

The role of acetyl-CoA carboxylase activity in normal liver metabolism and
pathophysiology in the context of obesity and cancer

Marin Elise Healy

Austin, Texas

MS, Biological and Physical Sciences, University of Virginia, 2013

MS, Exercise Science, The University of Texas at Austin, 2011

BS, Exercise Physiology, The University of Texas at San Antonio, 2008

A Dissertation Presented to the Graduate Faculty of the University of Virginia in
Candidacy for the Degree of Doctor of Philosophy

Department of Pharmacology

University of Virginia

August 2015

Kyle L. Hoehn, Ph.D.

Ira G. Schulman, Ph.D.

Norbert Leitinger, Ph.D.

Adam N. Goldfarb, M.D.

Marty W. Mayo, Ph.D.

Jill K. Slack-Davis, Ph.D.

David F. Kashatus, Ph.D.

ABSTRACT

The liver has a high capacity to store excess nutrients, primarily in the form of fat. However, excess lipid deposition in the liver can be problematic, as it is associated with metabolic disorders including fatty liver disease, type II diabetes, and liver cancer. The acetyl-CoA carboxylase (ACC) enzymes are major regulators of liver lipid content by catalyzing the conversion of excess glucose in the liver to fat, and by inhibiting mitochondrial fat oxidation. Thus, the ACC enzymes are potential drug targets because altering their activity could correct disease states associated with excess fat deposition. Using mice with genetic inhibition of liver ACC activity, we have uncovered a novel role for these enzymes in regulating protein acetylation that contributes to broad changes in cellular metabolism. At the level of whole-body physiology, we found that when a source of dietary fat was absent, LDKO mice have increased glucose disposal into the liver, reduction of peripheral adiposity, and improved whole-body glucose tolerance compared to controls. Under high-fat diet conditions, LDKO mice are protected from diet-induced fatty liver. However, a decrease in liver fat in this case is not sufficient to ameliorate diet-induced glucose intolerance. Finally, we investigated the role of ACC activity in tumorigenesis. Unexpectedly, inhibition of ACC activity increased susceptibility to carcinogen-induced liver tumor. Increased liver antioxidant defenses in LDKO mice protected cells from carcinogen-induced apoptosis and promoted tumor cell proliferation. This study identifies a protective role for ACC enzymes against tumorigenesis. Taken together, this work increases our understanding of liver nutrient metabolism and ACC activity, and highlights the complexity of liver metabolic compensatory mechanisms.

ACKNOWLEDGEMENTS

I am grateful for this opportunity to develop as a scientist at the University of Virginia. The past four years have been some of the best of my life, and this can be attributed to the wonderful people in my life.

I would like to start by thanking my family. My husband, Bobby Healy, did not hesitate to move to the other side of the country for this program. He has always encouraged me to push on through those long days in the lab and long nights studying. My brother, Owen Nelson, is always there to lift my spirits. Even as his older sister, I hope to be half as clever as he is one day. My mother, Leslie Nelson, is the best mother anyone could hope for. She's been in my corner from day one and has always challenged me to think big and pursue my dreams. Her confidence in me gives me the extra motivation to keep going, even if I'm not always quite as confident in myself. I dedicate my work to the memory of my father, Don Nelson, who passed away from cancer before his time. He instilled in me a curiosity for how things work and a passion to make the world a better place for those around me. I hope to carry his legacy forward by living life to the fullest, not taking a day for granted, and valuing relationships above accomplishments or possessions.

To my best friend, Chérie Nel, it's been quite an adventure! I remember years ago chatting about our hopes and dreams, and what life would look like when we were adults. Well, I still don't feel like an adult, but it's fun to look back and see how far we've come. Even though we've been geographically separated, you will always be close to my heart and I'm looking forward to many more adventures to come.

I'm grateful for the community here in Charlottesville, Virginia. I have had the opportunity to develop friendships with many wonderful people who have supported Bobby and me during our time here and genuinely invested in our lives. There are many people who I don't have space to mention, but specifically I'd like to thank Kyle and Christine Hoover, Bill Bray, Tash Kumar, Steven and Erica Griffith, Eric and Suzi Stauffer, Caitlin Secrist, and Sarah Booth. Even though I'm just passing through, I will hold these friendships dear for years to come.

My time here at the University of Virginia has provided an incredible framework for fostering my personal and scientific growth, and many of the faculty have actively invested in my training. I'm grateful for Doug Bayliss, Paula Barrett and Jolene Kidd, for guiding me through this process and getting me to the other side in one piece. My thesis committee members have given excellent insight and have been essential to shaping my project. I am particularly thankful for Ira Schulman and Jill Slack-Davis for their mentorship concerning my project, as well as my career as a scientist. They have been incredible role models and truly sources of inspiration.

One of the main reasons I am so excited to come to work every day is because of my wonderful lab mates. I thank Jenny Chow for showing me the ropes with enduring patience, and for her friendship. I thank Frances Byrne for always being willing to share her infinite wisdom, and for being both a lab "mom" and a great friend. To my lab "brothers" Brandon Kenwood and Evan Taddeo, thanks for letting me punch you when I'm frustrated (which is a daily occurrence, I think). I am thankful for the opportunity to learn and mature as scientists together. I look forward to many years ahead as peers and,

moreover, as friends. I thank Stefan Hargett and Sujoy Lahiri for courageously jumping in and picking up where I left off.

Finally, I am grateful for my mentor, Kyle Hoehn. I have always thought Kyle was one of the smartest people I've known, and so I figured I'd be coming out ahead if I could absorb even a fraction of his knowledge, analytical ability, and ingenuity. I appreciate Kyle because he allowed me to think for myself, shape my project from its outset, and provide mentorship and guidance as I needed it along the way. He is so dedicated to mentorship that he would not hesitate to drop everything to discuss my project. Whether my problem was big or small, I always knew I would have his ear. I have Kyle to thank for my even stronger appreciation for science than when I came into his lab, and a continuing passion for making discoveries and contributing to scientific knowledge.

TABLE OF CONTENTS

ABSTRACT	I
TABLE OF CONTENTS	V
SUMMARY OF FIGURES	1
SUMMARY OF TABLES	5
 CHAPTER 1: INTRODUCTION TO LIVER FUNCTION AND ACETYL-COA CARBOXYLASES	
1.1 Normal liver metabolism and the role of acetyl-CoA carboxylases	11
1.1.1 Normal function of the liver in detoxification	11
1.1.2 Normal function of the liver in whole-body nutrient homeostasis	14
1.1.3 Normal function of the liver in cholesterol homeostasis	21
1.1.4 Normal function of the liver in fatty acid production	23
1.1.5 Function of acetyl-CoA and the acetyl-CoA carboxylases in protein acetylation	28
1.2 Acetyl-CoA carboxylases in the context of obesity and metabolic disease.....	32
1.2.1 Pathologies associated with fatty liver.....	32
1.2.2 Evidence linking lipogenesis to fatty liver and the role of ACC enzymes	35
1.2.3 Review of studies that have targeted liver lipogenesis	36
1.3 Acetyl-CoA carboxylases in the context of liver cancer	38
1.3.1 Epidemiology of liver cancer.....	38

1.3.2 Overview of current detection and treatment strategies for liver cancer	39
1.3.3 Environmental and genetic etiology of liver cancer	42
1.3.4 Evidence of roles for lipogenesis and ACC enzymes in liver cancer	48
CHAPTER 2: EFFECTS OF GENETIC INHIBITION OF LIVER ACETYL-COA CARBOXYLASES ON WHOLE-BODY AND LIVER METABOLISM.....	50
2.1 Use of liver-specific ACC1 and ACC2 double knockout mice to define how loss of liver ACC activity affects normal liver and whole-body physiology in mice fed a normal chow diet.....	51
2.1.1 Background	51
2.1.2 Increased hepatic triglyceride accumulation in the absence of ACC activity..	51
2.1.3 Liver ACC inhibition disrupted acetyl-CoA homeostasis and altered protein acetylation	66
2.1.4 Subcellular compartmentalization of ACC-dependent changes in protein acetylation	66
2.1.5 Discussion	78
2.1.6 Summary	81
2.2 Effect of liver ACC deletion on liver and whole-body metabolic homeostasis in mice challenged with a high-carbohydrate diet	82
2.2.1 Background	82
2.2.2 Results.....	82

2.2.3 Discussion	89
2.2.4 Summary	91
2.3 Effect of liver ACC deletion on liver and whole-body metabolic homeostasis in mice challenged with a high-fat diet	92
2.3.1 Background	92
2.3.2 Results	92
2.3.3 Discussion	95
2.3.4 Summary	95
CHAPTER 3: METABOLIC CONSEQUENCES OF PROTEIN ACETYLATION MEDIATED BY THE ACC ENZYMES	97
3.1 Effect of ACC activity on PGC-1 α protein acetylation and cellular metabolism...	98
3.1.1 Background	98
3.1.2 Results	98
3.1.3 Discussion	102
3.1.4 Summary	103
CHAPTER 4: THE ROLE OF DIETARY NUTRIENTS AND ACC ENZYMES IN HEPATOCELLULAR CARCINOMA.....	104
4.1 Effect of dietary nutrients on hepatocellular carcinoma promotion	105
4.1.1 Background	105
4.1.2 Dietary effects on tumor burden	106

4.1.3 Physiologic effects	112
4.1.4 Metabolic effects.....	118
4.1.5 Inflammation.....	122
4.1.6 Serum adipokines.....	122
4.1.7 Liver protein expression	123
4.1.8 Discussion	130
4.1.9 Summary	135
4.2 Effect of ACC inhibition on hepatocellular carcinoma development.....	136
4.2.1 Background	136
4.2.2 Results.....	137
4.2.3 Summary	162
CONCLUDING REMARKS AND FUTURE DIRECTIONS.....	163
PUBLICATIONS RESULTING FROM THIS WORK.....	170
METHODS	171
General mouse husbandry.....	171
Generation of LDKO and Flox mice	171
Breeding of wildtype C57BL/6N mice	171
Diets for study of metabolic effects in LDKO and Flox mice.....	172
Diets for liver cancer studies.....	172

Diets for DEN-treated wildtype mice	173
Diet for DEN-treated LDKO and Flox mice.....	173
Respirometry.....	174
Serum collection and preparation	174
Serum metabolite measurements	174
Histology and immunohistochemistry	175
DEN treatment of mice	175
Metabolic tolerance testing and insulin sensitivity.....	175
Triglyceride production and oral triglyceride tolerance assays	176
Tissue collection of DEN-treated mice and tumor analysis.....	176
Liver histology and immunohistochemistry	177
Protein isolation and Western blotting.....	178
RNA isolation and qPCR.....	179
Liver fat content.....	179
NADPH and NADH assays	180
GSH:GSSG assay.....	180
8-OHdG assay.....	180
Metabolomics in liver tissue of DEN-treated LDKO and Flox mice	181
Evaluating mRNA expression using Oncomine.	183

Cell culture.....	183
In vitro metabolic substrate competition assays and enzyme activity assays	184
Seahorse Extracellular Flux assays.....	185
Acetyl-CoA measurements	186
Acetylation proteomics	187
Sample preparation	187
LC-MS/MS and data processing.....	188
Bioinformatics.....	190
Statistical analyses	191
REFERENCES.....	193

SUMMARY OF FIGURES

Figure 1. The Phase II glutathione metabolism system	13
Figure 2. Glucose metabolism in the liver.....	20
Figure 3. Function of the acetyl-CoA carboxylase enzymes in promoting fat synthesis and inhibiting fat oxidation.....	25
Figure 4. Typical progression of nonalcoholic fatty liver disease.....	33
Figure 5. Loss of hepatic ACC activity increases fat storage.....	54
Figure 6. Body weight and organ mass.....	56
Figure 7. Diurnal respirometry.....	57
Figure 8. Respirometry changes in response to fasting.....	58
Figure 9. Insulin signaling through Akt.....	59
Figure 10. The loss of ACC decreases hepatic fat oxidation.....	63
Figure 11. PPAR α , SREBP1c, and PGC-1 α target gene transcription in LDOK vs. Flox liver.....	65
Figure 12. ACC inhibition alters liver acetyl-lysine proteome.....	69
Figure 13. Liver NAD ⁺ and acetyl-CoA levels.....	70
Figure 14. ACC-mediated alterations in protein acetylation are enriched for metabolic networks involved in intermediary nutrient metabolism.....	73
Figure 15. Schematic showing the protein acetylation sites in metabolic pathways that are most differentially acetylated in LDKO/Flox liver.....	75
Figure 16. Protein expression and activity of electron transport chain complexes.....	77

Figure 17. Liver ACC inhibition increases glucose disposal into liver glycogen and improves whole-body glucose tolerance compared to Flox controls.....	84
Figure 18. LDKO mice fed a fat-free diet have reduced adiposity and depletion of liver triglycerides compared to Flox controls.	86
Figure 19. LDKO mice fed a fat-free diet for 3 weeks have no alterations in whole-body oxygen consumption or respiratory exchange ratio compared to Flox controls.	88
Figure 20. Liver ACC deletion causes a reduction of liver triglycerides, but no significant improvement in whole-body glucose tolerance in mice fed a Western diet.	94
Figure 21. ACC inhibition increases PGC-1 α acetylation.....	100
Figure 22. Inhibition PGC-1 α acetylation is sufficient to reverse the defect in fatty acid oxidation in LDKO hepatocytes.	101
Figure 23. Dietary nutrient content has a strong influence on liver tumor burden and multiplicity in male mice treated with DEN.	109
Figure 24. Liver histology.....	110
Figure 25. High sugar diets increase liver tumor incidence in DEN-treated females.....	111
Figure 26. Liver tumor burden is highly correlated with liver fat content, but does not correlate with adiposity in males.	115
Figure 27. Dietary sugar is associated with increased liver triglycerides in females.	116
Figure 28. Food consumption, body weight, and liver weight in males.	117
Figure 29. Liver tumor burden is associated with post-prandial insulin, but not other parameters of whole-body glucose metabolism in males.	119

Figure 30. Association of liver tumor burden with parameters of whole-body glucose metabolism in males.	120
Figure 31. Glucose tolerance in females.....	121
Figure 32. Liver tumor burden is positively correlated with liver IL-6, but negatively associated with serum adiponectin and apoptosis in males.	125
Figure 33. Liver inflammatory markers in males.	126
Figure 34. Serum inflammatory markers in males.....	127
Figure 35. Liver protein expression.....	129
Figure 36. Summary figure of dietary effects on liver tumor burden in mice treated with DEN	134
Figure 37. Liver cancer displays a lipogenic phenotype and liver cancer cells are programmed for dependency on lipogenesis.	141
Figure 38. ACC2 mRNA expression in HCC and inhibition of lipogenesis by SorA....	142
Figure 39. Mitochondrial function in liver non-cancer and cancer cells.	144
Figure 40. Liver ACC deletion increases diethylnitrosamine-induced tumorigenesis and liver cell proliferation in mice.....	147
Figure 41. Cleaved CASP3 staining in livers of DEN-treated Flox and LDKO mice....	148
Figure 42. Livers and tumors of LDKO mice are completely deficient in lipogenesis..	149
Figure 43. LDKO mice have no alterations in liver fat levels or whole-body physiology.	151
Figure 44. Metabolic gene expression and succinylcarnitine levels in livers of DEN-treated Flox and LDKO mice.....	153

Figure 45. Increased liver antioxidant status is a potential mechanism for increased cell proliferation and tumorigenesis in LDKO mice. 157

Figure 46. LDKO mice have higher liver glucokinase expression and antioxidant status. 158

Figure 47. LDKO livers maintain proliferation and are resistant to apoptosis acutely in response to DEN treatment. 160

Figure 48. Model for the role of sugars and acetyl-CoA carboxylase activity in liver and whole-body pathophysiology..... 169

SUMMARY OF TABLES

Table 1. Serum parameters of fed or 12 h-fasted LDKO and Flox mice.....	55
Table 2. Primer sequences	192

APPENDIX OF ABBREVIATIONS

¹⁸ F-FDG.	¹⁸ F-fluoro-2-deoxyglucose
2-AAF.	2-Acetylaminofluorene
8-OHdG.	8-Oxo-2'-deoxyguanosine
ABC.	ATP binding cassette
ACC.	Acetyl-CoA carboxylase
ACOX.	Acyl-CoA oxidase
AFP.	Alphafetoprotein
AMPK.	AMP-activated protein kinase
ASOs.	Antisense oligonucleotides
BMI.	Body mass index
CASP3.	Caspase 3
ChREBP.	Carbohydrate response element binding protein
CoA.	Coenzyme A
CPT1a.	Carnitine palmitoyl transferase 1a
CYP450.	Cytochrome P450
CYP7A.	Cholesterol 7 α hydroxylase
DAG.	Diacylglycerol
DCA.	Dioxycholic acid
DEN.	Diethylnitrosamine
DHAP.	Dihydroxyacetone phosphate
DNBA.	Dimethylbenzanthracene

ECAR.	Extracellular acidification rate
ER.	Endoplasmic reticulum
ETC.	Electron transport chain
F-1-P.	Fructose-1-phosphate
FASN.	Fatty acid synthase
Flox.	Floxed littermate control
G-6-P.	Glucose-6-phosphate
G6PD.	Glucose-6-phosphate dehydrogenase
GAD.	Glyceraldehyde
GEE.	γ -Glutamyl monoethyl ester
GEMMs.	Genetically engineered mouse models
HCA.	Hepatocellular adenoma
HCC.	Hepatocellular carcinoma
HIV.	Human immunodeficiency virus
HMGCR.	HMG-CoA reductase
HOMA-IR.	Homeostatic assessment model of insulin resistance
HPF.	Hyperplastic foci
i.p.	Intraperitoneal
LDKO.	Liver-specific ACC1 and ACC2 double knockout
LXR.	Liver X receptor
MCAD.	Medium chain acyl-CoA dehydrogenase
MRP.	Multidrug resistance-associated protein

mTOR.	Mammalian target of rapamycin
NAFLD.	Non-alcoholic fatty liver disease
NAM.	Nicotinamide, Nicotinamide
NASH.	Nonalcoholic steatohepatitis
OCR.	Oxygen consumption rate
OXPHOS.	Oxidative phosphorylation
PEPCK1.	Phosphoenolpyruvate carboxylase 1
PET.	Positron emission tomography
PFK.	Phosphofructokinase
PGC-1 α .	PPAR γ coactivator-1 α
PKC.	Protein kinase C
PPAR.	Peroxisomal proliferator-activated receptor
PPP.	Pentose phosphate pathway
R-5-P.	Ribulose-5-phosphate
RER.	Respiratory exchange ratio
RFA.	Radiofrequency ablation
Scap.	SREBP cleavage activating protein
SEM.	Standard error of the mean
SorA.	Sorafenib
SRE.	Sterol regulatory element
SREBP.	Sterol regulatory element binding protein
TACE.	Transarterial chemoembolization

TCA.	Tricarboxylic acid
VLDL.	Very low density lipoprotein
VO ₂ .	Oxygen consumption rate
β-HAD.	3-hydroxyacyl-CoA dehydrogenase

**CHAPTER 1: INTRODUCTION TO LIVER FUNCTION AND ACETYL-COA
CARBOXYLASES**

1.1 Normal liver metabolism and the role of acetyl-CoA carboxylases

1.1.1 Normal function of the liver in detoxification

The liver is the main site of detoxification in the body. It has a remarkable capability to metabolize a wide array of xenobiotics which are not produced by the body such as drugs, carcinogens, and pollutants, as well as endobiotics which are produced by the body such as fatty acids, hormones, vitamins, and amines^{1,2}. Ingested xenobiotics enter from the gastrointestinal tract to the hepatic portal vein, which feeds into the liver. Thus, most ingested xenobiotics encounter the liver and are metabolized before entering general circulation. The liver is well-vascularized, allowing xenobiotics and endobiotics that have made their way into general circulation to return to the liver where they can be metabolized.

Metabolizing a vast array of endobiotics and xenobiotics, including those never before encountered by the liver, is a demanding task which involves three phases. Phase I metabolism is carried out by Cytochrome P450 (CYP450) enzymes. This CYP450 family encompasses multiple enzymes that have similar mechanisms but varied substrate preferences³. Many of the CYP450 enzymes are inducible such that expression is increased upon exposure to certain compounds⁴. There is also significant genetic heterogeneity in CYP450 enzyme expression between ethnic populations, potentially causing drug metabolism to vary greatly depending on an individual's genetic background⁵. Regardless of the specific CYP450 enzyme or substrate, a typical Phase I enzyme reaction is characterized by use of oxygen and NADH to add a reactive oxygen group such as a hydroxyl radical, thereby activating the molecule³.

The activated molecule is often more toxic than the parent molecule because the associated free radical can cause oxidative lipid, protein, and DNA damage⁶ unless it directly proceeds to Phase II metabolism, which is carried out by a wide variety of enzymes spanning multiple gene families. These enzymes have a common function to conjugate the reactive group of a molecule resulting in its transformation to a water-soluble compound that can be eliminated from the body³. Glutathione (γ -glutamyl cysteinyl glycine) is a major component of the Phase II conjugation system in the liver⁷. GSH, which is glutathione reduced at its free thiol group, is conjugated to xenobiotics by the enzyme glutathione *S*-transferase, forming a glutathione *S*-conjugate. Additionally, the enzyme glutathione peroxidase catalyzes the transfer of an electron from GSH to a reactive oxygen group of an active molecule to form a hydrogen peroxide species which decomposes to water and oxygen, allowing GSH to function as an antioxidant. The glutathione molecule, now oxidized at its free thiol group, is unstable and rapidly forms a disulfide bond with another oxidized glutathione molecule, forming GSSG⁷. Oxidation of NADPH, catalyzed by the enzyme glutathione reductase, is required for reduction of GSSG back to GSH⁸. The glutathione metabolism system is shown in Figure 1. The ratio of GSH:GSSG represents the antioxidant capacity of a tissue^{9,10} and regulates essential cellular processes such as detoxification, growth, and survival¹¹⁻¹³.

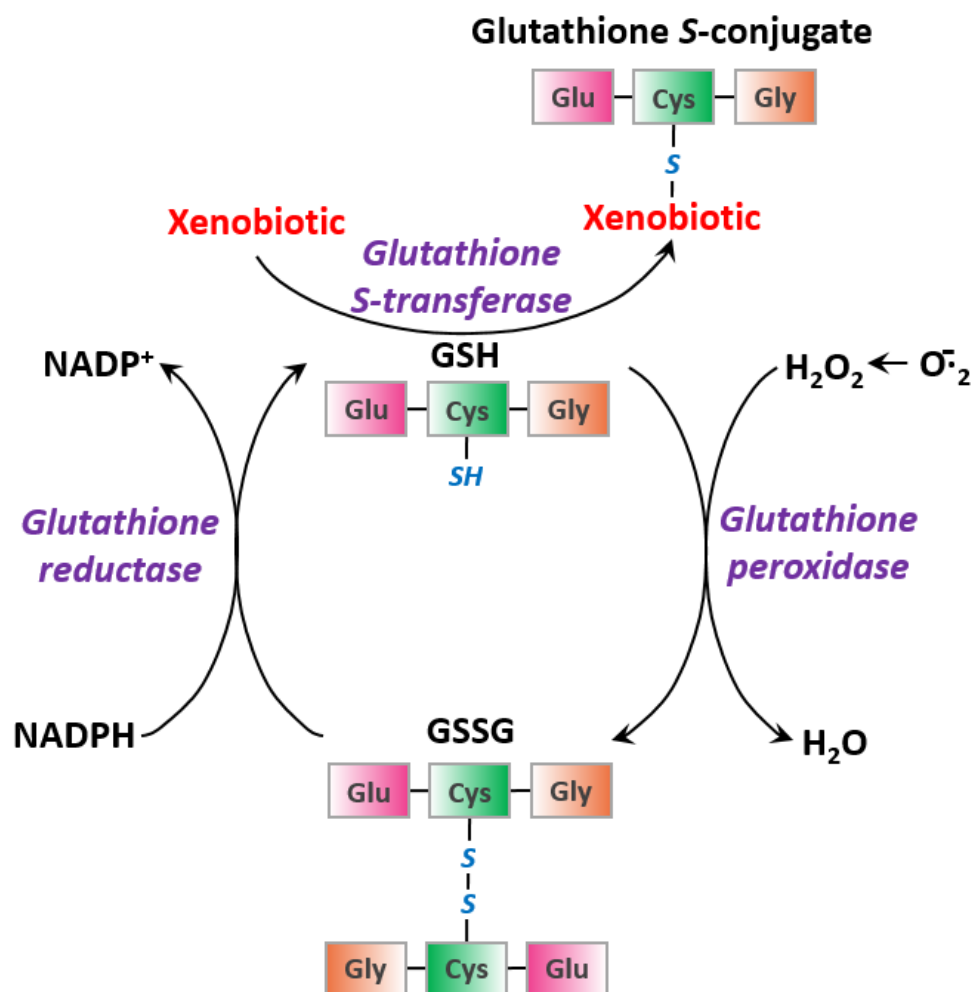


Figure 1. The Phase II glutathione metabolism system

GSH, the reduced form of glutathione, is conjugated to xenobiotics by the enzyme glutathione *S*-transferase, forming a glutathione *S*-conjugate. GSH also participates in a redox reaction to convert hydrogen peroxide (H_2O_2) to water (H_2O) which is catalyzed by the enzyme glutathione peroxidase. Oxidized glutathione is unstable and readily joins to another oxidized glutathione molecule via a disulfide bond to form GSSG. The enzyme glutathione reductase catalyzes the reduction of GSSG to GSH using NADPH.

Phase III metabolism is the final step of the liver detoxification process and involves antiporters which unidirectionally transport conjugated molecules outside the cell for elimination. This is an ATP-dependent process carried out by proteins of the multidrug resistance-associated protein (MRP) family, which are efflux transporters belonging to the ATP-binding cassette (ABC) superfamily of transport proteins¹⁴. The MRP family acquired its name because its members were originally observed to export chemotherapy drugs out of cancer cells, rendering the drugs ineffective¹⁵. After exiting the cell, these water-soluble conjugates are then eliminated from the body in the urine (Goodman and Gilman's *The Pharmacological Basis of Therapeutics*, Twelfth Edition).

1.1.2 Normal function of the liver in whole-body nutrient homeostasis

The liver is a key organ regulating whole-body nutrient homeostasis. When blood glucose levels drop, such as occurs during food deprivation, glucagon is released by the pancreatic alpha cells¹⁶ and promotes release of glucose and fatty acids which are stored in the liver back into circulation for maintenance of normal blood glucose levels and utilization by other organs. This nutrient source is particularly important for highly metabolically-active organs which have a low capacity for glucose and lipid storage such as the brain, cardiac muscle, and red blood cells^{17,18}. When blood glucose levels are high, such as after consumption of a meal, insulin is released by the pancreatic beta cells¹⁹. Insulin decreases liver glucose production by inhibiting glucagon production from pancreatic alpha cells, by inhibiting gluconeogenic enzyme activity, and by suppressing gluconeogenic enzyme expression^{20,21}. Insulin also enhances glucose disposal from the

blood into peripheral tissues such as skeletal muscle, adipose tissue, and the liver²². In skeletal muscle and adipose tissue, insulin stimulates translocation of the insulin-responsive glucose transporter GLUT4 to the plasma membrane to promote the transport of circulating glucose into the tissue²³ for energy production or storage in the form of lipid or glycogen. The liver is unique from adipose and skeletal muscle in that it does not express a glucose transporter such as GLUT4 that translocates to the surface of the cell in response to insulin. Rather, the liver expresses the glucose transporter GLUT2 and the fructose transporter GLUT5, which are constitutively localized to the plasma membrane of hepatocytes^{24,25}.

After transport into the liver, glucose is phosphorylated to glucose-6-phosphate (G-6-P) by glucokinase²⁶. G-6-P is then converted to glucose-1-phosphate by phosphoglucomutase and to UDP-glucose by UDP-glucose pyrophosphorylase, then joined to a chain of glucose polymers by glucogen synthase to make glycogen, which is the storage form of glucose molecules^{27,28}. The majority of G-6-P produced in the liver is shunted to the Pentose Phosphate Pathway (PPP) for production of nucleotides and amino acids²⁹. The first step of the PPP, the conversion of G-6-P to 6-phosphogluconate catalyzed by the enzyme glucose-6-phosphate dehydrogenase (G6PD), is the main source of NADPH production in the cell^{30,31}. NADPH is an important reducing agent for GSH production (discussed in the previous section *1.1.1 Normal function of the liver in detoxification*) and for biosynthetic processes such as cholesterol and lipid synthesis^{32,33}. The remaining G-6-P proceeds through glycolysis, which is a series of enzymatic reactions that yields NADH³⁴, an important reducing factor for mitochondrial oxidative

metabolism, and ATP, used for energy-dependent processes throughout the cell³⁵. Rate of flux through glycolysis is regulated by activity of the enzyme phosphofructokinase (PFK), which converts G-6-P to fructose-1,6-bisphosphate. G-6-P enters glycolysis as a 6-carbon molecule, and the final product of glycolysis is two 3-carbon pyruvate molecules.

The liver is the main site of fructose metabolism in the body because it highly expresses the fructose transporter GLUT5, which facilitates uptake of fructose into the liver from hepatic portal circulation. Because the liver efficiently takes up fructose from the portal circulation, very little appears in the blood after ingestion compared to glucose³⁶. Upon transport into the liver, fructose is converted to fructose-1-phosphate (F-1-P) by fructokinase, which is also highly expressed in the liver. F-1-P is converted to glyceraldehyde (GAD) and dihydroxyacetone phosphate (DHAP) by aldolase. GAD and DHAP are converted to G-3-P by G-3-P dehydrogenase. In a multi-step process, G-3-P is converted to G-6-P, which is processed to glycogen or converted to 6-PG by G6PD to proceed through the PPP. The rate of conversion G-3-P to G-6-P is limited by fructose biphosphatase activity. Alternatively, G-3-P is converted to ribose-5-phosphate (R-5-P) by transketolase and enters the PPP downstream of PFK and G6PD to form nucleotides and amino acids. Although fructose is able to enter the PPP via the mechanisms described, the rate of fructose flux through the PPP is approximately 25% that of glucose³⁷. Finally, G-3-P proceeds through glycolysis to produce pyruvate. Because G-3-P enters glycolysis downstream of PFK, the rate of pyruvate production from fructose is higher than that of glucose³⁷.

In normal liver tissue, pyruvate is transported into the mitochondria and converted to acetyl-CoA via decarboxylation and addition of coenzyme A (CoA). Acetyl-CoA is also produced from β -oxidation of fatty acids in the mitochondria³⁸. Acetyl-CoA proceeds through the tricarboxylic acid (TCA) cycle, which produces the reducing cofactors NADH and FADH₂³⁹ necessary for mitochondrial oxidative phosphorylation (OXPHOS). OXPHOS is conducted by the electron transport chain (ETC) enzymes, which are embedded in the mitochondrial inner membrane⁴⁰. Electrons from NADH or FADH₂ enter the ETC at complexes I and II, respectively. Electrons are passed from complexes I or II to complex III, and from complex III to complex IV. Complex IV then passes electrons to molecular oxygen, which is the final electron acceptor in the ETC. As electrons are passed along the ETC, complexes I, III and IV create an electrochemical proton gradient by pumping protons from the inner mitochondrial matrix to the inner membrane space between the mitochondrial inner and outer membranes. This gradient drives ATP synthase to catalyze ATP production from ADP and inorganic phosphate⁴¹.

In addition to producing reducing factors for the ETC, the TCA cycle produces important intermediates that feed into other metabolic pathways. One such metabolite is citrate, which, in addition to being a TCA cycle intermediate, is transported to the cytosol by the mitochondrial citrate transporter protein and converted to oxaloacetate and acetyl-CoA by ATP citrate lyase. Oxaloacetate is converted to malate by malate dehydrogenase or to pyruvate by the enzymes phosphoenolpyruvate carboxykinase and pyruvate kinase. Malate and pyruvate are shuttled back into the mitochondria to replenish the TCA cycle⁴² or used for gluconeogenesis⁴³. Acetyl-CoA serves as a precursor for lipid and cholesterol

synthesis⁴⁴. The liver glucose metabolism pathway is illustrated in Figure 2. Although citrate is considered to be the major source of cytosolic acetyl-CoA in cells under most conditions, acetate, which is derived from ketone and ethanol metabolism, is also converted to acetyl-CoA by the cytosolic enzyme acetyl-CoA synthetase⁴⁴.

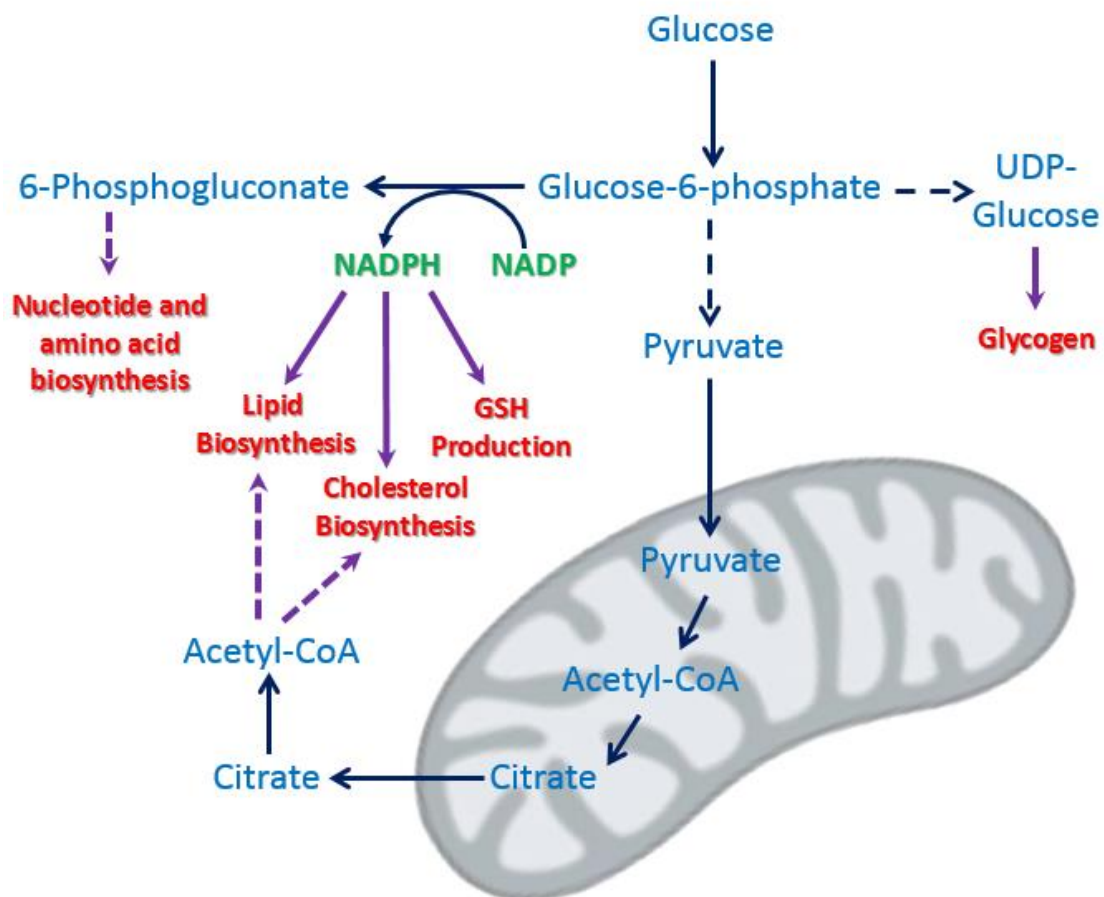


Figure 2. Glucose metabolism in the liver.

After entering the liver, glucose is converted to glucose-6-phosphate. Glucose-6-phosphate can be converted to glycogen, which is the storage form of glucose molecules. Glucose-6-phosphate can also be used for production of 6-phosphogluconate in a reaction yielding NADPH. 6-Phosphogluconate can be used for nucleotide and amino acid biosynthesis. NADPH is used in lipid and cholesterol biosynthesis, and for GSH production. Glucose-6-phosphate can also be converted to pyruvate, which is converted to acetyl-CoA in the mitochondria. Acetyl-CoA is converted to citrate for transport out of the mitochondria. In the cytoplasm, citrate can be converted back to acetyl-CoA, which is the precursor for lipid and cholesterol synthesis.

1.1.3 Normal function of the liver in cholesterol homeostasis

Cholesterol is an amphipathic lipid that is a major component of cell membranes and is a critical precursor to bile salts, steroid hormones, and fat-soluble vitamins. The liver is the primary organ for cholesterol synthesis, degradation and excretion, and it has a central role in regulating whole-body cholesterol homeostasis^{45,46}.

Cholesterol is synthesized in the liver from acetyl-CoA in a series of steps that are tightly regulated by multiple feedback mechanisms. The rate-limiting enzyme in the cholesterol biosynthesis pathway is HMG-CoA reductase (HMGCR), which catalyzes formation of mevalonate from acetyl-CoA and is the first committed step of the cholesterol synthesis pathway⁴⁷. HMG-CoA reductase is regulated by product feedback-inhibition at several levels including transcription and protein degradation^{48,49}.

When cells are depleted of cholesterol, transcription of HMG-CoA reductase increases through binding of sterol regulatory element binding protein (SREBP)-2 to DNA sterol regulatory elements (SREs) in gene promoters. Conversely, when cholesterol levels are high, SREBP-2 transcriptional activity decreases. After synthesis, the SREBP-2 protein is inserted into the endoplasmic reticulum (ER) membrane as a hairpin structure with the N- and C-terminal domains facing the cytosol. The C-terminus is normally bound to SREBP cleavage activating protein (Scap). Scap binds oxysterols, which signal high cholesterol levels, and thus functions as the cholesterol sensor in this system. When Scap is bound to oxysterol, it binds to the ER membrane protein Insig, causing the Scap-SREBP complex to be retained at the ER membrane. When cholesterol levels are low, the SREBP-Scap complex is freed from Insig to enter the Golgi where the N-terminal

domain of SREBP-2 is cleaved. The N-terminus of SREBP-2 then localizes to the nucleus where it binds to SRE elements and acts as a transcription factor⁵⁰⁻⁵².

HMGCR protein has a long half-life, thus its product-stimulated degradation plays an important role in regulating total HMGCR levels in the cell⁴⁹. Like SREBP, HMGCR is embedded in the ER membrane, and Insig is involved in regulating its degradation. Lanosterol, which is synthesized from mevalonate in the cholesterol synthesis pathway, binds to HMGCR and causes it to associate with Insig, resulting in ubiquitination and proteasomal degradation of HMGCR⁵³.

Cholesterol has multiple fates in the liver including storage, conversion to bile acids, or packaging and export. Cholesterol is stored in lipid droplets as cholesterol esters, and cholesterol is released from the droplets upon hydrolysis of the ester bonds by ester hydrolases⁵⁴. Conversion of cholesterol to bile acids and subsequent excretion represents a major route for decreasing liver cholesterol levels and maintaining the intestinal bile pool, which is necessary for digestion of dietary fats and lipid-soluble vitamins⁵⁵. Cholesterol 7 α hydroxylase (CYP7A) is a CYP450 enzyme which catalyzes the first and rate-limiting step in the bile synthesis pathway by oxidizing cholesterol to form 7 α hydroxycholesterol^{56,57}. Bile acid response elements within the CYP7A gene repress activity of the CYP7A promoter in the presence of bile acids⁵⁸, thereby regulating bile acid production by product feedback-inhibition.

Another important mechanism for lowering liver cholesterol levels and supplying cholesterol to other tissues is cholesterol packaging and export. In the liver, cholesterol is packaged in very-low-density lipoproteins (VLDLs), which are lipid-containing particles

encased by amphipathic proteins and phospholipids that make the particles soluble in circulation⁵⁹. Cholesterol and cholesterol esters represent approximately 10% and 4% of VLDL contents, respectively⁶⁰. VLDL particles are released from the liver into circulation, where the protein components of the particle are modified, allowing the particles to be endocytosed at peripheral tissues such as adipose, skeletal muscle, and cardiac muscle⁶¹.

1.1.4 Normal function of the liver in fatty acid production

Acetyl-CoA derived from cytosolic citrate or acetate is converted to fat by the process *de novo* lipogenesis. The liver is an exceptionally lipogenic tissue and plays an important role in synthesizing and storing fat under high nutrient conditions, and exporting fat to other organs under low nutrient conditions⁶². The liver has finite glycogen storage capacity; thus under conditions of high glucose availability, lipogenesis acts as a 'glucose sink' by converting glucose precursors to an efficient nutrient-dense form for storage⁶³. Lipogenesis is intricately regulated on multiple levels in order to appropriately respond to liver and whole-body nutrient status.

The rate-limiting enzymes in lipogenesis are acetyl-CoA carboxylase (ACC) 1 and 2, which catalyze the carboxylation of cytosolic acetyl-CoA to malonyl-CoA. The ACCs are multi-subunit enzymes encoded by separate genes that have biotin carboxylase and carboxyltransferase domains which coordinate a two-step reaction. First, the biotin carboxylase subunit catalyzes the transfer of a carboxyl group from bicarbonate to biotin

in an ATP-dependent reaction. Second, the carboxyltransferase subunit catalyzes the transfer of the carboxyl group from biotin to acetyl-CoA to form malonyl-CoA^{64,65}.

While ACC1 and ACC2 perform the same reaction to convert acetyl-CoA to malonyl-CoA, they have distinct functions which are dictated by their intracellular locations. ACC1 is localized to the cytosol, and so the malonyl-CoA it produces is readily used by other cytosolic enzymes involved in lipogenesis. ACC2 has an additional mitochondrial targeting sequence on its N-terminal domain which causes it to associate with the mitochondrial outer membrane⁶⁶. The malonyl-CoA produced by ACC2 readily blocks mitochondrial fatty acid oxidation by allosterically inhibiting carnitine palmitoyltransferase (CPT1a), which transports fatty acids across the mitochondrial membrane⁶⁷. By promoting fatty acid synthesis and inhibiting its oxidation, the net effect of ACC enzyme activity is to promote liver fat storage. The individual roles of ACC1 and ACC2 are illustrated in Figure 3.

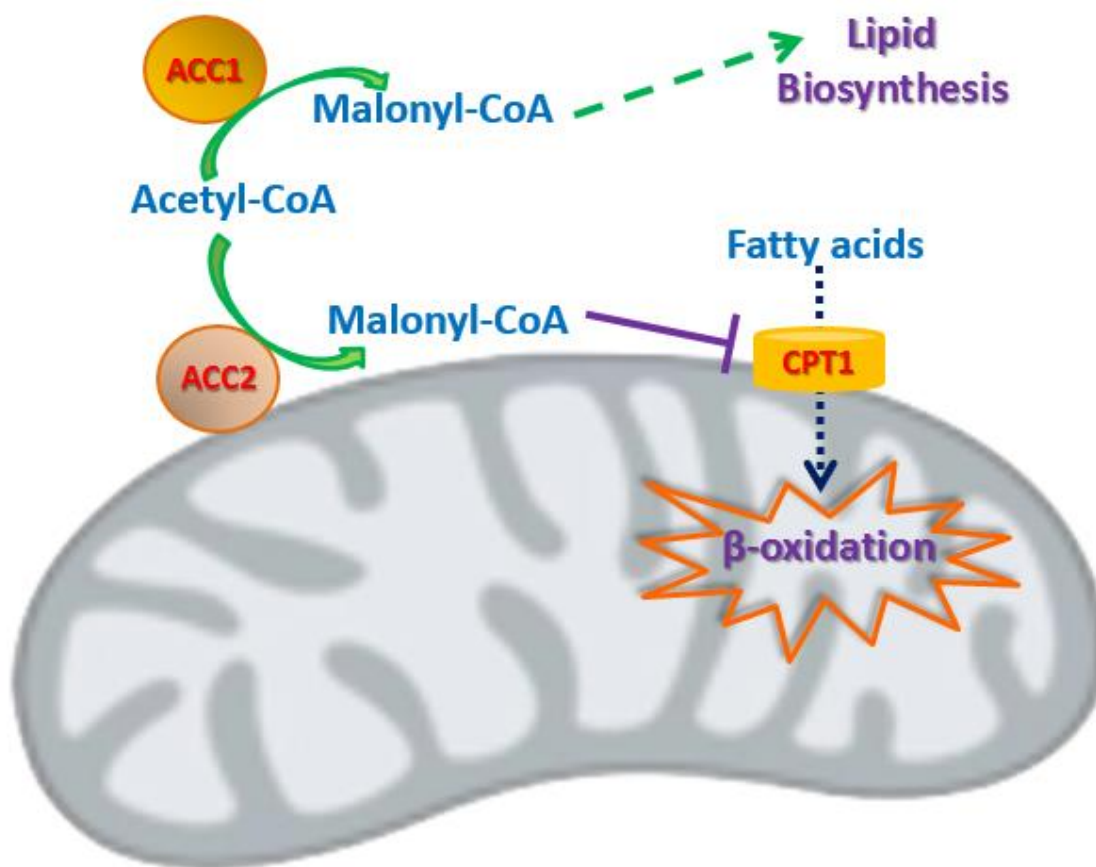


Figure 3. Function of the acetyl-CoA carboxylase enzymes in promoting fat synthesis and inhibiting fat oxidation.

The acetyl-CoA carboxylase (ACC) enzymes ACC1 and ACC2 catalyze the same reaction to convert acetyl-CoA to malonyl-CoA. However, they have different functions based on their intracellular locations. ACC1 is localized to the cytoplasm, and the malonyl-CoA it produces is readily utilized for lipid biosynthesis. ACC2 is localized to the mitochondrial outer membrane, and the malonyl-CoA it produces inhibits CPT1, blocking transport of fatty acids into the mitochondria for oxidation.

The ACC enzymes are sensitive to the nutritional status of the cell via two post-translational mechanisms. First, ACC1 is allosterically activated by citrate, as high citrate levels signify high cellular nutrient status and the availability of lipid precursors. Citrate enhances ACC1 activity by inducing polymerization of isolated ACC1 dimers into filamentous structures of up to 30 protomers, which enhance enzyme stability^{68,69}. Second, ACC1 and ACC2 are phosphorylated by AMP-activated protein kinase (AMPK). Under conditions of low cellular ATP, AMPK phosphorylates ACC resulting in its deactivation⁷⁰. By these mechanisms, the ACC enzymes are switched on under conditions of high nutritional status to promote storage of excess nutrients in the form of fat, and switched off under conditions of low nutrient status to allow ATP generation via mitochondrial lipid oxidation.

The ACC enzymes are also highly regulated at the transcriptional level. ACC transcription is induced in the liver by high carbohydrate feeding but decreased by feeding of long chain saturated fat⁷¹. Many of the effects of a high carbohydrate diet on increasing ACC transcription are attributed to the effects of insulin, which concomitantly increases with blood glucose. The ability of insulin to induce ACC expression is contingent upon the transcription factor SREBP1c^{72,73} in co-operation with the transcription factor liver X receptor (LXR). Regulation of SREBP1c activity in response to insulin is thought to be LXR-dependent via an LXR response element within the SREBP1c promoter⁷⁴. In contrast, polyunsaturated fatty acids interfere with binding of LXR to its response element, resulting in lower SREBP1c induction⁷⁵. There is evidence that insulin activates LXR through the protein complex mammalian target of rapamycin

(mTOR), which leads to phosphorylation of LXR on activating sites^{76,77}, signaling LXR translocation to the nucleus where it binds to the LXR response element on the SREBP1c promoter.

Similarly to SREBP2, activation of SREBP1c requires proteolytic cleavage to liberate its active N-terminal domain. In contrast to SREBP2, however, cleavage of SREBP1c is not regulated by sterols⁷⁸. Rather, cleavage of SREBP1c is regulated by a unique mechanism involving insulin. Acute insulin exposure causes rapid cleavage of SREBP1c, and the presence of insulin is required to achieve production of mature SREBP1c⁷⁹. While the exact mechanism remains unclear, it has been shown that insulin-induced cleavage of SREBP1c requires mTOR activity, but this process is distinct from mTOR regulation of SREBP1c transcription via LXR⁷⁷.

Deletion of SREBP1c in mice results in only a partial decrease in ACC induction in response to high-carbohydrate feeding⁸⁰, indicative of an additional transcription factor involved in stimulating ACC transcription in the presence of high glucose. Experiments using isolated hepatocytes have revealed that glucose directly activates ACC transcription independently of insulin⁸¹ mediated by the transcription factor carbohydrate response element binding protein (ChREBP)⁸². G-6-P, which signifies high intracellular levels of glucose or fructose, stimulates ChREBP translocation to the nucleus and transcriptional activation by mechanisms which are still under investigation⁸³.

The product of the ACC enzymes, malonyl-CoA, can be linked to another malonyl-CoA molecule to form palmitoyl-CoA in a 7-cycle process which is catalyzed by the enzyme fatty acid synthase (FASN). This reaction is expensive in terms of reductive

and energetic costs, as it consumes 14 molecules of NADPH and 7 molecules of ATP⁸⁴. Palmitoyl-CoA is then converted to palmitate, a fully-saturated lipid which is 16 carbons in length (16:0), by the enzyme palmitoyl-ACP thioesterase⁸⁵. Elongation of palmitate by elongase enzymes forms lipids of varied chain lengths. Additionally, desaturase enzymes introduce carbon-carbon double bonds to make unsaturated lipids. The primary products of lipogenesis are the saturated fatty acids palmitate (16:0) and stearate (18:0), along with the unsaturated fatty acids palmitoleate (palmitate that is saturated at the seventh carbon; 16:1n-7) and oleate (stearate that is saturated at the ninth carbon; 18:1n-9)⁸⁶.

Fatty acids synthesized in the liver are incorporated into cell membranes, esterified and stored, or packaged and exported. *De novo* synthesized lipids which are converted to phospholipids are readily incorporated into cell membranes. Inhibition of lipogenesis has been shown to cause membrane defects and interfere with proliferation of rapidly-dividing prostate cancer cells⁸⁷. Fatty acids are stored in the liver in the form of triglycerides, which are compartmentalized into lipid droplets encased by phospholipids⁸⁸. Finally, fatty acids in the liver are packaged in VLDL particles to be exported and delivered through circulation to other tissues. Triglycerides and phospholipids represent approximately 60% and 13% of VLDL contents, respectively⁶⁰.

1.1.5 Function of acetyl-CoA and the acetyl-CoA carboxylases in protein acetylation

In addition to being a necessary prerequisite for cholesterol and lipid biosynthesis, acetyl-CoA is becoming increasingly appreciated as an important regulator of metabolic homeostasis, particularly as a substrate for post-translational modification of proteins. It

was first discovered that nuclear histone proteins are reversibly acetylated on lysine residues, and that these modifications represent a main mechanism for regulation of chromatin arrangement, DNA accessibility, and gene transcription^{89,90}. More recently, owing to improvements in mass spectrometry proteomics, over one thousand non-histone acetylated proteins have been identified in the liver⁹¹. Interestingly, enzymes involved in intermediary metabolism are preferentially acetylated even when accounting for protein abundance⁹². The metabolic processes encompassing these acetylated proteins include glycolysis, gluconeogenesis, the TCA cycle, the urea cycle, fatty acid metabolism, and glycogen metabolism. The effects of acetylation on protein function are varied. Activities of the fatty acid oxidation enzyme enoyl-coenzyme A hydratase/3-hydroxyacyl-coenzyme A and the TCA cycle enzyme malate dehydrogenase are twice as high when acetylated. Activity of the glycolytic enzyme phosphoglycerate mutase-1 is also enhanced when acetylated⁹³. Conversely, activity of the urea cycle enzyme argininosuccinate lyase decreased when acetylated. Acetylation prolonged the half-life of the gluconeogenic enzyme phosphoenolpyruvate carboxykinase 1 (PEPCK1) was affected by its acetylation state, such that acetylation of PEPCK1 prolonged the protein half-life⁹². These examples illustrate that protein acetylation significantly affects the activity or stability of an enzyme, and the mechanism by which an enzyme is regulated by acetylation varies greatly depending on its role in a greater metabolic network.

How acetylation affects the function of particular enzymes throughout metabolism remains to be elucidated. However, a well-established target of regulation by acetylation is the transcriptional co-activator peroxisomal proliferator-activated receptor

(PPAR) γ coactivator-1 α (PGC-1 α)⁹⁴. PGC-1 α is a critical regulator of metabolic flexibility by controlling expression of genes involved in mitochondrial biogenesis, fatty acid oxidation⁹⁵, and gluconeogenesis⁹⁶. PGC-1 α is highly sensitive to the energy status of a cell through reversible acetylation. SIRT1, a deacetylase enzyme that is active under low-energy conditions⁹⁷, deacetylates and activates PGC-1 α . Alternatively, PGC-1 α is acetylated and deactivated by the histone acetyltransferase enzyme GCN5 under high energy conditions⁹⁴. When active, PGC-1 α triggers mitochondrial biogenesis and promotes transcription of genes encoding fatty acid oxidation and gluconeogenesis enzymes. Collectively, liver PGC-1 α activation under nutrient deprivation causes a shift in metabolism to decrease glucose catabolism, increase fat catabolism, and increase glucose release from the liver in order to maintain blood glucose levels and sustain the metabolic needs of other tissues.

Another transcription factor that known to be acetylated is ChREBP. Acetylation of ChREBP occurs under high glucose conditions in the liver and likely contributes to its transcriptional activity, resulting in upregulation of lipogenic genes⁹⁸.

Transfer of an acetyl group from acetyl-CoA occurs enzymatically⁹⁹ or non-enzymatically¹⁰⁰. GCN5 was originally identified as a nuclear histone acetyltransferase that functioned to add the acetyl group from acetyl-CoA to a lysine residue of histone proteins¹⁰¹. More recently, GCN5 was found to acetylate PGC-1 α and influence its activity⁹⁴. Although acetyltransferases are actively recruited to histones, acetyl-CoA synthesis is rate-limiting for histone acetylation^{102,103}, demonstrating that enzymatic acetylation is also regulated by levels of the reaction substrate, acetyl-CoA.

Since the ACC enzymes catalyze the conversion of acetyl-CoA to malonyl-CoA, they compete with acetyltransferases for intracellular acetyl-CoA pools. It has been confirmed in yeast that ACC inhibition increases the intracellular acetyl-CoA pool. As acetyl-CoA can freely distribute between the cytosol and nucleus, ACC inhibition in the cytosol was sufficient to increase histone acetylation^{91,104}. However, this phenomenon has not yet been tested in a mammalian system. While acetyl-CoA can freely move between the cytosol and nucleus because of the presence of nuclear pores, it is impermeable to other organelles such as mitochondria and peroxisomes, causing these organelles to rely on intra-organelle acetyl-CoA production or shuttle transport systems. Acetate can be transported bi-directionally across the cellular cytoplasmic membrane by monocarboxylate transporter proteins¹⁰⁵. Thus, the effect of ACC inhibition on organelle-specific acetyl-CoA pools and protein acetylation has yet to be determined.

1.2 Acetyl-CoA carboxylases in the context of obesity and metabolic disease

1.2.1 Pathologies associated with fatty liver

Non-alcoholic fatty liver disease (NAFLD) is defined as the accumulation of fat in hepatocytes exceeding 5% of the liver weight in a patient without significant history of alcohol use. NAFLD is the most common liver disorder in Western society, affecting over 30% of Americans^{106,107}. NAFLD encompasses a progressive spectrum of liver abnormalities from steatosis (fatty liver) to steatohepatitis (fatty liver with inflammation) to cirrhosis (steatohepatitis with fibrosis), which can progress to liver cancer and end-stage liver failure¹⁰⁸. The typical progression of NAFLD is depicted in Figure 4. While the pathogenesis of many NAFLD cases is cryptic, some established causes include rapid weight loss, glucocorticoids, antiviral medications, genetic defects in lipid storage, human immunodeficiency virus (HIV) infection, and environmental hepatotoxins¹⁰⁹. Obesity, type 2 diabetes, and hyperlipidemia commonly co-exist with NAFLD and are thought to contribute to its development. Of patients with NAFLD, obesity has been observed in 30-100%, type 2 diabetes has been observed in 10-75%, and hyperlipidemia has been observed in 20-95%^{108,110-113}. NAFLD itself is a risk factor for several pathologies including glucose intolerance/insulin resistance^{114,115}, hypertriglyceridemia¹¹⁶, hypertension and cardiovascular disease¹¹⁷.

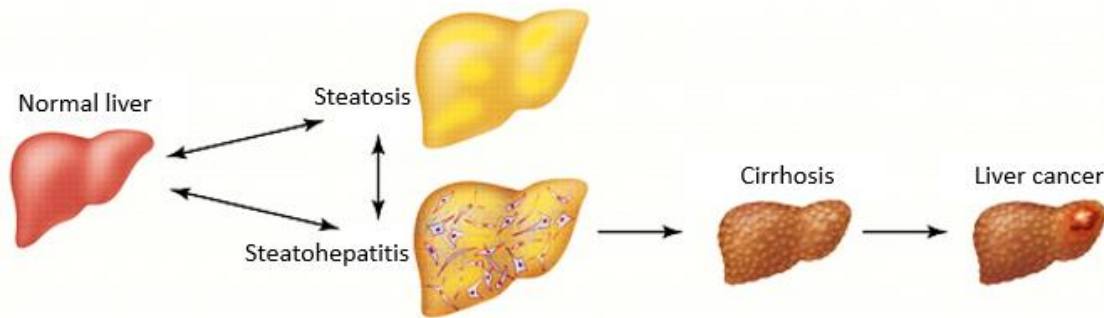


Figure 4. Typical progression of nonalcoholic fatty liver disease.

Nonalcoholic fatty liver disease (NAFLD) encompasses a progression of liver diseases from steatosis to steatohepatitis to cirrhosis, which can lead to liver cancer. Steatosis and steatohepatitis are reversible, whereas cirrhosis features permanent liver damage. NAFLD can initiate as steatosis or steatohepatitis, and these two conditions can be interchangeable. Figure adapted from Cohen, Horton, and Hobbs. Human fatty liver disease: old questions and new insights. *Science*. 2011;332:1519-23.

Although NAFLD is a common feature in obesity, the association between fatty liver and glucose intolerance/insulin resistance is thought to be independent of peripheral adiposity^{111,118–120}. In a study by Lee, et al.¹¹¹, reduced glucose tolerance was as common in lean as obese patients with NAFLD. In a study by Marchesini, et al.¹²¹, patients with NAFLD had an increased prevalence of insulin resistance compared to patients without NAFLD regardless of body mass index. Furthermore, hepatic insulin resistance is a strong predictor of whole-body insulin resistance¹²². However, the contribution of lipogenesis to hepatic insulin resistance and/or whole body glucose intolerance is controversial and is currently under investigation.

Evidence exists to suggest that pathogenic accumulation of liver lipid, particularly diacylglycerol (DAG), disrupts the insulin signaling cascade by activating protein kinase C (PKC) and stimulating its translocation to the plasma membrane. PKC decreases insulin receptor phosphorylation, leading to impairments in downstream pathways causing reduced glycogen synthesis and an inability to appropriately restrain hepatic glucose release¹²³. Hepatic lipogenesis contributes to increased steady-state levels of DAG¹²⁴; thus hepatic lipogenesis may play a causal role in whole-body glucose intolerance and insulin resistance¹²⁵. In support of a causal role of lipogenesis in insulin resistance, glucose intolerance and NAFLD, mice expressing constitutively active ACC1 and ACC2 featured elevated liver lipogenesis, fatty liver, and hepatic insulin resistance, coincident with whole-body glucose intolerance and insulin resistance¹²⁶. A major confounding factor in interpreting these results is that the ACC enzymes were constitutively active throughout the whole-body rather than specifically targeted to the

liver and so were shown in this study to also affect lipid accumulation and insulin sensitivity in skeletal muscle¹²⁶. Thus, it remains unclear whether increased liver lipogenesis is sufficient to drive NAFLD and whole-body insulin resistance or glucose intolerance.

1.2.2 Evidence linking lipogenesis to fatty liver and the role of ACC enzymes

Liver lipid accumulation occurs by several mechanisms including 1) increased uptake of exogenous lipid, 2) decreased export of triglyceride, 3) decreased oxidation of stored lipid, and 4) increased *de novo* synthesis of lipid¹²⁷. While *de novo* lipogenesis contributes only 5% of stored liver lipids in normal fasted conditions¹²⁸, enhanced lipogenesis is the single greatest contributor to liver lipid accumulation in patients with NAFLD, accounting for as much as 26% of liver lipids even in the fasted state¹²⁹. In a study by Diraison, et al.¹³⁰, *de novo* synthesized lipids increased more than 3-fold in patients with NAFLD compared to controls, whereas re-esterification of exogenous free fatty acids was decreased, and no significant differences were detected in fat oxidation or triglyceride export. Most NAFLD patients also have elevated blood glucose and/or insulin, which both promote expression of the ACC enzymes, potentially linking poor diet and obesity to development of NAFLD. ACC expression is increased in livers of patients with NAFLD^{131,132}, as well as levels of oleate (18:1n9)¹³³, which is a product of lipogenesis⁸⁶. Although these studies implicate a role for lipogenesis and the ACC enzymes, it is not clear whether hepatic lipogenesis is causal in NAFLD and/or glucose intolerance. It has been proposed that inhibiting liver lipogenesis would decrease liver fat

accumulation and improve whole-body glucose tolerance in the context of NAFLD, although sufficient *in vivo* studies in this area are lacking.

1.2.3 Review of studies that have targeted liver lipogenesis

Testing the role of liver lipogenesis in whole-body and liver physiology has proven challenging. Lipogenesis is necessary during embryonic development, as constitutive deletion of ACC1 or FASN is embryonic lethal^{134,135}. Liver-specific ACC1 knockout mice were successfully generated by using *loxP* sequences to delete *Acc1* driven by hepatocyte-specific Cre recombinase^{136,137}. Although these mice completely lacked liver ACC1 expression, ACC2 expression increased^{136,137} and, interestingly, these hepatocytes were capable of lipogenesis to a similar extent as wild-type hepatocytes. Lipogenesis in ACC1-null hepatocytes was blocked by administration of a pharmacological pan-ACC inhibitor¹³⁶. This demonstrates that, although ACC1 is normally associated with lipogenesis, there is not a strict cytosolic-specific pool of malonyl-CoA, and ACC2 is capable of compensating for the lipogenic activity of ACC1 in its absence. In another study, antisense oligonucleotides (ASOs) against ACC1 and ACC2 administered to rats by tailvein injection decreased liver ACC1 and ACC2 protein expression by 80%, decreased liver triglyceride levels, and improved insulin sensitivity¹³⁸. A major caveat to this study is that the ASOs were not specifically administered to the liver, and ACC expression was also decreased in adipose tissue to the same extent as the liver. In the only study to-date to achieve liver-specific inhibition of lipogenesis, FASN, which is the enzyme downstream of ACC that converts malonyl-CoA to fatty acid, was deleted specifically in mouse hepatocytes. Paradoxically, liver-specific

deletion of FASN caused an increase in liver fat storage when mice were fasted or fed a fat-free diet for 4 days, as a result of decreased mitochondrial fat oxidation⁹⁸. Lack of *de novo* synthesized fatty acids reduces expression of PPAR α target genes in the liver, including those involved in mitochondrial fat oxidation⁹⁸, indicating that *de novo* synthesized fats are important PPAR α ligands. Taken together, the role of liver lipogenesis and ACC activity in NAFLD and glucose intolerance has not been fully elucidated with existing models.

1.3 Acetyl-CoA carboxylases in the context of liver cancer

1.3.1 Epidemiology of liver cancer

Liver cancer is the fifth most-common cancer in men and the ninth most-common in women, accounting for 7.5% and 3.4% of all cancers worldwide in men and women, respectively¹³⁹. Hepatocellular carcinoma (HCC) is the most common liver malignancy and represents 85-90% of liver cancer cases¹⁴⁰. Rates of HCC incidence are approximately 2-fold higher in men compared to women, such that cumulative lifetime risk of HCC is 0.88% in men and 0.42% in women¹⁴¹.

Incidence of HCC is highest in developing countries (including Eastern and South-Eastern Asia, and Northern and Western Africa) with an average age of diagnosis of 20 years, most likely due to higher incidence of chronic hepatitis virus infection¹⁴¹. HCC incidence in these countries is decreasing, however, with the introduction of vaccines against Hepatitis B infection. While incidence in developed countries (including North America, Europe, and Australia) is lower in comparison with underdeveloped countries¹³⁹, rates are increasing in developed countries in recent decades with an average age of diagnosis of 50 years¹⁴¹. In the United States, rates of HCC incidence have more than tripled between the years 1975 and 2011¹³⁹.

HCC is a highly lethal disease, with a yearly fatality ratio of 1, meaning that most patients do not survive a year¹⁴¹. In the US, HCC 5-year survival rate is 8.3%, and HCC is inevitably fatal in underdeveloped countries. HCC is the second-highest cause of cancer-related death in men and the sixth-highest in women worldwide. HCC accounts for 11.2% and 6.3% of total cancer-related deaths in men and women, respectively¹³⁹.

1.3.2 Overview of current detection and treatment strategies for liver cancer

Early detection of HCC is necessary for optimistic patient prognosis. While methods for detecting HCC have vastly improved in recent years, survival after diagnosis remains bleak, indicating room for improvement in HCC screening and detection. For decades, alphafetoprotein (AFP) has been used as a serum marker for HCC. AFP is a glycoprotein normally produced in fetal liver. Its expression is repressed in the adult liver but re-expression occurs in many HCC cases. However, it is increasingly apparent that AFP is not ideally specific for HCC, as it can be highly elevated in chronic inflammatory liver disease even in the absence of HCC. A more troubling problem with using AFP as a screening tool for HCC is that it is not adequately sensitive, detecting approximately only 40% of HCC cases^{142,143}. AFP does, however, have prognostic value, as tumors associated with serum AFP value of greater than 100 ng/mL are more likely to be multifocal and invasive¹⁴³.

Due to the lack of a specific and sensitive serum screening tool, currently the most reliable method for HCC detection is imaging. While abdominal imaging techniques have advanced considerably in recent years to allow more sensitive liver tumor detection, it remains a challenge to detect tumors smaller than 2 cm in diameter. Magnetic resonance imaging is the most sensitive imaging tool, as it identifies almost 80% of tumors, including 63% of tumors less than 2 cm. However, due to challenges in detecting small tumors, most HCC cases are not diagnosed until later stages. For many types of cancer, positron emission tomography (PET) using ¹⁸F-fluoro-2-deoxyglucose (¹⁸F-FDG)

is a reasonably specific and sensitive imaging tool for tumors in contrast to surrounding non-tumor tissue. However, less than 50% of HCC cases are detected using this method. ^{11}C -acetate is more specific and sensitive for HCC compared to ^{18}F -FDG¹⁴⁴, likely due to a propensity for HCC to utilize acetate as a lipogenic substrate (discussed further in the following section *1.3.4 Evidence for roles of lipogenesis and ACC enzymes in liver cancer*).

Detection of a tumor by imaging is often sufficient for designing an informed treatment plan, but a tumor biopsy is performed if the tumor grade will influence the treatment approach. Early grade HCC is pathologically characterized by well-differentiated cells with increased cell density and hyperplasia compared to surrounding areas and a thin irregular trabecular pattern. Progressed grade HCC takes on a nodule-in-nodule appearance, pathologically characterized by cell undifferentiation and enlargement, large trabecular structures, and invasiveness¹⁴⁵. In addition to expert pathological analysis, the biopsy is often evaluated by immunohistochemistry for glypican 3, heat shock protein 70, and glutamine synthetase, as positivity for all 3 of these stains confirms HCC¹⁴⁶.

After diagnosis, staging of HCC for determining a treatment strategy is a complex matter because HCC commonly occurs in the setting of underlying fibrotic liver disease that may have a significant impact on prognosis and treatment. The system most commonly used by clinicians and in clinical trials to treat HCC is the Barcelona Clinic Liver Cancer classification scheme¹⁴⁶. Accordingly, HCC patients are eligible for liver resection if there is no severe underlying liver disease as assessed by measurements of

portal vein pressure and serum bilirubin levels, and if the HCC is in a very early stage, defined by only one liver tumor less than 2 cm that has not invaded into the vasculature or metastasized to a distant site. If HCC is still in an early stage, defined by a single tumor less than 3 cm and no invasion into the hepatic portal vein, but portal pressure or bilirubin is elevated, a liver transplantation is recommended. Liver transplantation in the setting of hepatitis-related liver fibrosis is associated with diminished patient survival and it is very likely that fibrosis and HCC will recur in the transplanted liver¹⁴⁷⁻¹⁵¹. Therefore, if the HCC is in an early stage but associated diseases such as hepatitis infection and fibrosis are present, radiofrequency (RFA) ablation is recommended. Liver resection, transplantation, or RFA are considered potentially curative treatments¹⁴⁶.

Unfortunately, most HCC patients are not eligible for these curative treatments due to late-stage HCC diagnosis or underlying disease and are left with only palliative treatment options. For example, if HCC is in an intermediate stage, defined by the presence of multiple tumor nodes, then treatment by transarterial chemoembolization (TACE) is recommended. This method involves catheterization of the hepatic artery and local delivery of a chemotherapeutic agent, typically doxorubicin or cisplatin¹⁵². In a large 8510 patient study, 1-year survival for patients with unresectable HCC treated with TACE was 82%¹⁵³, showing a benefit for many patients who qualify for this treatment, although a cure is rarely achieved. If the HCC has progressed to advanced stage, defined by invasion of the tumor cells into the hepatic portal vein, then the standard of care is Sorafenib, which is a small molecule inhibitor with activity against multiple kinases including Raf-1, B-Raf, vascular endothelial growth factor receptor 2, and platelet-

derived growth factor receptor. Sorafenib is the only systemic therapy approved for advanced stage HCC, but only a minority of patients are responsive and it extends patient lifespan in aggregate by only months¹⁵⁴. The most common cause of death among HCC patients is liver failure caused by uncontrolled tumor progression¹⁵⁵.

1.3.3 Environmental and genetic etiology of liver cancer

Risk of HCC is highly linked to environmental factors including hepatitis infection, aflatoxin exposure, excess alcohol consumption, obesity, and NAFLD^{140,156}. In humans, development of HCC is a gradual process that can take as long as 30 years to manifest after an initial insult. While it is clear that liver disease follows a typical progression from steatosis to cirrhosis to preneoplastic hepatocyte dysplasia to HCC¹⁵⁷, the genetic programs driving this process are not well understood. Many of the alterations in gene expression during the preneoplastic phase of HCC occur by epigenetic mechanisms in the absence of genetic mutations. For example, increased expression of hepatocyte growth and inflammatory factors are a common feature of cirrhosis and preneoplasia, and are thought to be important for early hepatocyte proliferation^{158,159}. Although these epigenetic alterations are not sufficient for malignancy, they create conditions which increase the stochastic likelihood of generating hepatocyte populations that have a critical combination of genetic mutations that drive cancerous transformation. Erosion of telomeres, which may occur in highly proliferative hepatocytes, produces mitotic non-disjunction and chromosome disruption^{160,161}. Additionally, oxidative and nitrosative damage to the genomic DNA, which occurs in the setting of chronic liver inflammation and cirrhosis, leads to genetic mutations if not properly repaired¹⁶².

The genetic profile of HCC is quite heterogeneous, in most cases containing structural alterations in many genes and chromosomes which may simultaneously affect gene expression across multiple pathways regulating proliferation, death, differentiation, and genomic integrity¹⁶³. Although DNA damage and resulting mutations may occur at random, it is reasonable to speculate that particular clonal populations have a survival and proliferative advantage during tumor formation. Studies supporting this theory have identified some commonalities in genetic signatures across HCC. The most common oncogene driver observed in HCC is activation of β -catenin, which can occur by activating mutations in β -catenin or deletion of negative regulators of β -catenin¹⁶⁴⁻¹⁶⁷. TP53 is a frequently mutated tumor suppressor in HCC¹⁶⁴⁻¹⁶⁷; however TP53 is only a weak tumor suppressor in a mouse model of HCC¹⁶⁸, highlighting cooperation with other stress regulators and tumor suppressors. Mutations in *Arid1A* and *Arid2*, which remodel chromatin, are also prevalent in HCC. Other observations include frequent loss of cell cycle regulatory genes such as *ATM* and *MLH1*, and mutations in epigenetic regulators such as *MLL3* and *MLL*¹⁶⁴⁻¹⁶⁷. One study identified enrichment of positive regulators of cell cycle including *CDK4*, *CDC25A*, *CDC7* and *MAPK3*¹⁶⁹ to be associated with poor-prognosis HCC. Interpretation of these findings is confounded by the relatively small number of HCC tumors that have been sequenced to date (approximately 100, compared to >1000 in many other types of cancer)¹⁶³. Most investigators are in agreement that the most striking finding from sequencing thus far is the overall complex heterogeneity across HCC cases.

Which genes are critical drivers of HCC or merely bystanders remains to be defined; however, some progress has been made in understanding the molecular mechanisms of HCC by utilizing mouse models. The most commonly used model of HCC is treatment of neonates with the chemical carcinogen diethylnitrosamine (DEN). DEN is a prodrug that is converted to its active form when metabolized by liver CYP450 enzymes. Activated DEN causes both nitrosative and oxidative DNA damage, which lead to genetic mutations and tumor outgrowth with a latency of 5 to 10 months¹⁷⁰. Tumors induced by DEN reflect the genetic heterogeneity of human HCC and genetically resemble poor-prognosis HCC¹⁶⁹. The sexual dimorphism of HCC is also recapitulated in the DEN model, with females being more resistant to developing tumors. This difference has been attributed to the stimulating effects of androgens on liver cancer through Foxa1 and Foxa2¹⁷¹; however, the exact mechanisms leading to increased HCC in response to androgens have not been clarified. Other chemical models include feeding aflatoxin or peroxisome proliferators or administration of carbon tetrachloride. These models have relatively long latency, ranging from 12 to 24 months¹⁷⁰. Alternatively, implantation models have much shorter latency, producing tumors in a matter of days to weeks. However, these models have been proven inadequate for HCC research because they fail to fully interact with the unique inflammatory and regenerative nature of the liver¹⁷². Therefore, chemical models are favored in HCC research because they mimic the process of random DNA injury, inflammation, cell hyperproliferation, malignant cell selection, and tumor outgrowth that is characteristic of human HCC.

Genetically engineered mouse models (GEMMs) are vital tools for understanding roles of individual proteins in liver tumor etiology. Using GEMMs, liver oncogenes sufficient to cause liver neoplasia have been identified including Hepatitis B surface antigen, SV40, c-Myc and H-Ras¹⁷³⁻¹⁷⁶. Additionally, liver tumor suppressors that have been identified include Rb, TP53 and PTEN¹⁷⁴. Because the genetic profile of human HCC is exceptionally diverse, GEMMs may not recapitulate HCC as authentically as the chemical models discussed. However, GEMMs have been combined with chemical models in order to better understand the roles of particular proteins within the complex setting of HCC.

Studies using the DEN model of liver cancer, in some cases combined with GEMMs, have provided some valuable insight into mechanisms of HCC initiation and progression. One major advancement was determining the cell type of origin in HCC. Hepatocytes are unique from many other differentiated cell types in that they have a robust regenerative capacity. It had been known for several decades that both hepatocytes and liver progenitor cells are able to proliferate in order to restore damaged liver tissue, such as after a partial hepatectomy¹⁷⁷; however, it was not clear whether hepatocellular carcinoma arose from liver progenitor cells or from differentiated hepatocytes. To resolve this question, Bratlet et al. (2002)¹⁷⁸ used two different strategies to label hepatic cells: (a) inducing liver cell proliferation by feeding rats with 2-acetylaminofluorene (2-AAF) which stimulates oval cell proliferation and suppresses hepatocyte proliferation and labeling proliferating cells by retrovirus infection with beta-galactosidase; and (b) performing a partial hepatectomy to stimulate replication of mature hepatocytes, followed

by infection of proliferating cells with retrovirus containing the β -galactosidase before 2-AAF feeding. Using the second strategy, the authors were able to demonstrate selective hepatocyte labeling. Mice were then treated with DEN and, after disease onset, tumors were removed from the liver and inspected for expression of β -galactosidase. The authors observed that the tumor cells expressed β -galactosidase, indicating that they were of hepatocyte origin¹⁷⁸. This study has had a major impact in the field by placing hepatocyte physiology at the center of HCC research.

It had been recognized that inflammation may act as a tumor promoter in a small subset of human cancers, but a role for inflammation in etiology for HCC was not appreciated until Maeda et al. (2005)¹⁷⁹ demonstrated that inflammation was an important mechanism in DEN-induced tumorigenesis. In this study, inactivation of hepatocyte NF- κ B, a transcription factor which promotes expression of inflammatory cytokines, increased cell death in response to DEN. Hepatocyte death signaled to resident liver macrophages (Kupffer cells) to increase inflammatory cytokine production, ultimately increasing proliferation of surviving cells and increasing the likelihood of tumor development. This process of compensatory hyperproliferation is thought to be highly relevant in human HCC.

Because environmental factors have such a heavy influence on HCC risk, there has been considerable effort to understand their roles in HCC initiation and progression. For example, obesity has been identified as a significant risk factor for both HCC incidence and mortality in multiple epidemiological studies¹⁸⁰⁻¹⁸². The increasing prevalence of obesity in developed countries may at least partially explain the recent

increase in HCC incidence. In order to better understand the molecular mechanisms contributing to liver cancer risk in the context of obesity, Park et al. (2010)¹⁸³ fed DEN-treated mice with an obesigenic Western diet, which is high in fat and sugar. Remarkably, mice fed the Western diet developed significantly more tumor than normal chow-fed controls. While tumor incidence in males was relatively high regardless of diet (85 to 100%), males fed the Western diet had more and larger liver tumors. As expected, females fed normal chow had lower tumor incidence than males (40%), but females fed the Western diet had a 2-fold increase in tumor incidence (80%). Genetic deletion of the IL-6 or TNF receptor genes partially attenuated DEN-induced liver tumor development in mice fed the Western diet¹⁸³, implicating these inflammatory cytokines in promoting liver cancer in the context of an obesigenic diet. However, whether obesity *per se*, an obesity-related disorder such as fatty liver or hyperinsulinemia, and/or a diet component such as high fat or high sugar was the major driver of liver tumor is not clear. Another study to investigate the links between obesity and liver tumor was by Yashimoto et al. (2013)¹⁸⁴. The authors showed that a Western diet altered the gut microbiome, causing an increase in deoxycholic acid (DCA), a bile acid which is known to be secreted from gut microbiota¹⁸⁵. DCA caused an inflammatory response in the liver and promoted liver tumor induced by the chemical carcinogen dimethylbenzanthracene (DNBA), which could be partially attenuated by administration of antibiotics or knockout of IL-1 β ¹⁸⁴. Interestingly, DCA administration to DNBA-treated mice fed a normal chow diet was not sufficient to induce significant liver tumor, implicating another obesity- or diet-associated factor as a culprit in HCC promotion.

In summary, little is currently known about the molecular etiology of HCC or interactions between environmental factors and liver tumor development. Mechanistic studies investigating the relationship between HCC and environmental factors such as hepatitis infection, aflatoxin exposure, alcohol consumption, poor diet, or fatty liver are lacking. Therefore, continued investigation in the area is crucial for developing new preventive and therapeutic strategies for HCC.

1.3.4 Evidence of roles for lipogenesis and ACC enzymes in liver cancer

A hallmark of cancerous cells is alterations in metabolism which promote survival, proliferation, and metastasis. The most extensively characterized metabolic phenotype of cancer cells is increased aerobic glycolysis, coined the “Warburg effect” after Dr. Otto Warburg who first described this phenomenon in the 1920s¹⁸⁶. The Warburg effect is marked by increased glucose uptake and conversion to lactate in the cytosol rather than conversion to pyruvate in the mitochondria, even in the presence of ample oxygen. Further studies since this initial observation have expounded on the relevance of the Warburg effect to tumor metabolism. The Warburg effect is now considered to be advantageous for cancer because it promotes survival in hypoxic conditions of the tumor microenvironment, the lactate produced may assist in degrading extracellular matrix to allow tumor metastasis to areas of higher oxygen and nutrient availability, and pathways stemming from glycolysis synthesize materials to support rapid cell growth and proliferation¹⁸⁷. For example, glucose which enters glycolysis can be diverted to the PPP for production of the reductive molecule NADPH which is used

for antioxidant defense and biosynthetic processes such as lipid synthesis, as well as production of nucleotides and amino acids which are used for DNA repair and as building blocks for new cells¹⁸⁸.

Glycolysis also supplies glucose precursors that are incorporated into lipids via lipogenesis. Although less characterized than glycolysis in the context of cancer metabolism, upregulation of lipogenesis is similarly observed in cancer¹⁸⁹, including HCC, despite its characteristic genetic heterogeneity. In a study by Yahagi, et al.¹⁹⁰, all ten patients examined had increased expression of ACC1 in tumor tissue compared to surrounding liver tissue. Moreover, the extent of lipogenic enzyme expression in liver tumor has been correlated with increased clinical aggressiveness¹⁹¹ and poorer patient survival¹⁹². Genetic inhibition of ACC1 caused growth inhibition and apoptosis in the HCC cell line HuH¹⁹¹. Several theories exist for why lipogenesis is important for cancer cell survival and proliferation even in the presence of ample exogenous fatty acids; these include: (a) lipogenesis-derived phospholipids can be incorporated into new membranes to support rapid cell proliferation, whereas exogenous lipids are preferentially stored or oxidized⁸⁷; (b) lipogenesis produces saturated lipids which preferentially form lipid rafts to facilitate cancer cell growth factor signaling^{193–196}; and (c) saturated lipids produced by lipogenesis are less susceptible to peroxidation and therefore cause less cancer cell toxicity¹⁹⁷. For these reasons, there is considerable interest in targeting lipogenesis for prevention or treatment of HCC; however, the role of lipogenesis in cancer is poorly understood, and inhibition of lipogenesis in the context of liver cancer remains to be tested *in vivo*.

**CHAPTER 2: EFFECTS OF GENETIC INHIBITION OF LIVER ACETYL-COA
CARBOXYLASES ON WHOLE-BODY AND LIVER METABOLISM**

2.1 Use of liver-specific ACC1 and ACC2 double knockout mice to define how loss of liver ACC activity affects normal liver and whole-body physiology in mice fed a normal chow diet

2.1.1 Background

Both ACC isotypes are susceptible to dysregulation and are commonly over-expressed or over-activated in disease states associated with fatty liver^{109,132,190,198}. Simple hepatosteatosis alone is thought to have a benign course^{109,198}, but up to 25% of patients progress to advanced diseases¹⁰⁹. Fatty liver disease is a risk factor for insulin resistance, diabetes, and hepatocellular cancer. Thus, there is considerable interest in developing small molecule drugs that inhibit ACC enzymes^{199,200}. Recently, it was shown that chronic activation of ACC enzymes in mice is sufficient to increase hepatic fat accumulation¹²⁶; however, it remains unclear how the complete and chronic inhibition of ACC activity will impact liver lipid content, whole body metabolic physiology, or the metabolic fate of cytosolic acetyl-CoA in hepatocytes. To investigate these questions, we generated and characterized liver-specific ACC1 and ACC2 double knockout mice.

2.1.2 Increased hepatic triglyceride accumulation in the absence of ACC activity

Other groups have reported single gene knockout of either ACC1 or ACC2 individually in mice^{136,137,201,202}. However, no studies have genetically knocked out both ACC enzymes specifically in mouse liver. In this study we generated liver-specific ACC1 and ACC2 double knockout (LDKO) mice, as follows. ACC1 and ACC2 floxed mice were bred with mice expressing Cre under the control of a liver-specific albumin promoter. Knockout was confirmed at the mRNA and protein levels in liver tissue

(Figure 5A and B). To verify that ACC enzymatic activity was deficient in the liver, we isolated primary hepatocytes from LDKO and flox control (Flox) mice and tested their capacity to utilize ^{14}C -acetate (a cell-permeable precursor to cytosolic acetyl-CoA) for lipogenesis. Hepatocytes from LDKO mice were completely deficient in lipogenic conversion of acetate into lipid, but were fully capable of synthesizing sterols from this substrate (Figure 5C). The utilization of ^{14}C -acetate for sterol synthesis was expected because this process does not require ACC activity. Compared to Flox controls, LDKO mice had similar body weight and adiposity (Figure 6), and had normal energy expenditure and respiratory quotient in both fed and fasted states (Figure 7). The LDKO mice also demonstrated normal responses to metabolic challenges with a bolus injection of glucose, pyruvate, or insulin (Figure 5D and F). LDKO mice had similar serum glucose, insulin, free fatty acid, and triglyceride levels to Flox controls in both the fed and fasted states, but had 22% less ($p < 0.05$) serum cholesterol in the fasted state (Table 1). Hepatocytes and liver tissue demonstrated normal insulin stimulation of Akt (Figure 9). Together, these data demonstrate that loss of ACC activity in the liver does not adversely affect whole body nutrient handling or insulin sensitivity. However, we did find that LDKO liver mass was increased (Figure 5G) concomitant with increased triglyceride content (Figure 5H). Histological analysis of liver tissue by Oil-red-O and H&E staining revealed that LDKO hepatocytes accumulated microvesicular fat (Figure 5I), a phenotype normally associated with a defect in fat oxidation²⁰³. ACC enzymes normally function to promote fat storage; therefore, the finding that ACC deletion increases basal liver fat accumulation was unexpected.

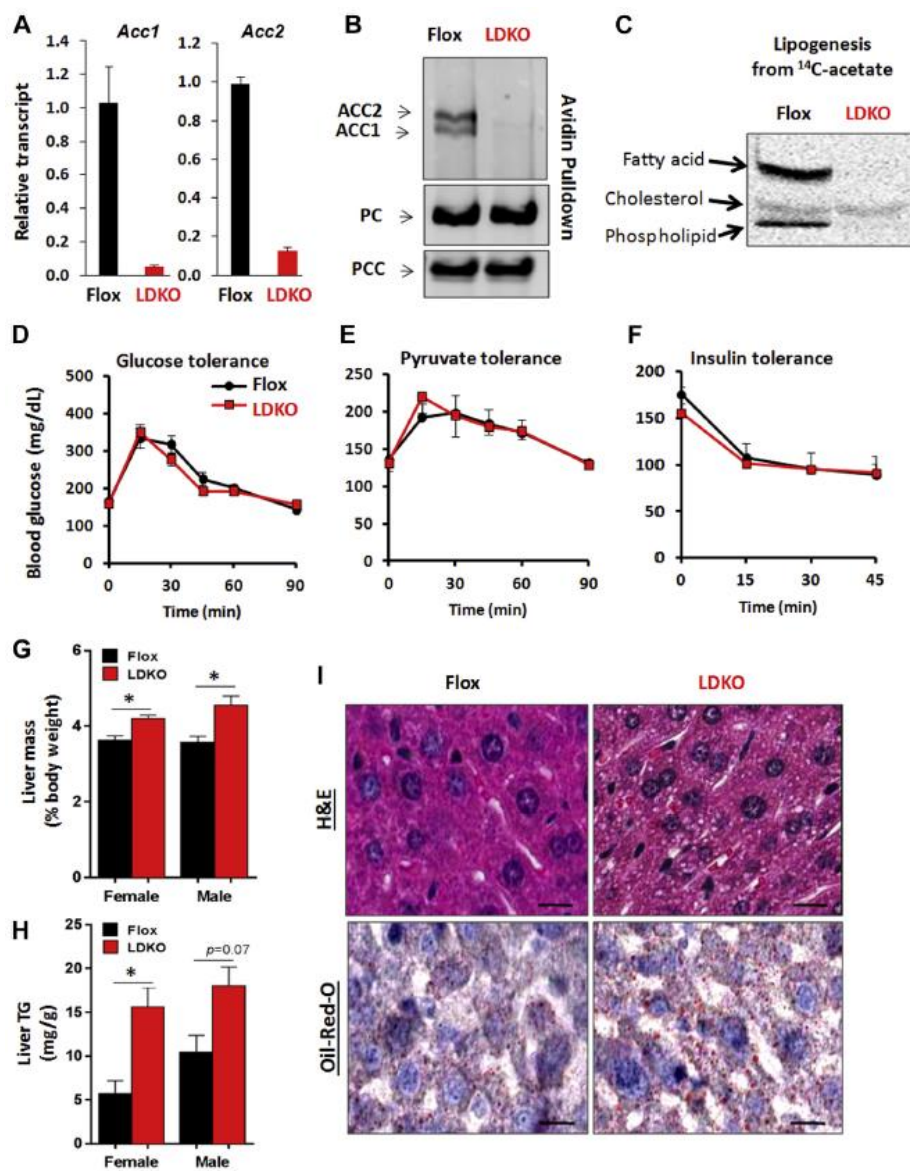


Figure 5. Loss of hepatic ACC activity increases fat storage.

A) Liver *Acc1* and *Acc2* mRNA transcripts quantified by qPCR in Flox control and LDKO mice ($p < 0.0001$, $n=10$, Mann-Whitney). (B) Avidin-bead pulldown with immunoblotting for ACC enzymes in liver lysates from flox and liver-specific ACC1 and ACC2 knockout (LDKO) mice, with pyruvate carboxylase (PC) and propionyl-CoA carboxylase (PCC) enzymes serving as protein loading controls. (C) Incorporation of ^{14}C -acetate into fatty acids and sterols in primary hepatocytes. (D-F) Glucose, pyruvate and insulin tolerance tests (D and E, $n=5$; F, $n=3$). (G) Liver to body weight percentage and (H) triglyceride content of Flox and LDKO mice (female LDKO ($n=8$) and Flox ($n=5$), male LDKO ($n=5$) and Flox ($n=3$); $*p < 0.05$, Mann-Whitney.). Data expressed as mean \pm SEM. (I) Representative liver sections stained with hematoxylin and eosin (H&E) and Oil-Red-O; Scale bars = 100 μm .

Table 1. Serum parameters of fed or 12 h-fasted LDKO and Flox mice

	Fed		Fasted	
	Flox	LDKO	Flox	LDKO
Triglyceride (mg/dL)	204.5 ± 28.8 (9)	233.8 ± 27.0 (10)	156.0 ± 12.9 (9)	136.3 ± 5.0 (11)
Cholesterol (mg/dL)	91.4 ± 6.7 (9)	71.9 ± 5.4 (10)	93.6 ± 6.0 (9)	73.5 ± 3.7 (11)
Free fatty acid (mM)	0.92 ± 0.11 (9)	0.87 ± 0.09 (10)	1.40 ± 0.15 (9)	1.15 ± 0.12 (11)
Glucose (mg/dL)	170.8 ± 18.5 (6)	171.3 ± 22.9 (4)	124.9 ± 7.6 (17)	144.5 ± 7.9 (17)
Insulin (ng/ml)	0.97 ± 0.12	1.34 ± 0.27	0.42 ± 0.08	0.51 ± 0.11

Data expressed as mean ± SEM. * Significant difference ($p < 0.05$) between Flox vs. LDKO of same condition (fed or fasted). Parentheses indicate the number of mice per group.

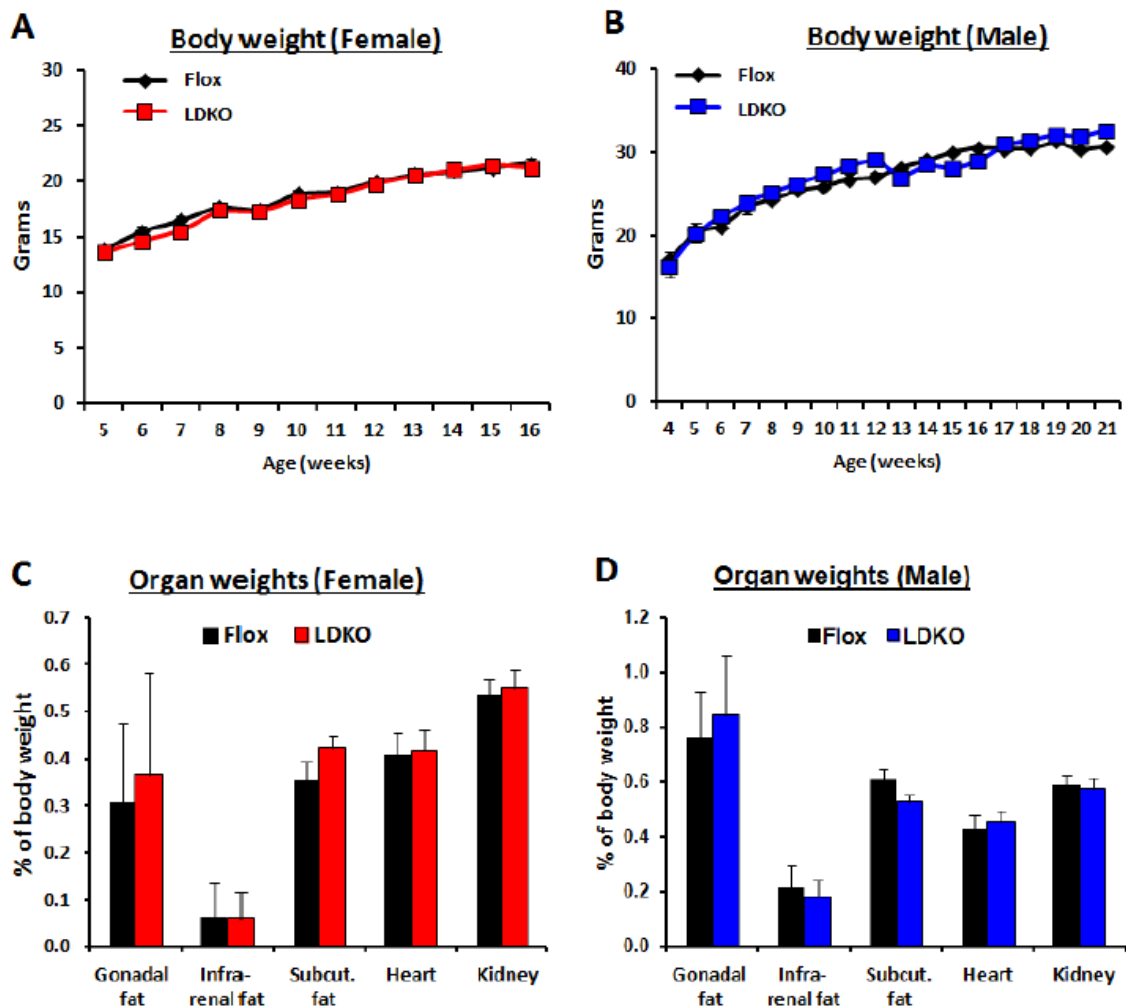


Figure 6. Body weight and organ mass.

A and C) Female body weight ($n > 6$) and organ weights ($n = 5$ Flox, $n = 8$ LDKO), and (B and D) male body weight ($n > 6$) and organ weights ($n = 5$ Flox, $n = 9$ LDKO). Data expressed as mean \pm SEM.

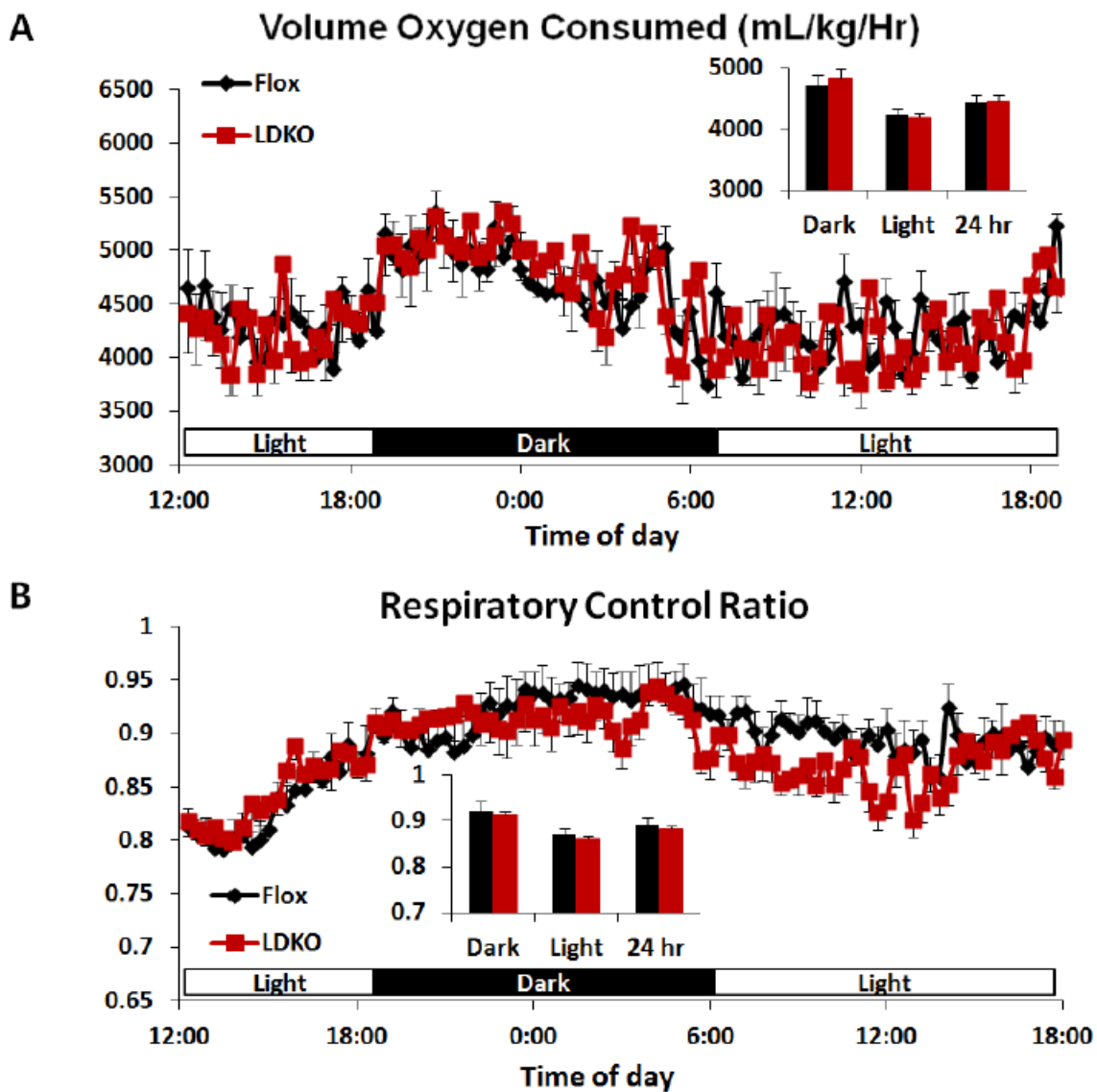


Figure 7. Diurnal respirometry.

Indirect calorimetry was used to determine (A) VO_2 and (B) RER in 22 week-old female Flox and LDKO mice at the fed state. Data expressed as mean \pm SEM (n=8).

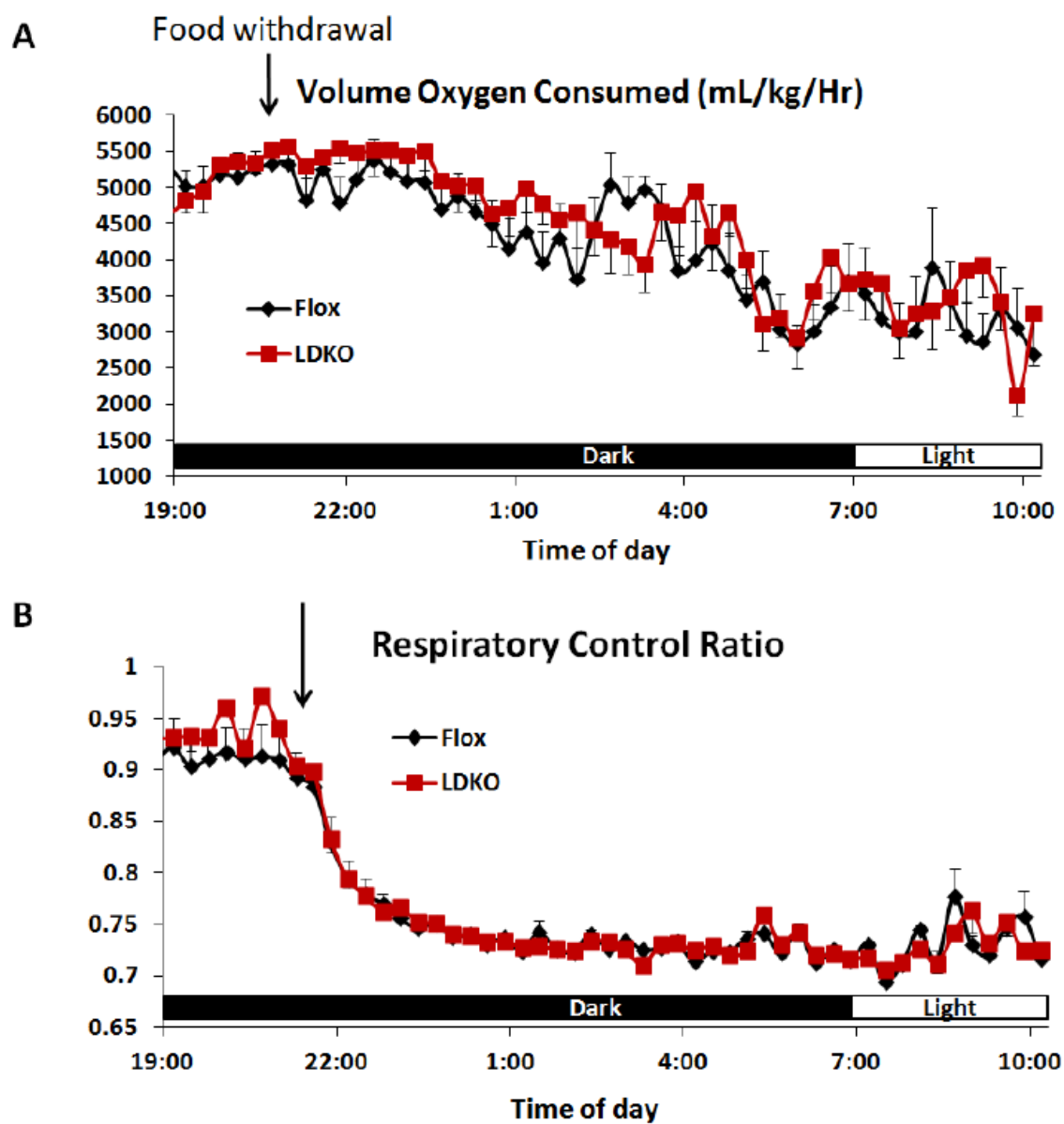


Figure 8. Respirometry changes in response to fasting.

Indirect calorimetry measurements were used to determine (A) VO_2 and (B) RER in 22 week-old female Flox and LDKO mice at the fasted state. Data expressed as mean \pm SEM (n=4).

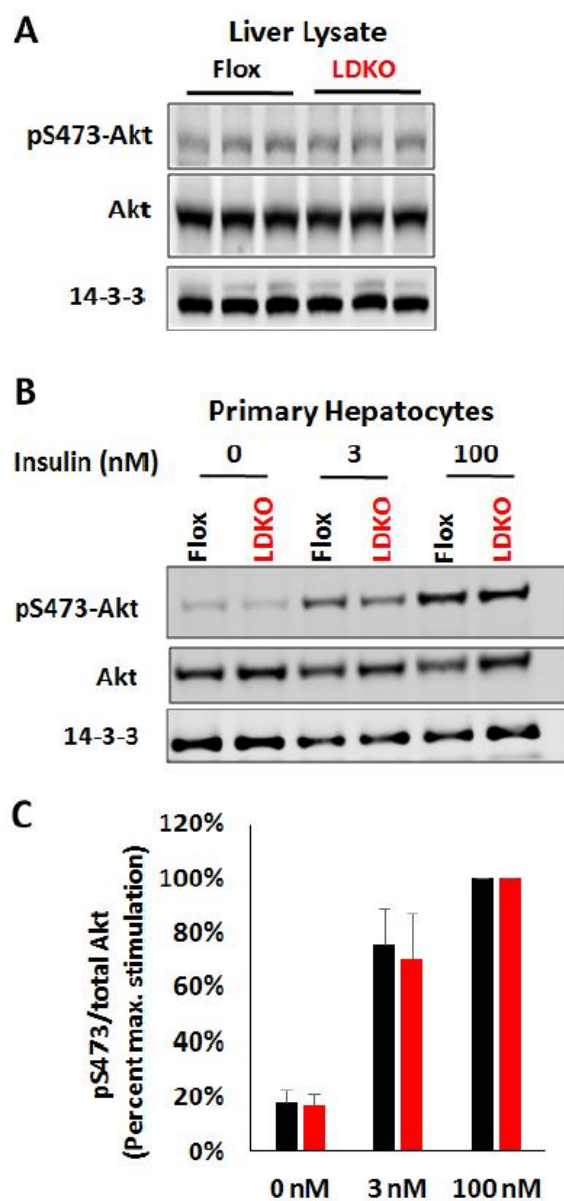


Figure 9. Insulin signaling through Akt.

A) Western blot analysis of Akt phosphorylation in liver tissue from LDKO and Flox mice (n=3 mice). (B) Representative Western blot of whole cell lysates from primary hepatocytes stimulated with 3 or 100 nM insulin for 10 min. (C) Quantification of phospho-Akt/total Akt from (B) (n=4-5). Data expressed as mean \pm SEM.

2.1.3 ACC inhibition paradoxically suppresses fatty acid oxidation

Hepatic fat accumulation can be caused by numerous mechanisms including defective lipid export, increased lipid intake, increased lipid synthesis, or decreased fat oxidation. Lipid synthesis can be ruled out (Figure 5C); therefore, we measured triglyceride export from the liver, the clearance of triglyceride after a bolus oral gavage of safflower oil, and the oxidation of the saturated fatty acid palmitate (Figure 10A and C). The rate of lipid efflux from the liver was measured by treating LDKO and Flox mice with the lipoprotein lipase inhibitor, Poloxamer 407, and monitoring serum triglyceride accumulation over time (Figure 10A). LDKO mice had greater rates of triglyceride export from the liver compared to Flox control mice (Figure 10A), thus indicating the increase in hepatic fat in LDKO mice was not due to impaired lipid efflux from the liver. We next challenged LDKO and Flox mice with an oral bolus of safflower oil and measured triglyceride appearance and clearance from the serum. This experiment showed that LDKO mice had normal uptake and clearance of lipid (Figure 10B). Finally, we measured fatty acid oxidation in LDKO and Flox primary hepatocytes using ^{14}C -palmitate. This experiment revealed that LDKO hepatocytes had a significant decrease in fatty acid oxidation compared to Flox controls (48% decrease, $p < 10^{-4}$, Figure 10C). The mechanism(s) of reduced fat oxidation were investigated in more detail by assaying the activity of key enzymes in the mitochondrial and peroxisomal fatty acid oxidation pathways in liver lysates. Compared to Flox control tissue, LDKO liver lysates had decreased activity of mitochondrial 3-hydroxyacyl-CoA dehydrogenase (β -HAD, $p=0.002$), mitochondrial medium-chain acyl-CoA dehydrogenase (MCAD, $p=0.07$), and

peroxisomal acyl-CoA oxidase (ACOX, $p=0.002$) (Figure 10D-F). The LDKO liver tissue also had lower mRNA and protein expression of CPT1a; the rate-limiting enzyme in mitochondrial fat oxidation (Figure 10G and H). Furthermore, LDKO mice showed a trend for impaired fasting-induced ketone production; an indirect marker of hepatic fat oxidation in vivo (Figure 10I). To determine whether the decrease in fat oxidation was compensated by altered glucose utilization, as predicted by the Randle cycle²⁰⁴, we measured the rate of glycolysis in isolated primary hepatocytes from LDKO and Flox mice. These data revealed a 40% increase in glycolysis in LDKO hepatocytes compared to Flox controls (Figure 10J). Collectively, these data identify that inhibition of ACC enzymes leads to reprogramming of hepatic glucose and fatty acid metabolism that resembles the chronic fed state.

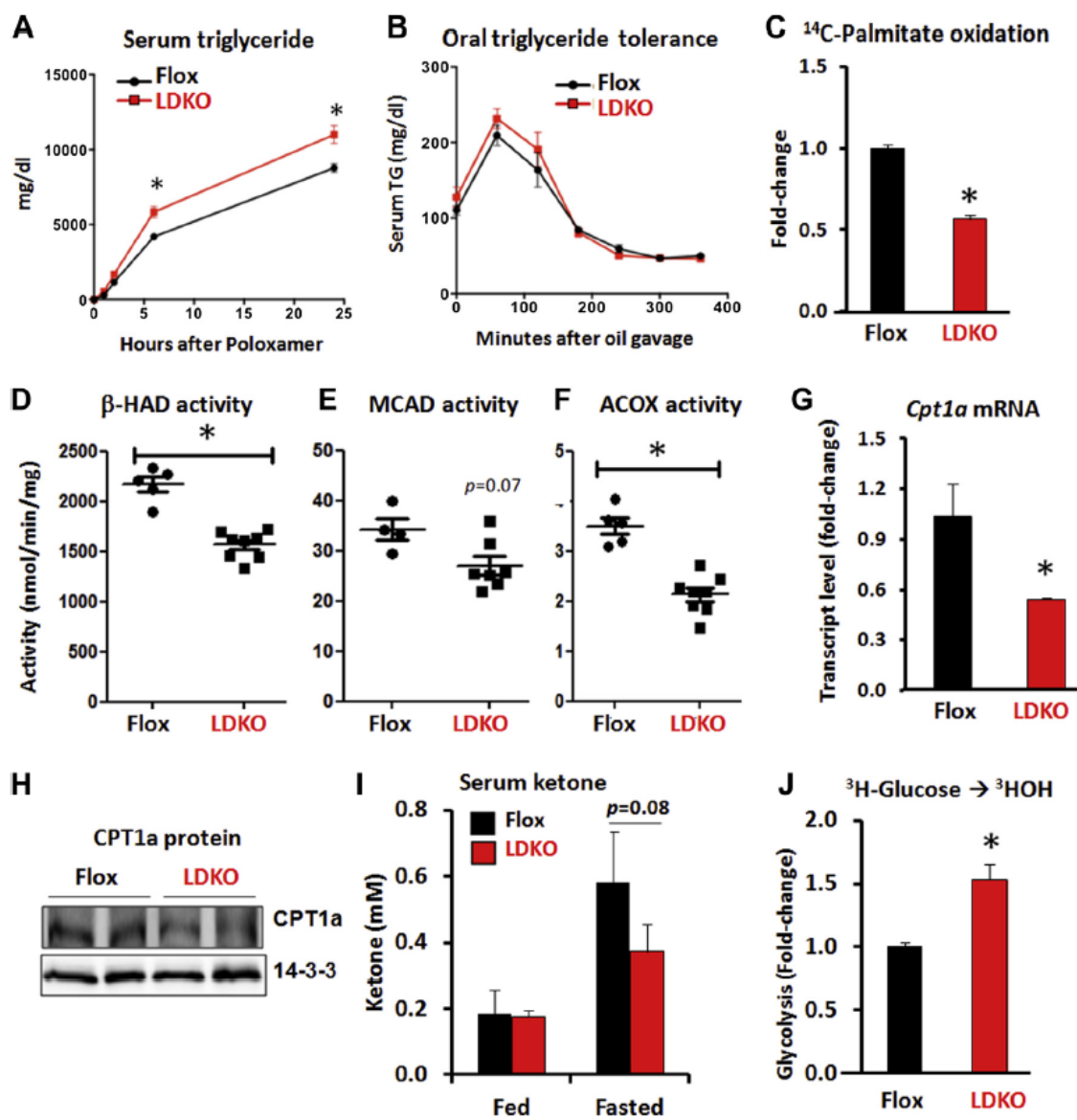


Figure 10. The loss of ACC decreases hepatic fat oxidation.

A) Hepatic triglyceride production assessed by serum triglyceride levels at time points after i.p. treatment of 1 g/kg lipoprotein lipase inhibitor, Poloxamer 407 (n=5 LDKO, n=4 Flox). (B) Oral triglyceride tolerance assessed by serum triglyceride levels at various time points after a bolus of safflower oil (n=5). Data expressed as mean SEM; *p < 0.0001, multiple unpaired t-test with correction using Holm-Sidak method. (C) Rate of palmitate oxidation in isolated primary hepatocytes (*p < 0.001, Mann-Whitney, seven independent experiments). Enzyme activity assays of (D) 3-hydroxyacyl-CoA dehydrogenase (β -HAD), (E) media-chain acyl-CoA dehydrogenase (MCAD), and (F) peroxisomal acyl-CoA oxidase (ACOX) in liver tissue (*p < 0.05, Mann-Whitney, n=7 LDKO vs. n=5 Flox). (G and H) Hepatic CPT1a transcript levels and protein expression. 14-3-3 serves as a protein loading control. (I) Serum ketone levels at fed and fasted states (Mann-Whitney; n=5 flox vs. n=10 LDKO). (J) Rate of glycolysis in isolated primary hepatocytes (*p < 0.01, Mann-Whitney, five independent experiments). Data expressed as mean \pm SEM.

Peroxisomal proliferator-activated receptor alpha (PPAR α) regulates the expression of several hepatic genes involved in fat oxidation, including *Cpt1a*. Therefore, we investigated transcriptional changes in pathways involved in nutrient metabolism including 5 other PPAR α -regulated genes: *Pdk4*, *Fgf21*, *Acox1*, *Hmgcs2* and *Ppara*. In contrast to *Cpt1a*, no other PPAR α -regulated genes were down regulated and both *Pdk4* and *Hmgcs2* were upregulated in liver tissue from LDKO mice compared to controls (Figure 11A). Furthermore, there were no statistically significant transcriptional changes in other glucose or fatty acid metabolic genes regulated by *Srebp1c*, *Pgc-1 α* or *Pgc-1 β* (Figure 11B and D). These data also show that the decreases in ACOX and MCAD activity in LDKO liver tissue (Figure 11D and F) was not due to alterations in transcription of their respective genes, *Acox1* and *Acadm* (Figure 11A and D).

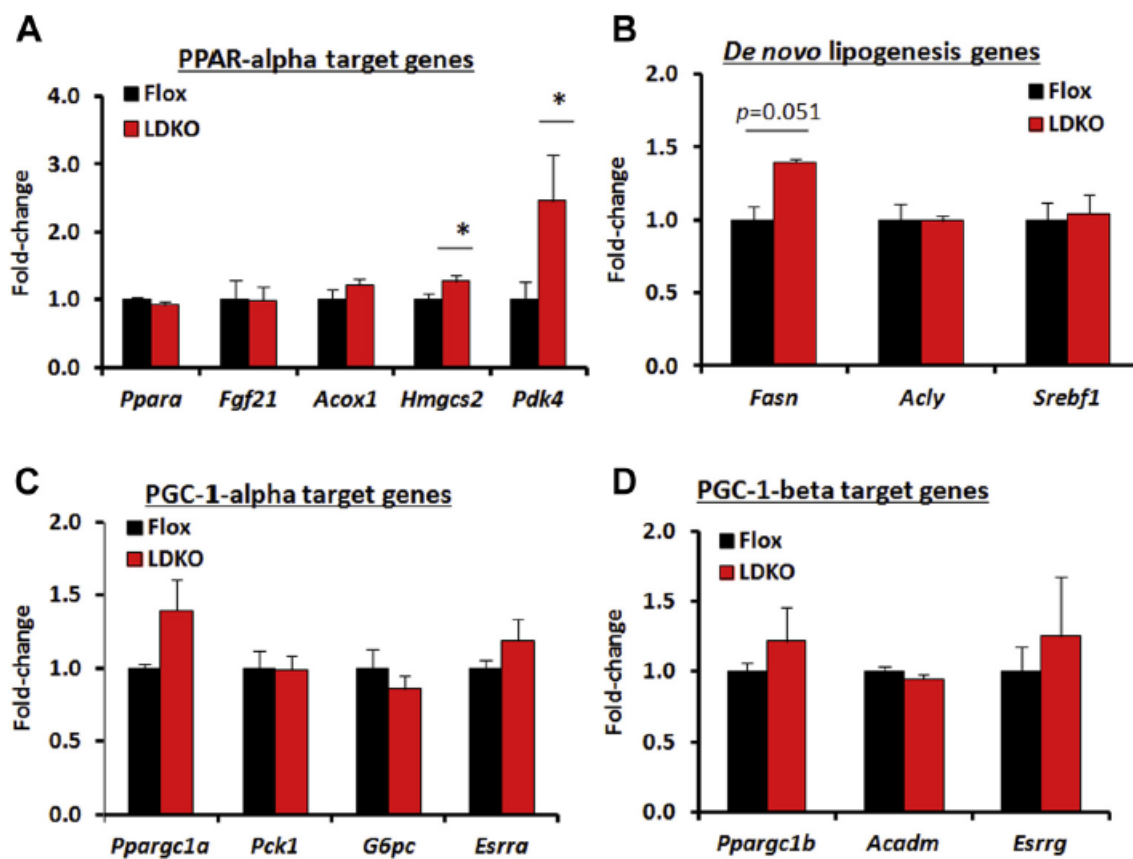


Figure 11. PPAR α , SREBP1c, and PGC-1 α target gene transcription in LDKO vs. Flox liver.

A-D) qPCR analysis of target genes regulated by PPAR α , SREBP1c, PGC-1 α and PGC-1 β . Data expressed as mean \pm SEM (n=5, *p < 0.05 LDKO vs. Flox).

2.1.3 Liver ACC inhibition disrupted acetyl-CoA homeostasis and altered protein acetylation

Acetyl-CoA is a versatile cellular metabolite utilized for ATP production, cholesterol and lipid biosynthesis, and protein acetylation. Given the high flux of acetyl-CoA through ACC enzymes for lipogenesis, we investigated whether the perturbation of ACC activity could impact acetyl-CoA utilization for protein acetylation. Primary hepatocytes and liver tissue from LDKO and Flox control mice were immunoblotted with an antibody that recognizes acetylated lysine residues (Figure 12A and B). Compared to Flox controls, the LDKO tissues and cells had increased immunoblotting signals across a broad range of molecular weights (Figure 12A and B). Since deacetylase enzymes may also regulate protein acetylation, we measured NAD⁺ levels and compared the acetylation pattern of ACC-deficient cells with the pattern caused by the NAD⁺-dependent deacetylase inhibitor, nicotinamide (NAM). NAD⁺ levels were similar in Flox and LDKO liver lysates (Figure 13A), and NAM treatment induced a different pattern of protein acetylation than was observed with ACC inhibition (Figure 12A). These data reveal that ACC inhibition promotes global protein acetylation, and indicate that NAD⁺-dependent deacetylase inhibition cannot account for the changes in lysine acetylation.

2.1.4 Subcellular compartmentalization of ACC-dependent changes in protein acetylation

It was recently shown in *Saccharomyces cerevisiae* that ACC1 inhibition increases nuclear histone acetylation¹⁰⁴; however, the Western blots demonstrated lysine hyper-acetylation across a broad range of protein molecular weights that are not

indicative of histones. To identify the proteins that were hyper-acetylated, we enriched for acetyl-peptides by an anti-acetyl-lysine antibody pulldown and quantified them by proteomics (Figure 12C). This approach resulted in the quantification of 26,843 acetylated peptides corresponding to 3586 unique acetylation sites on 1151 proteins. After normalization to protein abundance, the distribution of acetylation site relative abundances were positively biased (mean $\text{Log}_2(\text{LDKO}/\text{Flox}) = 0.30$), signifying global hyperacetylation in the LDKO liver. Specifically, 788 acetylation sites were increased by greater than 2-fold (22% of the unique sites identified) (Figure 12D). Curiously however, 274 acetylation sites (8% of the unique sites identified) were decreased by more than 2-fold compared to Flox controls. Since ACC enzymes only have access to cytoplasmic acetyl-CoA, we investigated whether subcellular protein distribution correlated with lysine acetylation. These analyses identified a significant enrichment in the acetylation of proteins in the extramitochondrial space and hypo-acetylation of proteins located in mitochondria (Figure 12E and Figure 14A).

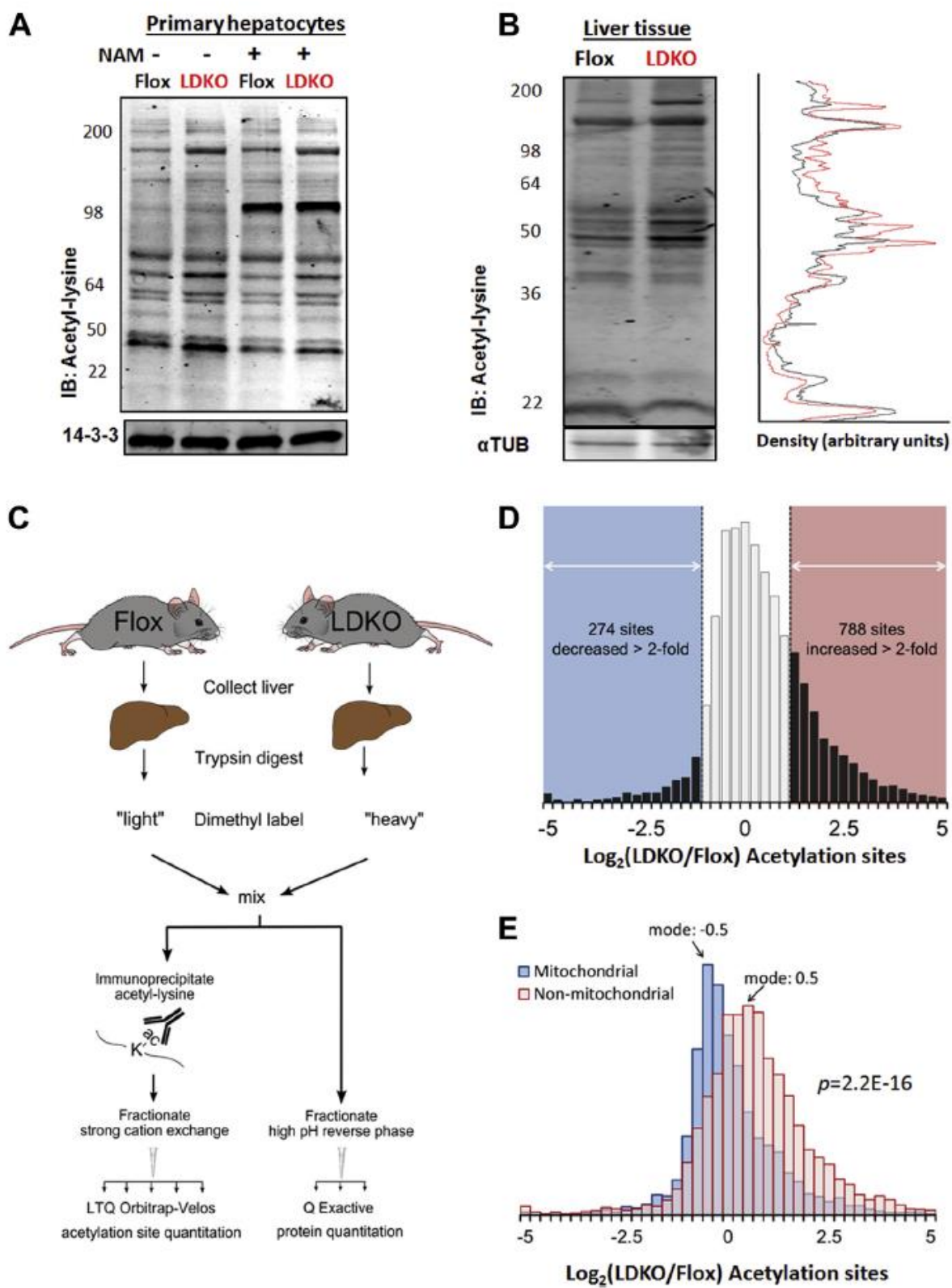


Figure 12. ACC inhibition alters liver acetyl-lysine proteome.

A) Acetyl-lysine immunoblotting of whole cell lysates of primary hepatocytes treated with or without 5 mM nicotinamide, isolated from LDKO and Flox mice. (B) Acetyl-lysine immunoblotting of liver tissue from LDKO and Flox mice with line scan analysis. (C) Work flow of quantitative acetylproteomics experiments on Flox and LDKO livers. (D) Distribution of relative abundances in acetylation sites between LDKO and Flox mice, expressed in logarithmic scale (\log_2) for the entire proteome and (E) mitochondrial vs. non mitochondrial proteins according to Mitocarta classification (n=3, p=2.2e-16, Mann-Whitney).

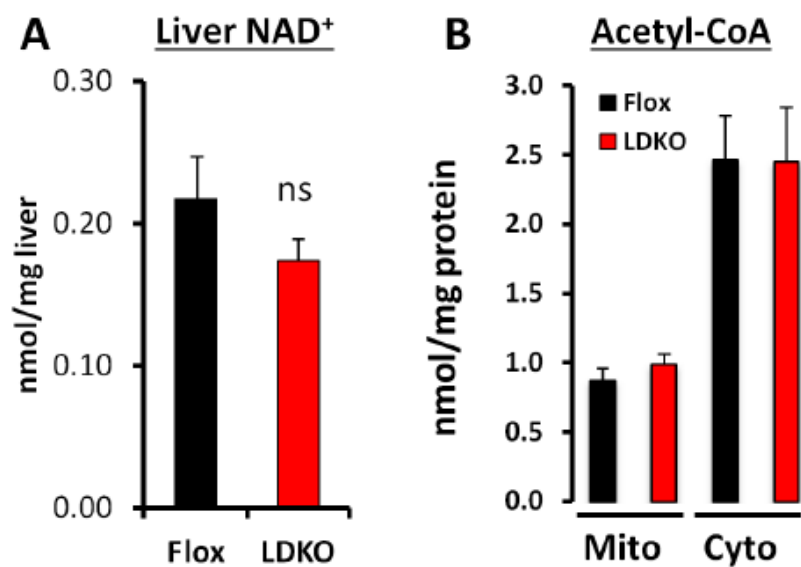


Figure 13. Liver NAD⁺ and acetyl-CoA levels.

A) NAD⁺ level in liver lysates. (B) Acetyl-CoA levels in mitochondrial and cytoplasmic fractions of mouse liver (n=4). Data expressed as mean \pm SEM. ns, non-significant.

We next evaluated whether altered protein acetylation patterns caused by ACC inhibition were biased toward particular biological or metabolic pathways. Functional enrichment analysis identified that proteins involved in intermediary nutrient metabolism were highly acetylated in the liver tissue of LDKO mice compared to Flox controls (eight out of the ten most acetylated pathways, Figure 14B). In livers from LDKO mice, glycolytic and peroxisomal fatty acid metabolic enzymes were generally hyper-acetylated, while mitochondrial proteins involved in fat oxidation and the tricarboxylic acid cycle (TCA) were generally unaffected or hypo-acetylated compared to Flox controls (Figure 14C and Figure 15).

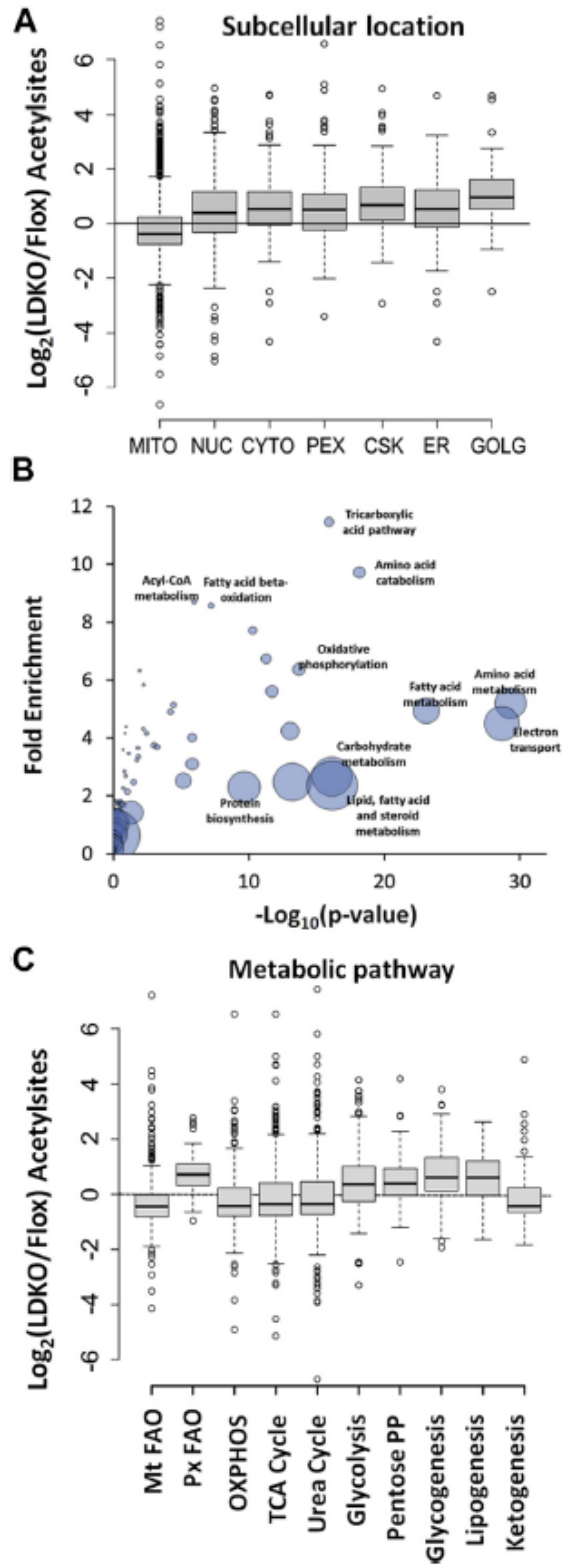


Figure 14. ACC-mediated alterations in protein acetylation are enriched for metabolic networks involved in intermediary nutrient metabolism.

A) Boxplot distribution of acetylation site of proteins based on their annotated subcellular localizations. (B) Functional enrichment analysis of acetylated proteins identifies that metabolic networks are significantly affected. Bubble size represents the number of proteins in each cluster. (C) Boxplot distribution of protein acetylation sites based on their metabolic process.

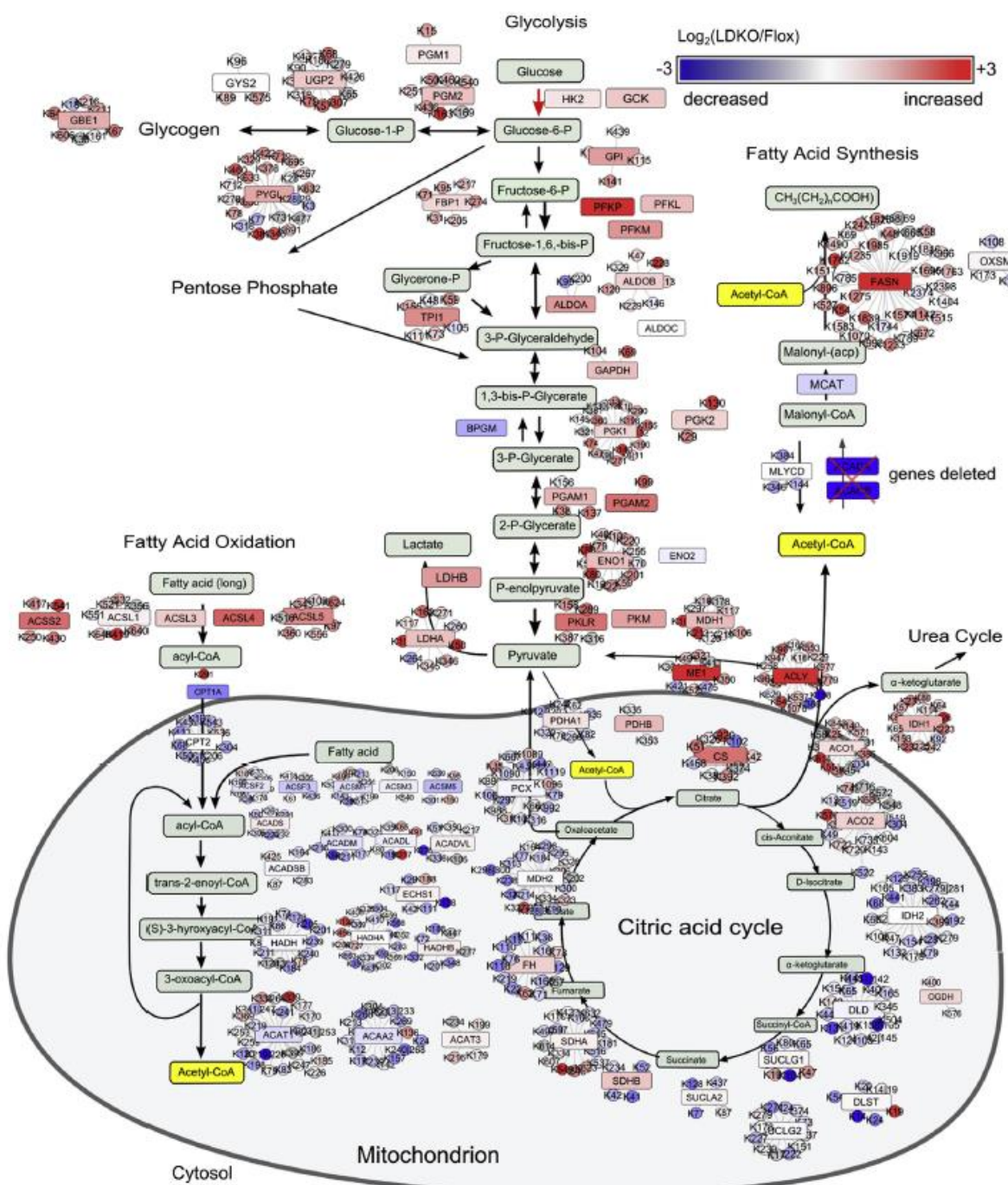


Figure 15. Schematic showing the protein acetylation sites in metabolic pathways that are most differentially acetylated in LDKO/Flox liver.

Pathway color scheme: *Red*, increased in LDKO vs. Flox; *blue*, decreased; *red* or *blue box*, enzymes; *circles*, acetylation status of each enzyme.

To determine whether protein acetylation corresponded with acetyl-CoA levels, we measured acetyl-CoA in mitochondrial and cytoplasmic fractions of Flox control and LDKO liver tissues. Curiously, both mitochondrial and cytoplasmic acetyl-CoA levels were similar between Flox and LDKO liver tissues (Figure 13B). These data suggest that alterations in metabolic substrate flux or increased protein acetylation balance cellular acetyl-CoA levels independently of functional ACC enzymes. Since mitochondria were generally hypo-acetylated, we investigated the activity and acetylation status of complexes I, II and IV of the electron transport chain (ETC) and citrate synthase of the TCA cycle (TCA). The expression of all ETC complexes was similar between Flox and LDKO livers as determined by Western blot using antibodies against complex I subunit NDUFB8, complex II subunit of 30 kDa, complex III core protein 2, complex IV subunit I and complex V alpha subunit (Figure 16A). However, proteomics analysis of acetylated ETC components revealed variable differences in the expression and acetylation of other individual components of the ETC (Figure 16B). To determine whether these changes affected complex activity, we measured their activity (Figure 16C). LDKO liver lysates had increased activity of ETC complex I, lower activity of complex II, and similar activity of complex IV compared to control (Figure 16C). In addition, citrate synthase enzyme activity was increased in LDKO tissue lysates (Figure 16C).

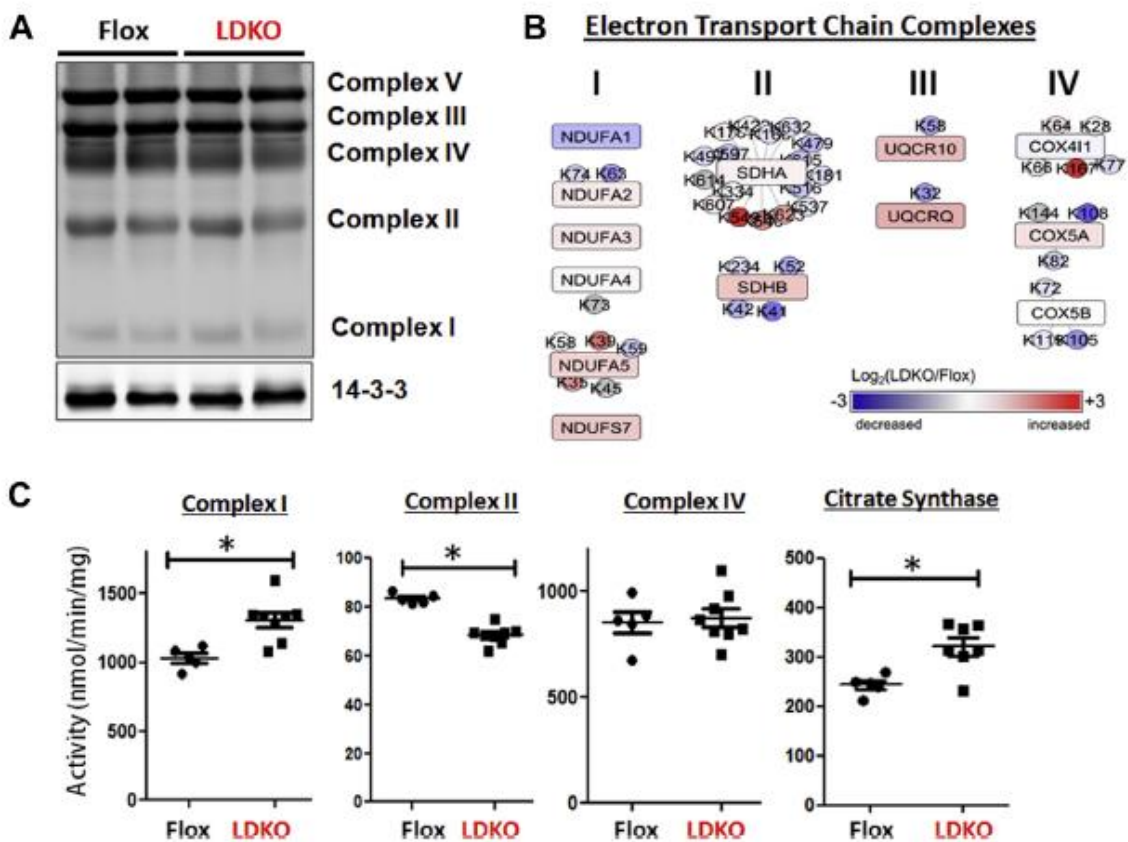


Figure 16. Protein expression and activity of electron transport chain complexes.

A) Western blot analysis of a liver lysates from LDKO and Flox mice separated by SDS-PAGE and immunoblotted with five monoclonal antibodies recognizing a representative protein in each complex involved in mitochondrial oxidative phosphorylation. (B) Changes in protein expression (boxes) and acetylation (circles) of electron transport chain complexes I, II, III, and IV. (C) Enzyme activity of complexes I, II, and IV, and citrate synthase in tissue lysates from LDKO and Flox control liver (n=5 Flox, n=8 LDKO, *p < 0.05, Mann-Whitney, n=5 Flox, n=8 LDKO). Data expressed as mean SEM.

2.1.5 Discussion

ACC enzymes are attractive drug targets for fatty liver diseases because inhibition of their activity is predicted to decrease lipogenesis, increase fat oxidation, and thereby reduce fat storage. Our observation that the deletion of ACC activity in the liver promotes excess fat accumulation is entirely unexpected based on previous work in this area. The only study to genetically target both ACC enzymes *in vivo* utilized antisense oligonucleotides (ASOs) in rats. The ASO markedly decreased ACC expression in both adipose tissue and liver, and resulted in a decrease in hepatic fat and improved insulin sensitivity when rats were fed a high-fat diet¹³⁸. The phenotype of the LDKO mouse and ASO treatment are not directly comparable for many reasons including differences in the species of rodent, the diet, the duration of inhibition, and the different tissues targeted. Regardless of these discrepancies, the LDKO mouse described herein has allowed us to evaluate the consequences of hepatic ACC inhibition on liver fat metabolism and whole animal physiology. Importantly, the increase in liver fat storage in LDKO mice reveals a gap in knowledge concerning the role of ACC enzymes in liver fat metabolism. The increase in liver fat in LDKO hepatocytes is likely caused by reduced fatty acid oxidation, as supported by our findings demonstrating decreased CPT1a expression; decreased fasting ketone production; accumulation of microvesicular fat; and reduced activities of peroxisomal acyl-CoA oxidase, mitochondrial β HAD and mitochondrial MCAD enzymes in the LDKO liver compared to Flox controls. Furthermore, since complex II is involved in FADH₂ oxidation that is driven by fatty acid catabolism, the reduced activity of this complex may also contribute to impaired fatty acid oxidation in

LDKO hepatocytes. These data indicate that ACC inhibition triggers multiple mechanisms to repress fatty acid oxidation. It has been suggested that newly synthesized lipids are ligands for PPAR α ^{98,205}. However, our data indicate that liver-derived lipogenesis is not required for PPAR α -mediated gene transcription since only CPT1a was decreased in LKDO liver tissue compared to Flox controls, while five other PPAR α regulated genes were unaltered or upregulated (*Pdk4* and *Hmgcs2*). Furthermore, we did not observe significant effects on other metabolic genes regulated by SREBP1c, PGC-1 α or PGC-1 β in LDKO mice. These data reveal the existence of a very precise, but unknown, mechanism whereby ACC inhibition specifically targets CPT1 α at the mRNA level to decrease fatty acid oxidation without disrupting other closely regulated genes involved in carbohydrate and mitochondrial metabolism. In organelles such as the nucleus, the regulation of protein acetylation is fairly well-characterized with respect to the roles of histone acetyltransferases and deacetylases. By contrast, the regulation of protein acetylation in the cytoplasm is insufficiently understood. In recent years, several reports have demonstrated that protein acetylation, particularly of cytoplasmic proteins, plays an important role in liver metabolism^{92,206}. In LDKO liver, protein hyper-acetylation was observed in all organelles except mitochondria, indicating an important regulatory role for ACC enzymes in the control of protein acetylation in the extra-mitochondrial space. It is likely that the metabolic phenotype of reduced fat oxidation and increased glycolysis observed in LKDO liver is related to the alterations in protein acetylation. For example, hyper-acetylation of glycolytic enzymes is known to promote glycolysis^{93,206,207}. The mechanisms that underlie the compartment-specific changes in

acetylation caused by ACC inhibition require further investigation, and several scenarios are possible. First, the loss of ACC activity in the extra-mitochondrial space may increase the availability of acetyl-CoA for protein acetyltransferases. Several acetyltransferases are known to localize in the cytoplasmic compartment including GCN5 and PCAF^{94,208,209}; however, it remains unclear whether these acetyltransferases have the broad substrate specificity or subcellular distribution necessary to mediate the hyper-acetylation observed in LDKO liver tissue. Another possibility is that the increase in protein hyperacetylation occurs non-enzymatically, as has been demonstrated previously^{99,100,210}. Studies in yeast demonstrate that ACC gene inhibition is sufficient to promote histone acetylation due to increased availability of acetyl-CoA⁹¹. Similarly, inhibition of AMPK in yeast activated ACC and led to reduced histone acetylation⁹¹. Therefore, a similar regulation of protein acetylation by ACC enzymes may also exist in the mammalian hepatocyte on non-histone proteins. Although we were unable to detect an increase in acetyl-CoA levels in LDKO liver, it remains possible that certain nutritional or hormone-activated states are required to observe acetyl-CoA accumulation. It is less likely that decreased NAD⁺-dependent deacetylase activity drives global protein acetylation since NAD⁺ levels were unchanged in LDKO tissue and nicotinamide did not increase protein acetylation with a similar pattern. Finally, it was recently shown that decreased activity of mitochondrial ETC complex I is associated with increased mitochondrial protein acetylation²¹¹. The LDKO liver had significantly higher complex I activity concomitant with a decrease in protein acetylation in mitochondria, thus it is possible that mitochondrial hypo-acetylation may be secondary to increased complex I activity. In

summary, we observe that complete inhibition of hepatocyte ACC enzymes triggers the activation of a compensatory pathway that preserves fat storage in the liver. We hypothesize that the mechanism linking the loss of ACC activity to increased fat storage is due to increased acetylation of key metabolic enzymes and transcriptional regulatory sensors. These sensors interpret hyper-acetylation as a nutrient replete state and coordinate the feeding response to decrease fatty acid oxidation; an appropriate response to nutrient excess. Future mutational studies are required to test this hypothesis and to define how specific acetyl-lysine sites identified in this study affect protein function.

2.1.6 Summary

Collectively, this new information advances our understanding of the role of ACC enzymes in hepatic nutrient metabolism and protein acetylation, and also reveals the existence of a therapeutic window for drug discovery efforts targeting ACC. One possibility is that an ideal ACC inhibitor would impair lipogenesis but maintain enough residual activity in specific subcellular compartments to prevent protein hyper-acetylation and avoid the compensatory inhibition of fat oxidation. These data also implicate acetyl-CoA, like malonyl-CoA, as a potent regulator of hepatic metabolic flexibility.

2.2 Effect of liver ACC deletion on liver and whole-body metabolic homeostasis in mice challenged with a high-carbohydrate diet

2.2.1 Background

The liver has a finite capacity to store glucose in the form of glycogen, and when glycogen stores are full, a high proportion of glucose taken into the liver from circulation is diverted to lipogenesis and stored as fat, which is a more energetically-efficient form of nutrient storage than glycogen in terms of calories per gram⁶³. Lipogenesis is a significant source of hepatic fat, accounting for approximately 25% of total stored fat in the liver in the fed state¹²⁸. Since hepatic lipogenesis is thought to be important as a ‘glucose sink’, we hypothesized that genetic inhibition of hepatic lipogenesis in mice would be detrimental for maintenance of blood glucose levels in the context of a high sugar diet. To test this, we fed Flox and LDKO mice a fat-free high-carbohydrate diet for 3 weeks, then performed a glucose tolerance test and traced glucose disposal into insulin-sensitive organs including the liver, skeletal muscle, and adipose tissue.

2.2.2 Results

Liver-specific ACC1 and ACC2 double knockout (LDKO) mice were generated as we have previously described²¹². LDKO mice and floxed littermate (Flox) controls were fed a 0% fat, high carbohydrate diet for 3 weeks. After 3 weeks, LDKO mice unexpectedly showed a marked increase in glucose clearance during a glucose tolerance test compared to Flox controls (Figure 17A and B). This phenomenon in the LDKO mice was accompanied by an increased rate of glucose incorporation into liver glycogen (Figure 17C). There were no differences in rates of glucose incorporation into skeletal

muscle glycogen or uptake into adipose tissue (Figure 17D and E), indicating that the liver was the primary organ responsible for increased glucose disposal.

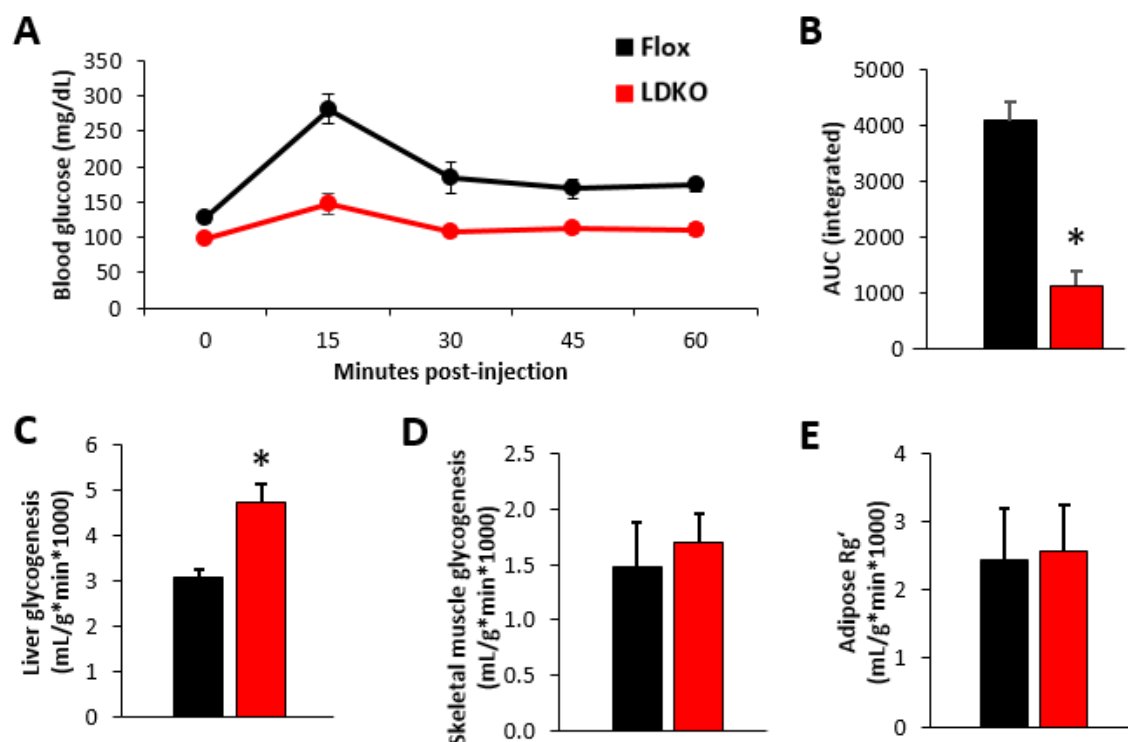


Figure 17. Liver ACC inhibition increases glucose disposal into liver glycogen and improves whole-body glucose tolerance compared to Flox controls.

A) Blood glucose levels over time and **(B)** area under the curve, and rates of incorporation of glucose into **(C)** liver glycogen, **(D)** skeletal muscle glycogen, and **(E)** adipose tissue during a glucose tolerance test of LDKO mice and Flox littermate controls after 3 weeks of fat-free diet feeding. * indicates significant difference, $p < 0.05$ ($n=5-6$). Data are represented as mean \pm SEM.

We proceeded to investigate additional factors that could influence whole-body glucose tolerance and incorporation of circulating glucose into liver glycogen. Although insulin is a strong stimulator of glycogen synthesis²¹³, there were no differences in post-prandial or overnight-fasted serum insulin levels between Flox and LDKO mice (Figure 18A). There were no differences in overall body weight (Figure 18B). However the LDKO mice had a significant decrease in fat mass (Figure 18C). Furthermore, livers of LDKO mice were depleted of triglyceride, had a significant reduction of cholesterol, and an increase in glycogen levels (Figure 18D-F) compared to Flox controls.

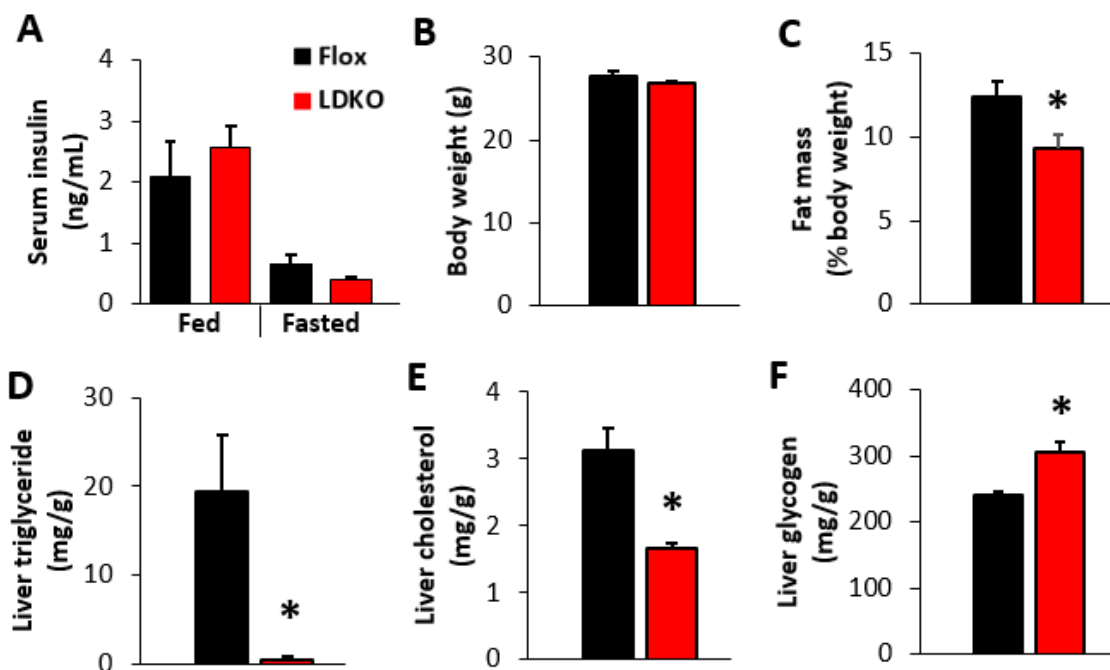


Figure 18. LDKO mice fed a fat-free diet have reduced adiposity and depletion of liver triglycerides compared to Flox controls.

A) Serum insulin levels, (B) body weight, (C) fat mass, and liver (D) triglyceride, (E) cholesterol, and (F) glycogen content of Flox and LDKO mice after 3 weeks of fat-free diet feeding. * indicates significant difference, $p < 0.05$ ($n=5-6$). Data are represented as mean \pm SEM.

LDKO mice did not exhibit any significant differences in whole-body oxygen consumption or respiratory exchange ratio (Figure 19A-B), indicating that the decreased adiposity in the LDKO mice was not due to changes in whole-body energy expenditure or utilization of fat or carbohydrates.

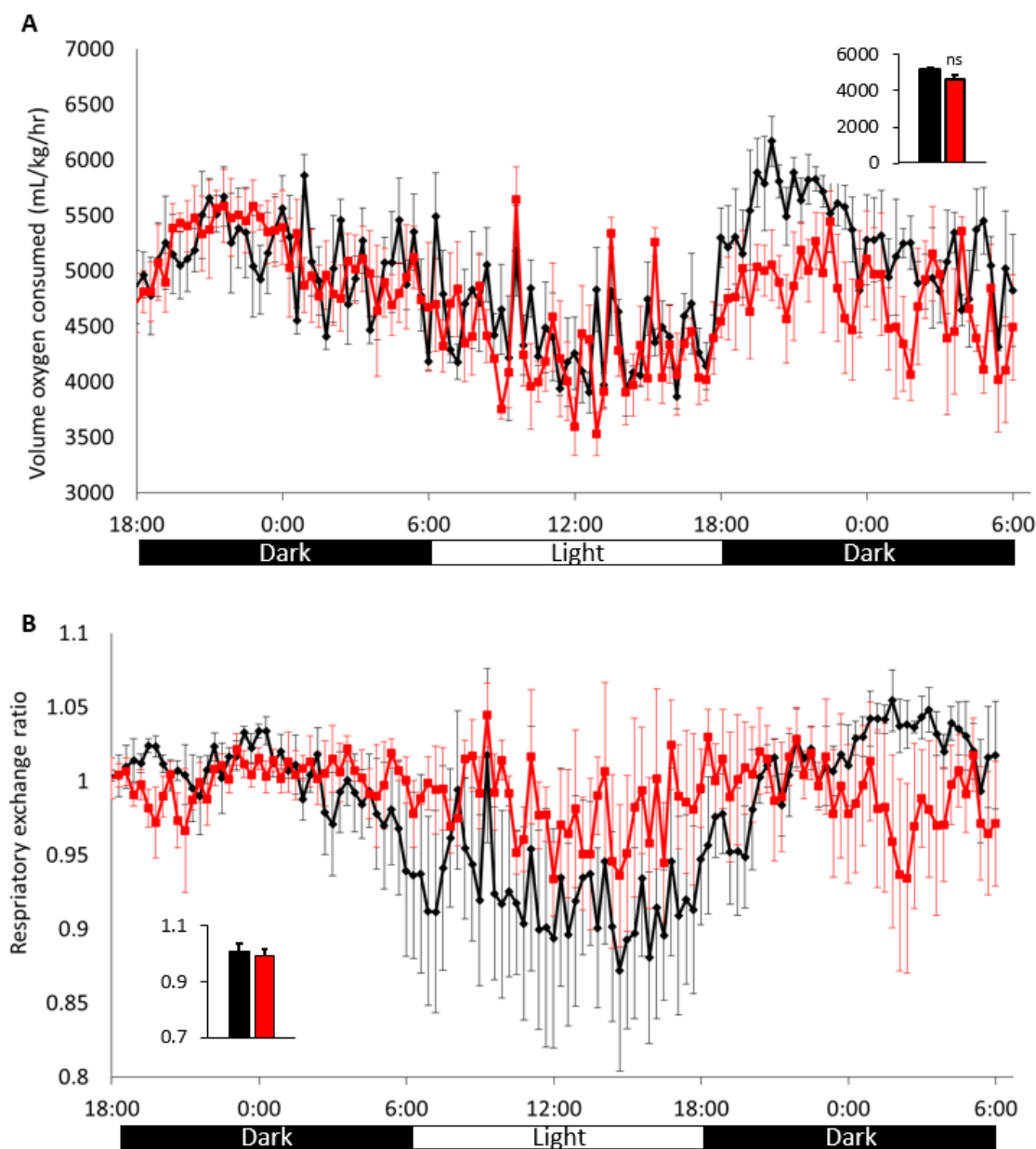


Figure 19. LDKO mice fed a fat-free diet for 3 weeks have no alterations in whole-body oxygen consumption or respiratory exchange ratio compared to Flox controls.

A) Volume of whole-body oxygen consumption and **(B)** respiratory exchange ratio during dark and light cycles in Flox and LDKO mice after 3 weeks of fat-free diet feeding (n=5-6). Data are represented as mean \pm SEM.

2.2.3 Discussion

Lipogenesis represents a major mechanism by which the liver stores excess glucose and so it has been thought that lipogenesis is important to maintain whole-body glucose homeostasis by acting as a glucose sink. Our results, however, demonstrate that inhibition of lipogenesis actually increases the rate of glucose disposal in mice that have been fed a fat-free high-carbohydrate diet, and this coincided with increased levels of stored liver glycogen. The improvement in glucose tolerance seen in the LDKO mice is extremely robust, and mainly due to increased glucose uptake by the liver. This finding was unexpected since hepatic lipogenesis was thought to be necessary to dispose of excess glucose in the context of a high carbohydrate diet. How this excess glucose is being stored or metabolized in the liver or other organs in the absence of hepatic lipogenesis is a question that will need to be addressed in future studies.

We have previously demonstrated that LDKO mice are unable to synthesize lipids *de novo* in the liver. When LDKO mice are fed a normal chow diet which contains a source of fat, they have an increase in liver triglyceride levels and no change in peripheral adiposity²¹². A previous study in mice with liver-specific deletion of FASN, which inhibits hepatic lipogenesis, showed an increase in liver lipid content even in mice on a high-carbohydrate fat-free diet for 4 days⁹⁸. In the current study, however, when the mice are completely restricted from a source of dietary fat for 3 weeks, there is a depletion of liver triglycerides and a reduction of peripheral adiposity. This suggests that when the liver cannot obtain exogenous lipids or synthesize its own lipids *de novo*, it signals to the adipose tissue to release lipids, likely to help meet the lipid demands of the liver and

other organs. However, with a persistent lack of dietary fat, adipose tissue can no longer compensate in order to maintain liver lipid levels, resulting in a decline of lipid levels in both the adipose and liver tissues. Interestingly, although cholesterol is synthesized by a pathway independent of lipogenesis, cholesterol levels were also significantly reduced in the LDKO livers.

How the liver is communicating to the adipose tissue to supply lipids is not known and will require further investigation, but may involve a liver-derived metabolite (e.g. acetyl-CoA or lipid product) or a liver-derived hormone (e.g. fibroblast growth factor) that is released into circulation. To investigate whether changes in adipose tissue observed in the LDKO mice can be attributed to a circulating factor, primary adipocytes should be treated with serum collected from Flox or LDKO mice fed a fat-free diet and differences in adipocyte lipid uptake, lipogenesis, oxidation, and release should be measured. If the LDKO serum contains a factor that influences adipocyte lipid metabolism as we hypothesize, it may be possible to identify the nature of this factor(s) by phase-extracting lipid and non-lipid serum components, or by heat-inactivating hormones. Individual components contained in LDKO serum that are found to be associated with changes in lipid metabolism may be added back to adipocytes to determine which factor(s) are sufficient to recapitulate a reduction in adiposity. If the factor(s) present in LDKO serum that reduces adiposity is identified, primary hepatocytes should be used to determine whether this factor(s) is released by LDKO hepatocytes directly, or whether this signal is secondary to liver-intrinsic effects of ACC inhibition.

2.2.4 Summary

Liver lipogenesis was thought to be a necessary means to store excess glucose in the context of high-carbohydrate feeding in order to maintain appropriate blood glucose levels. However, the present study demonstrates that inhibition of liver lipogenesis by genetic deletion of ACC1 and ACC2 paradoxically increased glucose disposal into the liver and improved whole-body glucose tolerance. ACC inhibition caused a depletion of liver triglycerides after 3 weeks of fat-free diet, accompanied by decreased adipose tissue, suggesting communication of the liver's nutrient status to the adipose tissue, resulting in adipose tissue compensation. This study demonstrates the ability of the liver to influence nutrient status of other organs such as adipose tissue and places the liver at the center of whole-body nutrient homeostasis.

2.3 Effect of liver ACC deletion on liver and whole-body metabolic homeostasis in mice challenged with a high-fat diet

2.3.1 Background

Liver lipid accumulation in NAFLD has been attributed to aberrant lipogenesis. In fasting individuals, lipogenesis normally contributes only 5% of stored liver, and may contribute up to 25% after consumption of a meal¹²⁸. In individuals with NAFLD, lipogenesis can account for about 25% of liver lipids even in the fasted state^{129,130,214}. Expression of the ACC enzymes and the products of lipogenesis are commonly increased in livers of NAFLD patients^{131,132,86,133}. Furthermore, excess accumulation of *de novo* synthesized lipids in the liver has been implicated in causing insulin resistance and glucose intolerance^{114,115,123,124}. Therefore, it has been proposed that inhibiting liver lipogenesis would decrease liver fat accumulation and improve whole-body glucose tolerance in the context of NAFLD. However, no study has previously examined the physiological effects of complete inhibition of hepatic lipogenesis in the context of NAFLD. To determine whether dual inhibition of liver ACC1 and ACC2 improves fatty liver and glucose intolerance in the context of NAFLD, we tested liver-specific ACC1 and ACC2 mice in the context of Western diet-induced fatty liver and glucose intolerance.

2.3.2 Results

Liver-specific ACC1 and ACC2 double knockout (LDKO) mice were generated as we have previously described²¹². LDKO mice and Flox controls were fed a 45% fat,

high sugar Western diet for 12 weeks. Compared to Flox controls, liver lipid levels were significantly reduced by over 60% in livers of the LDKO mice, whereas liver cholesterol levels were not different (Figure 20A-B). How does this compare to mice on normal chow? However, there were no significant differences in adipose tissue weight or body weight between LDKO mice and Flox controls (Figure 20C-D). Furthermore, whole-body glucose tolerance, assessed by a glucose tolerance test at 12 weeks of diet, was not significantly different between Flox and LDKO mice (Figure 20E-F).

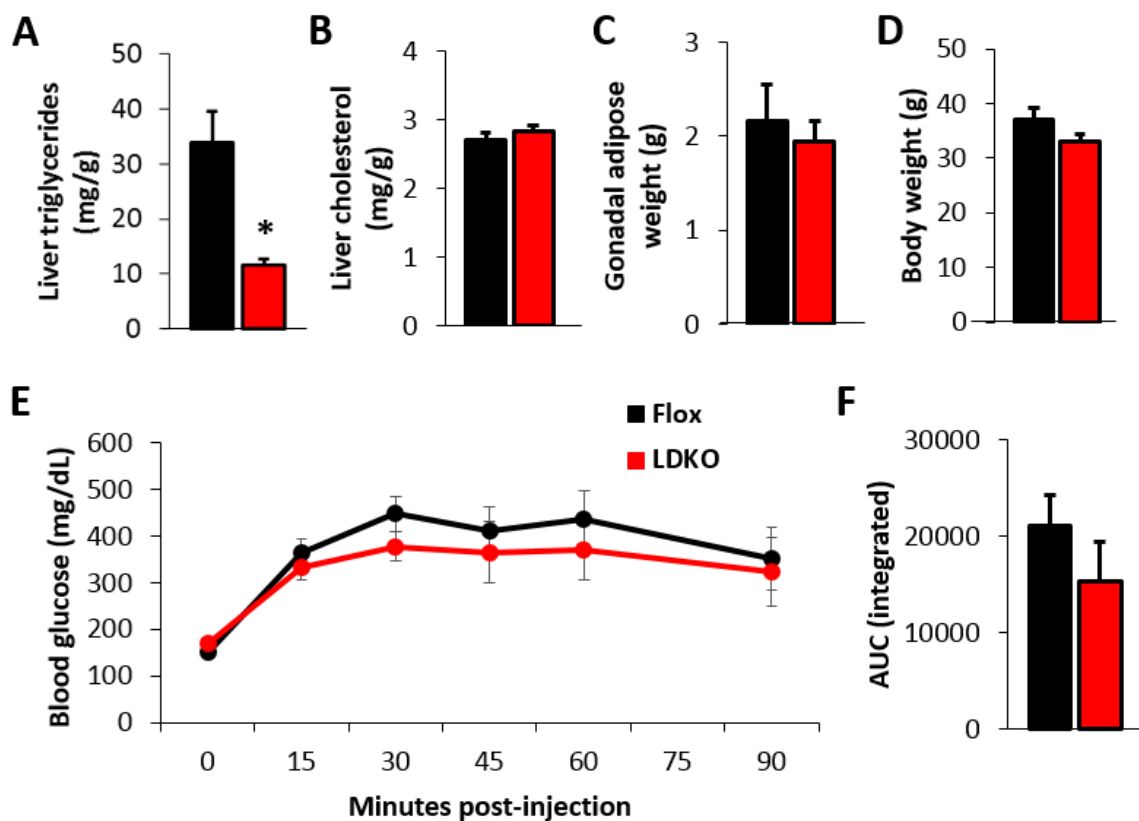


Figure 20. Liver ACC deletion causes a reduction of liver triglycerides, but no significant improvement in whole-body glucose tolerance in mice fed a Western diet.

Liver (A) triglyceride and (B) cholesterol content, (C) gonadal adipose weight, and (D) body weight of LDKO and Flox mice fed a Western diet. E) Blood glucose concentrations over time and (F) area under the curve (AUC) during a glucose tolerance test in LDKO and Flox mice fed a Western diet. * indicates significant difference, $p < 0.05$ ($n=6$). Data are represented as mean \pm SEM.

2.3.3 Discussion

The present study demonstrates that complete genetic inhibition of hepatic ACC1 and ACC2 significantly protected from Western diet-induced fatty liver; however, this reduction in liver fat was not sufficient to improve whole-body glucose tolerance. These results differ from a previous study that targeted liver ACC enzymes in rats using antisense oligonucleotides and observed protection from diet-induced fatty liver and glucose intolerance¹³⁸. However, the ASOs delivered by tailvein injection also targeted the adipose tissue, potentially explaining these different results¹³⁸. In another study, mice expressing constitutively active ACC1 and ACC2 had increased liver lipogenesis, and were susceptible to fatty liver and whole-body glucose intolerance which was refractory to metformin treatment¹²⁶. Similarly, these results may differ from our current results because the constitutive activation of ACC enzymes was also whole-body rather than specifically targeted to the liver¹²⁶. Nevertheless, we demonstrate that inhibition of hepatic lipogenesis is sufficient to completely prevent Western-diet induced fatty liver such that liver triglycerides are maintained at the level of chow-fed mice, but has no effect on whole-body glucose tolerance.

2.3.4 Summary

The present study demonstrates that decreasing liver fat levels by inhibiting ACC1 and ACC2 specifically in the liver is not sufficient to ameliorate diet-induced glucose intolerance. Future work should examine whether inhibition of ACC1 and ACC2 in other tissues such as adipose tissue or skeletal muscle is sufficient to improve whole-

body glucose tolerance in the context of a Western diet, and whether reduction of liver fat levels is required for such an effect.

**CHAPTER 3: METABOLIC CONSEQUENCES OF PROTEIN ACETYLATION
MEDIATED BY THE ACC ENZYMES**

3.1 Effect of ACC activity on PGC-1 α protein acetylation and cellular metabolism

3.1.1 Background

We have previously demonstrated that ACC inhibition alters protein acetylation at lysine residues, such that LDKO mice had overall increased global protein acetylation compared to Flox controls. This was accompanied by decreased expression of CPT1a, which is the rate-limiting enzyme in mitochondrial fat oxidation. A major inducer of CPT1a is PGC-1 α , a master regulator of hepatic metabolism^{95,96}. Interestingly, the activity of PGC-1 α is known to be regulated by acetylation. When acetylated, PGC-1 α is inactive and unable to trigger transcription of its target genes, causing a shift in metabolism toward glucose catabolism and away from fat catabolism.

Acetyl-CoA availability is rate-limiting for either enzymatic or non-enzymatic protein acetylation^{100,102,103}. Since the ACC enzymes catalyze the conversion of acetyl-CoA to malonyl-CoA, they compete for intracellular acetyl-CoA pools, influencing acetyl-CoA availability and protein acetylation^{91,104}. Therefore, fluctuations in acetyl-CoA availability caused by changes in ACC activity may be important to modulate PGC-1 α and may represent a major intersection between sensing cellular nutrient status and producing a coordinated transcriptional response. Therefore, in the present study, we test whether blocking PGC-1 α in ACC-deficient mice is sufficient to reverse the depression in fatty acid oxidation.

3.1.2 Results

Primary hepatocytes were isolated from liver-specific ACC1 and ACC2 double knockout (LDKO) mice and floxed littermate (Flox) controls that were fed normal chow

or a fat-free diet (FFD) for 4 days. We first validated that LDKO mice lacked expression of ACC1 and ACC2 in both normal chow and FFD conditions, whereas FFD induced ACC1 and ACC2 expression in Flox hepatocytes as expected (Figure 21A). Expression of the PGC-1 α target genes *Pck1* and *G6pc* was significantly lower in the LDKO livers (Figure 21B), indicating lower PGC-1 α activity. In Flox and LDKO liver lysates we immunoprecipitated proteins with acetylated lysine residues (AcK), then immunoblotted with an antibody against PGC-1 α . This revealed a higher levels of acetylated PGC-1 α protein in livers of LDKO mice fed normal chow compared to Flox controls. Compared to chow conditions, FFD conditions caused a greater increased in levels of acetylated PGC-1 α in both LDKO and Flox livers (Figure 21C). shRNA knockdown of GCN5, a protein acetyltransferase, or overexpression of non-acetylatable PGC-1 α (K13R) was sufficient to restore fatty acid oxidation in LDKO primary hepatocytes (Figure 22A-B). This demonstrates a complex layer of metabolic programming by liver ACC activity involving the regulation of intracellular acetyl-CoA availability which ultimately controls the dynamic switch between fat and glucose utilization.

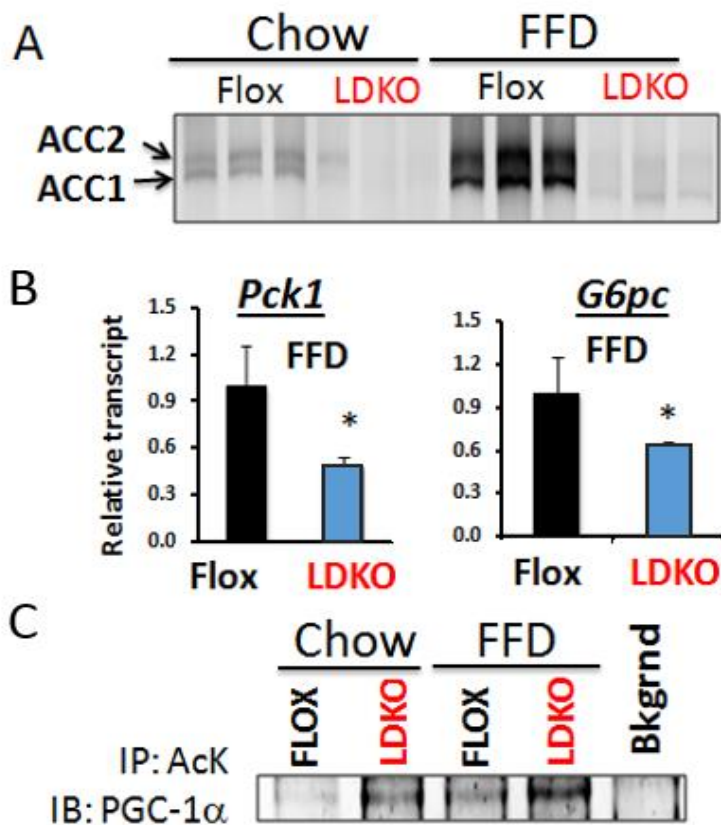


Figure 21. ACC inhibition increases PGC-1 α acetylation

A) Liver ACC1 and ACC2 expression is increased in the livers of flox mice fed a high-carbohydrate diet, but absent in the livers of LDKO mice. (B) LDKO mice fed a high-carbohydrate diet have reduced expression of gluconeogenic PGC-1 α target genes (C) and increased acetylated PGC-1 α . * indicates significant difference, $p < 0.05$ (n=5-6).

Data are represented as mean \pm SEM.

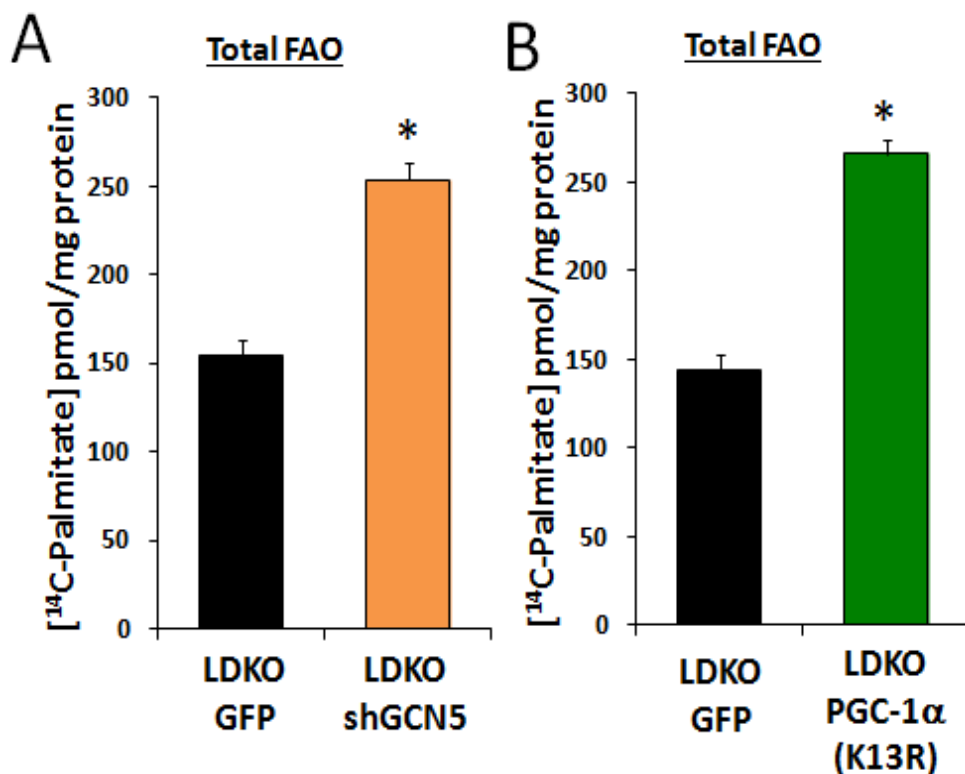


Figure 22. Inhibition PGC-1 α acetylation is sufficient to reverse the defect in fatty acid oxidation in LDKO hepatocytes.

Adenovirus-mediated knockdown of GCN5 (A) or over-expression of PGC-1 α (K13R) (B) increased fatty acid oxidation in primary LDKO hepatocytes. * indicates significant difference, $p < 0.05$ ($n=3$). Data are represented as mean \pm SEM.

3.1.3 Discussion

We have previously shown that inhibition of liver ACC activity causes an increase in global protein acetylation. Liver ACC inhibition also caused decreased expression of CPT1a, which is the rate-limiting enzyme in mitochondrial fatty acid oxidation. Because PGC-1 α is a major transcriptional regulator of CPT1a, we speculated that ACC activity may link cellular nutrient status with the transcriptional response by PGC1a to maintain metabolic flexibility.

The present study confirms that LDKO mice have increased acetylation of PGC-1 α in the liver. PGC-1 α is known to be acetylated by the acetyltransferase GCN5, although its non-enzymatic spontaneous acetylation may also be possible. Regardless, the probability of both enzymatic and non-enzymatic acetylation is influenced by the availability of acetyl-CoA. Treating cells with an inhibitor of GCN5 or expression a non-acetyltable mutant of PGC-1 α was sufficient to increase fatty acid oxidation in LDKO hepatocytes, demonstrating that the ACC enzymes regulate metabolism via influencing PGC-1 α acetylation. Therefore, we propose that inhibition of ACC activity increases the intracellular acetyl-CoA pool, causing increased acetylation of PGC-1 α by GCN5. In turn, acetylation of PGC-1 α reduces its transcriptional activity, leading to decreased expression of PGC-1 α target genes that regulate glucose metabolism and fatty acid oxidation, such as *Pck1*, *G6pc*, and *Cpt1a*.

ACC activity is highly regulated by cellular nutrient status at multiple levels. First, low ATP levels cause phosphorylation and inactivation of ACC by AMPK. Second, citrate, an important metabolite which represents the nutrient status of a cell, is

an allosteric regulator of ACC, causing ACC polymerization and activation. Third, ACC expression is regulated by transcription factors that are highly responsive to insulin and glucose levels. Because ACC integrates multiple nutritional inputs, it is poised to efficiently moderate downstream cellular metabolic adaptations. PGC-1 α is required for cellular metabolic flexibility and highly regulated by acetylation; thus, it is fitting that it is regulated by ACC activity. However, the protein acetylome is enriched for metabolic proteins, presenting the possibility that, in addition to PGC-1 α , other transcription factors or enzymes may be highly regulated by ACC activity. Further work will be required to determine how ACC activity influences metabolism on a broad scale.

3.1.4 Summary

ACC activity influences the intracellular acetyl-CoA pool, resulting in altered global protein acetylation and metabolic gene expression. ACC inhibition reduced expression of CPT1a, the rate limiting enzyme in mitochondrial fatty acid oxidation. The major transcription factor regulating CPT1a expression is PGC-1 α , and the transcriptional activity of PGC-1 α is known to be regulated by acetylation. Therefore, we tested whether ACC inhibition influenced PGC-1 α acetylation and activity. Herein we demonstrate that ACC inhibition causes increased PGC-1 α acetylation. Furthermore, inhibition of PGC-1 α acetylation restores the rate of fatty acid oxidation in hepatocytes lacking ACC activity. These data establish ACC activity as a major regulator of cellular metabolism at least in part by controlling acetylation of PGC-1 α .

**CHAPTER 4: THE ROLE OF DIETARY NUTRIENTS AND ACC ENZYMES IN
HEPATOCELLULAR CARCINOMA**

4.1 Effect of dietary nutrients on hepatocellular carcinoma promotion

4.1.1 Background

Environmental risk factors for primary liver cancer include viral hepatitis, aflatoxin, alcohol, and obesity^{215,216}. A recent study of more than 900,000 adults in the United States reported the relative risk of dying from liver cancer was 4.5 times greater for men and 1.7 times higher for women with baseline body mass index (BMI) ≥ 35 , compared to the reference groups with baseline BMI of 18.5 to 25¹⁸¹. Diabetes and hyperglycemia are also highly associated with liver cancer^{217–220}, as is dietary intake of sugar²²¹. However, the pathophysiologic mechanisms linking obesity and poor diet to liver tumor burden remain unclear and may involve a range of factors including hyperinsulinemia, insulin resistance, glucose intolerance, inflammation, and hepatic steatosis.

A commonly used model of experimental primary liver cancer in mice involves a single intraperitoneal injection of the pro-carcinogen diethylnitrosamine (DEN) in neonates. DEN is metabolized in the liver by CYP450 enzymes where it is converted to an active carcinogen that causes DNA alkylation and oxidative damage, leading to development of hepatocellular adenoma (HCA), which progresses to hepatocellular carcinoma (HCC), resembling poor-prognosis HCC in humans^{222–224}. In this study, we investigated the role of dietary fats and sugars on primary liver tumor burden in DEN-treated mice fed one of five diets: normal chow (NC) which is low in fat and sucrose; Western diet based on lard (WD-L) which is high in fat and sucrose; Western diet based on coconut oil (WD-C); fructose diet (FD) which is low in fat but high in sucrose and

fructose; and ketogenic diet (KD) which is high in fat but low in sucrose. These diets cause dissimilar metabolic phenotypes. For example, WD-L causes obesity, peripheral insulin resistance, glucose intolerance, and hepatic steatosis compared to NC. WD-C is calorically identical to WD-L, but it induces greater hepatic lipogenesis²²⁵, which has pathogenic and prognostic significance in primary liver cancer^{191,226}. FD was chosen because it is calorically identical to NC, but fructose induces lipogenesis and glucose intolerance in the absence of obesity^{227,228}. Finally, long-term KD promotes glucose intolerance with less hepatic steatosis compared to mice fed a WD²²⁹. These diets were used to determine how the intake of dietary sugars and fats impacts tumor burden in a mouse model of liver cancer.

4.1.2 Dietary effects on tumor burden

Figure 23A illustrates the study design. In brief, C57BL/6N mice were injected with DEN (25 mg/kg i.p.) at 14 days of age. The mice were weaned at 3 weeks of age and randomized to cages with non-littermates to avoid litter bias. From 6 weeks of age, mice were fed one of five diets with varying sugar and fat content. Metabolic analyses were performed at 22 weeks of age (16 weeks of study diet) and mice were euthanized at 32 weeks of age (26 weeks of study diet). We observed that tumor incidence was similar between diet groups (Figure 23B); however, tumor burden and multiplicity were significantly greater in all mice fed high-sugar diets (WD-L, WD-C, and FD) (Figure 23C–D) compared to mice fed NC. Mice fed KD, which was high in fat but low in sugar, had low tumor burden that was comparable to mice fed NC diet. Histological analysis

identified the majority of tumors as hepatocellular adenoma (HCA), but instances of HCC and HCC foci were observed in livers of mice fed the high-sugar diets (Figure 23E and Figure 24). The mouse with the median tumor burden for each diet group is shown as a representative image in Figure 23F. In addition to males, female C57BL/6 mice were similarly treated with DEN at 2 weeks of age and inspected for tumor at 40 weeks of age. Interestingly, tumor incidence was higher in female mice fed high sugar diets (Figure 25A-B).

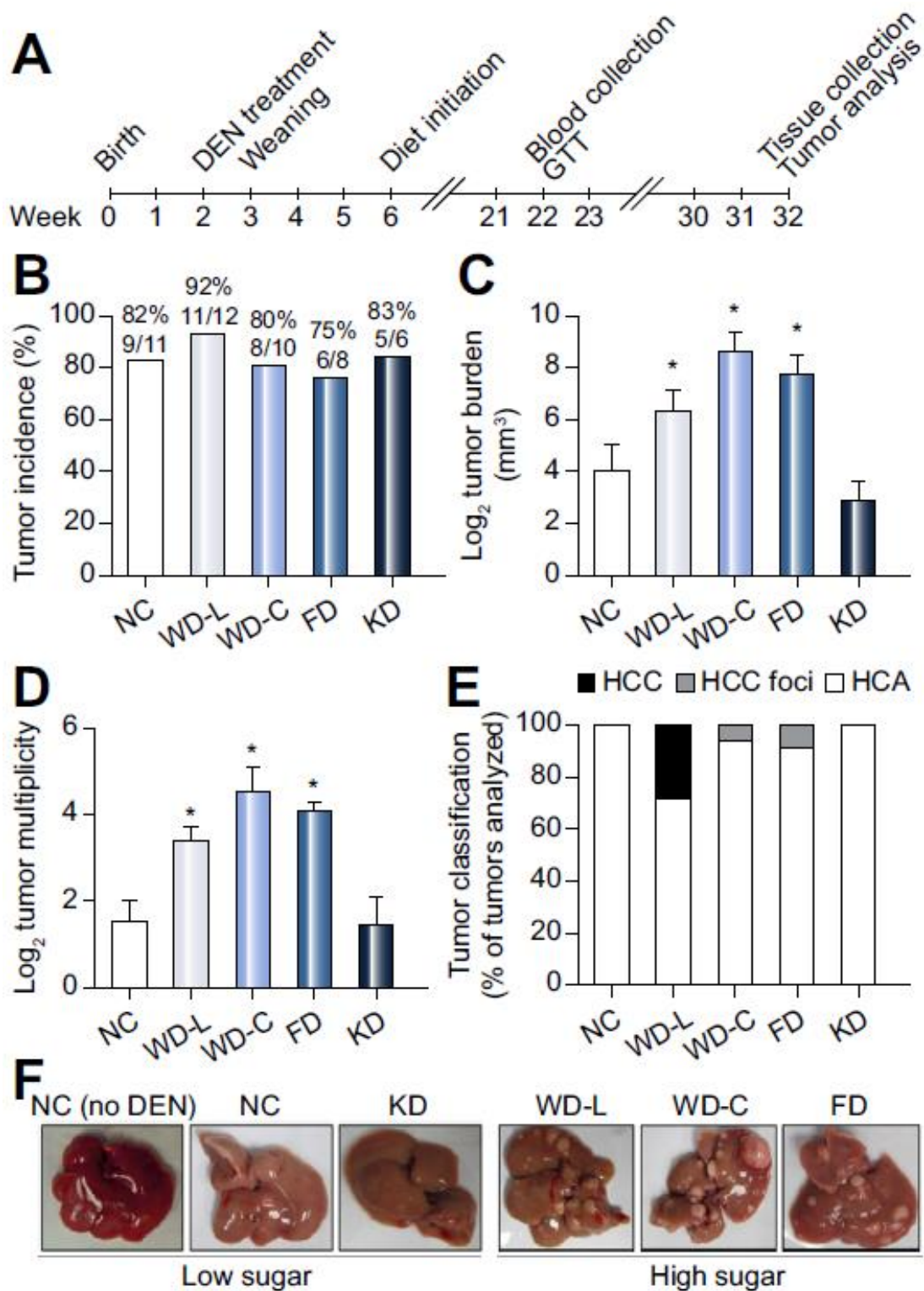


Figure 23. Dietary nutrient content has a strong influence on liver tumor burden and multiplicity in male mice treated with DEN.

A) Diagram of study design. (B) Tumor incidence, (C) average tumor burden, and (D) multiplicity of DEN-treated mice at 32 weeks of age. Data presented as mean \pm SEM. * indicates a significant difference compared to NC group, $p < 0.05$ ($n = 5-11$). (E) Histological classification of tumors observed ($n = 4-6$). HCC = hepatocellular carcinoma, HCA = hepatocellular adenoma. (F) Representative images of livers of DEN-treated mice and a liver from an age-matched mouse fed NC (NC no DEN) shown for comparison.

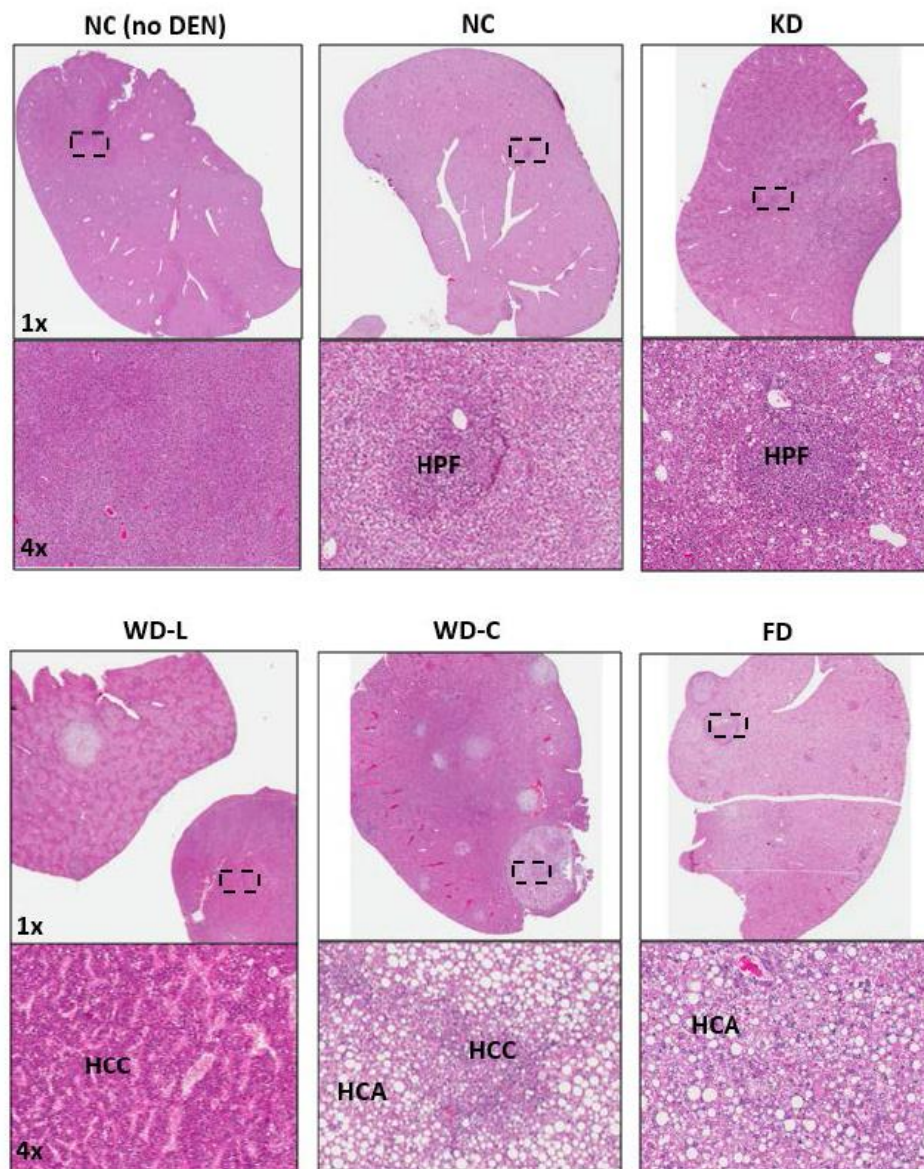


Figure 24. Liver histology.

Representative images of H&E-stained liver sections (large lobes) of 32-week-old male mice fed low sugar diets (NC, KD (top row)) or high sugar diets (WD-L, WD-C, or FD (bottom row)) from 6 to 32 weeks of age. A liver from an age-matched mouse fed NC (NC no DEN) is shown for comparison. HPF=hyperplastic foci, HCC=hepatocellular carcinoma, HCA=hepatocellular adenoma.

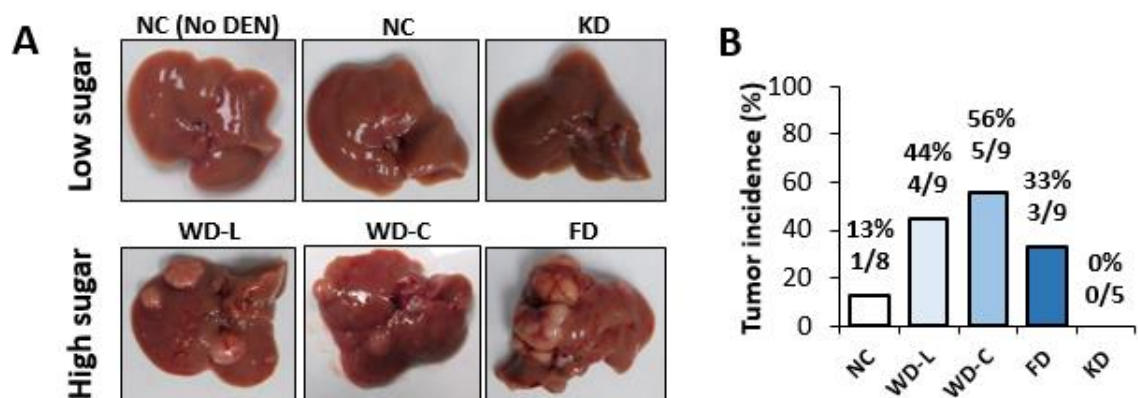


Figure 25. High sugar diets increase liver tumor incidence in DEN-treated females.

(A) Representative liver images and (B) liver tumor incidence of female C67BL/6 mice treated with DEN at 2 weeks of age and fed one of five experimental diets from 6 to 40 weeks of age.

4.1.3 Physiologic effects

DEN treatment significantly increased liver triglyceride stores in all dietary groups compared to control mice that did not receive DEN (Figure 26A). When comparing only DEN-injected mice, those fed WD-L and WD-C had significantly increased liver triglycerides compared with mice fed NC (Figure 26A). Liver cholesterol levels were significantly elevated in mice fed high sugar diets (WD-L, WD-C, and FD) compared with those fed NC (Figure 26B). When evaluated as independent parameters, both liver triglyceride (Figure 26A) and cholesterol (Figure 26B) significantly correlated with tumor burden. There were no differences in overall body weights between groups, but compared to mice fed NC, mice fed WD-C and KD had greater adiposity, whereas mice fed FD had a trend for lower adiposity (Figure 26C–E). Overall, there was no correlation between tumor burden and adiposity or body weight (Figure 26E and Figure 28B). This was particularly emphasized by the low tumor burden and high fat mass in mice fed KD and the high tumor burden and low fat mass of mice fed FD. Food consumption monitoring showed a trend for increased kCal intake in mice fed diets rich in fat (WD-L, WD-C, KD) (Figure 28A). In females, mice fed WD-L had significantly higher body weight compared to mice fed NC (Figure 27A). Both of the Western diets caused significantly higher adiposity in the female mice (Figure 27B). High sugar feeding was associated with significantly higher liver triglycerides in female mice, whereas mice fed KD had significantly lower liver triglycerides compared to mice fed NC (Figure 27C). In females, diet had no effect on liver cholesterol levels (Figure 27D). Male mice fed WD-C and FD had larger liver weight as a percentage of body weight compared to

mice fed NC, while mice fed KD had smaller liver weight as a percentage of body weight (Figure 28B–D).

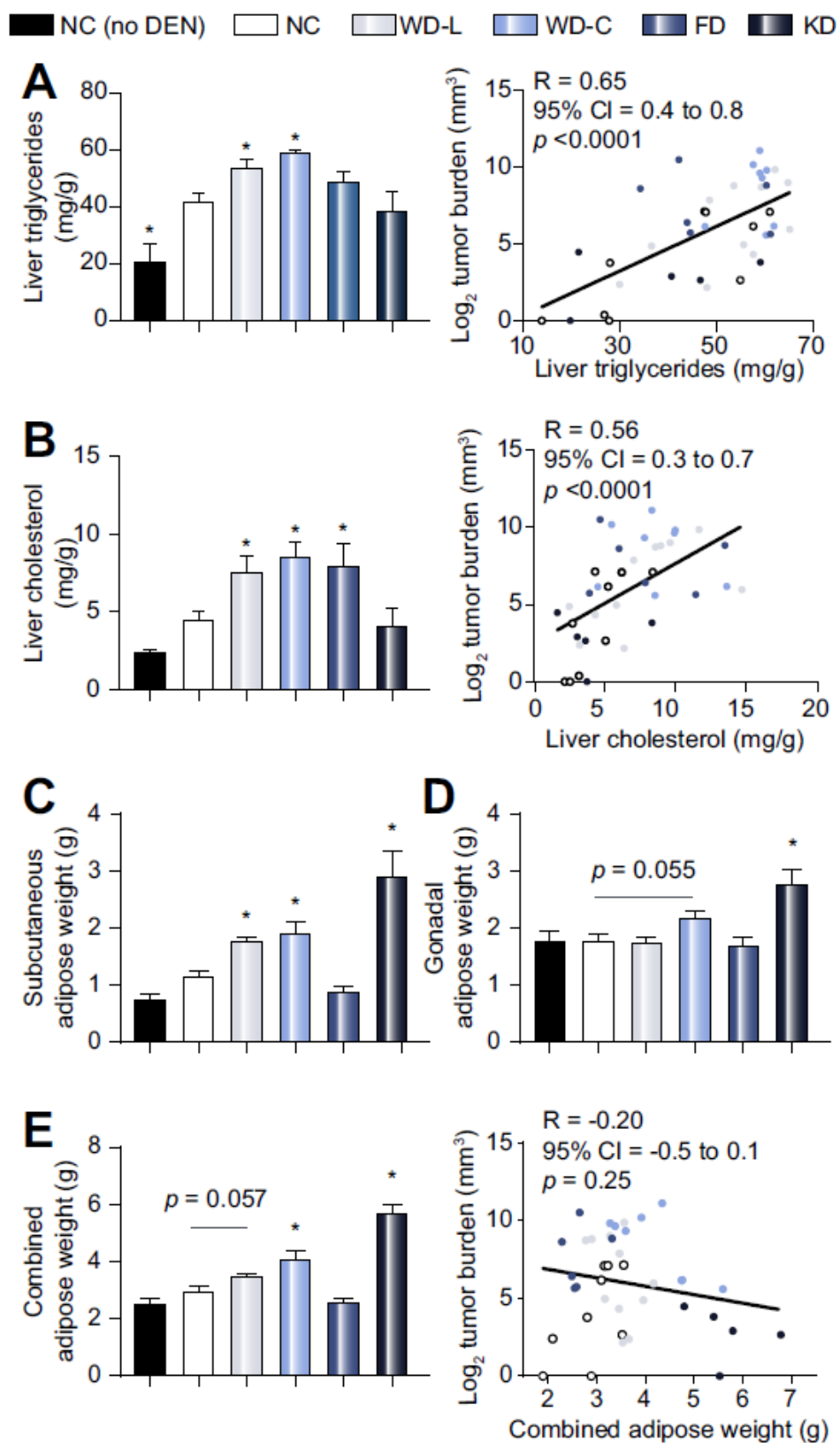


Figure 26. Liver tumor burden is highly correlated with liver fat content, but does not correlate with adiposity in males.

A) Triglycerides and (B) cholesterol were measured in non-tumor-involved liver lipid extracts from mice at 32 weeks of age. Data on the left are averaged per group and data sets on the right represent the correlation between lipid and tumor burden for each individual mouse. (C) Weights of subcutaneous adipose, (D) gonadal adipose, and (E) combined subcutaneous and gonadal adipose of mice at 32 weeks of age. Data in bar graphs are presented as mean \pm SEM. * indicates a significant difference compared to NC, $p < 0.05$ (n = 5–11).

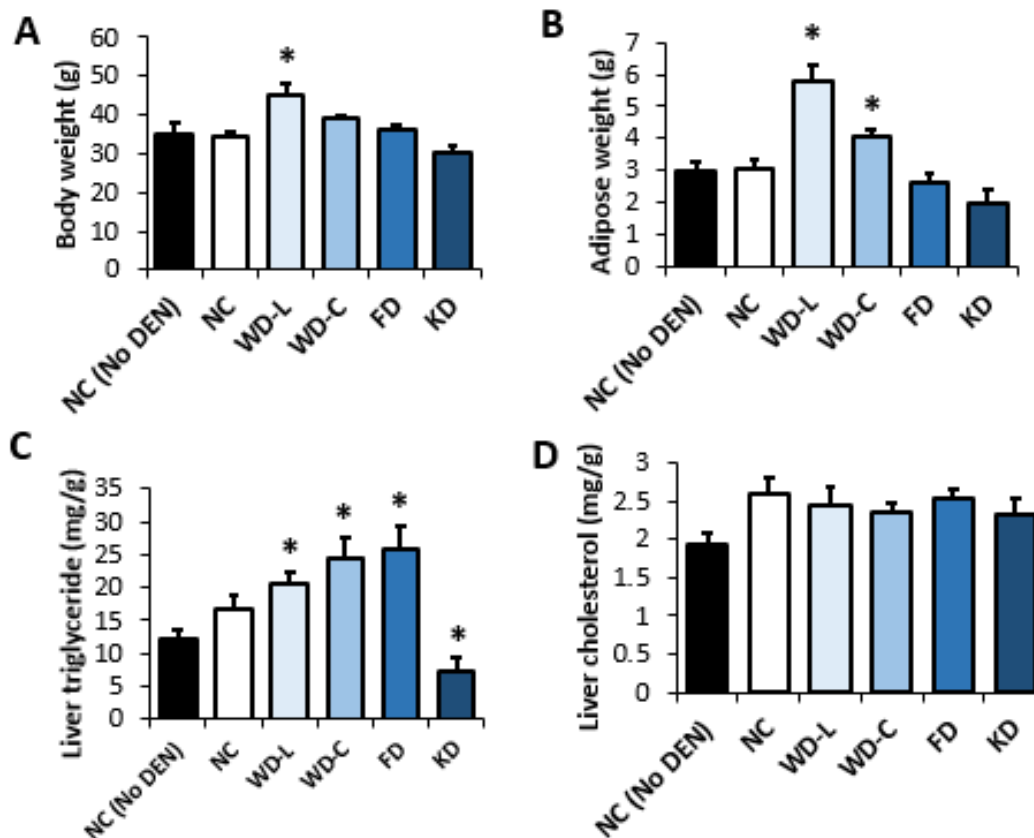


Figure 27. Dietary sugar is associated with increased liver triglycerides in females.

A) Body weights, (B) adipose tissue weights, (C) liver triglyceride content, and (D) liver cholesterol content of 40-week-old female wildtype C57BL/6N mice treated with DEN at 2 weeks of age. * indicates significant difference from NC, $p < 0.05$ ($n=5-9$). Error bars represent $\text{mean} \pm \text{SEM}$.

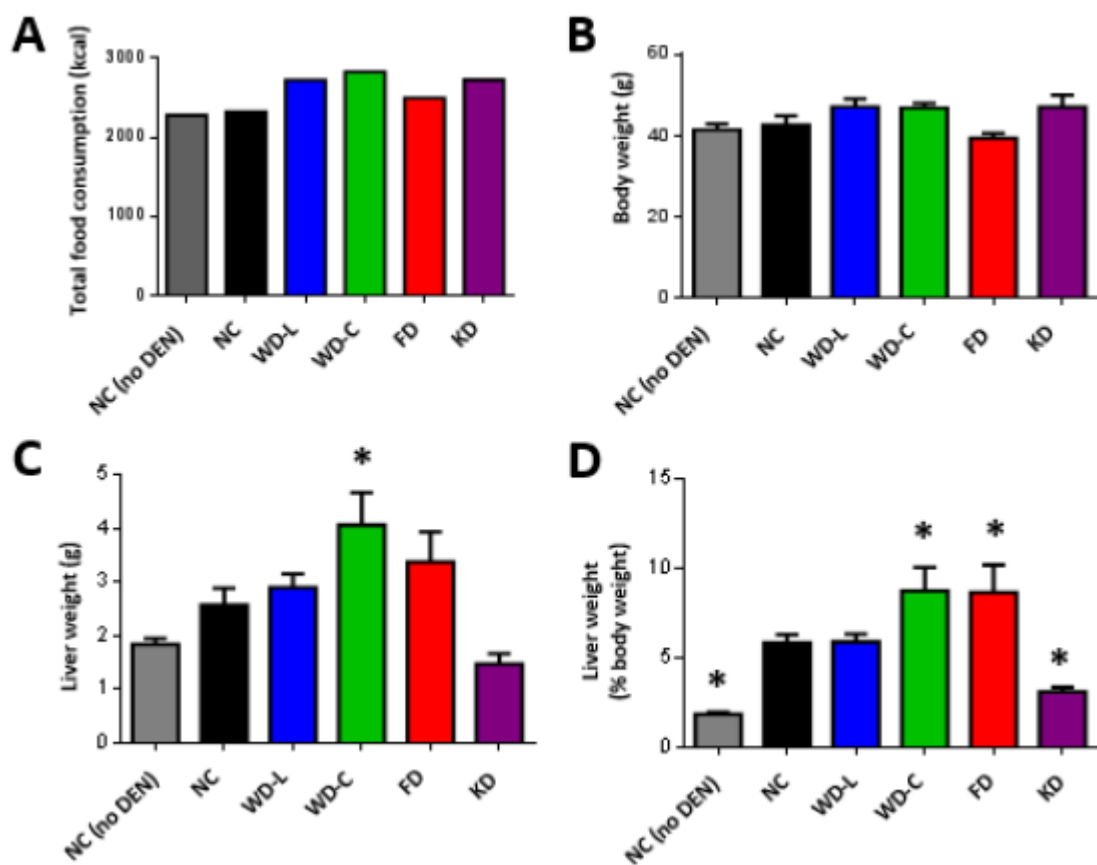


Figure 28. Food consumption, body weight, and liver weight in males.

A) Average cumulative food consumption per mouse over the course of the study. Data presented as mean. (B) Final body weight of mice at 32 weeks of age. Liver weight (C) and liver to body weight (D) of mice at 32 weeks of age. For B-D, data presented as mean \pm SEM. * indicates a significant difference compared to NC, $p < 0.05$ ($n = 5-11$).

4.1.4 Metabolic effects

At 16 weeks of diet, serum insulin and glucose levels were measured in random-fed (Figure 29A and B) and overnight-fasted mice (Figure 29C and D). Mice fed WD-L and WD-C had significantly elevated serum insulin levels in the postprandial fed state compared to mice fed NC. Furthermore, serum insulin levels in the postprandial state positively correlated with tumor burden when compared as independent parameters irrespective of diet (Figure 29A). Postprandial fed blood glucose levels were similar between all diet groups (Figure 29B). Fasting hyperglycemia was observed in mice fed WD-L and WD-C (Figure 29C), but fasting hyperinsulinemia was only observed in mice fed WD-C (Figure 29D). Homeostatic model assessment of insulin resistance (HOMA-IR) calculations indicated that mice fed WD-L and WD-C were insulin resistant under basal fasting conditions (Figure 29E). Furthermore, mice fed WD-L and KD diet displayed marked glucose intolerance compared to mice fed NC (Figure 29F). In sum, of the metabolic parameters evaluated, post-prandial insulin was the major factor associated with increased tumor burden. In contrast, tumor burden was not independently associated with fasting glucose, fasting insulin, glucose tolerance, or HOMA-IR (Figure 30A–D). In females, all mice on experimental diets had significantly worse glucose tolerance compared to mice fed NC (Figure 31A-B).

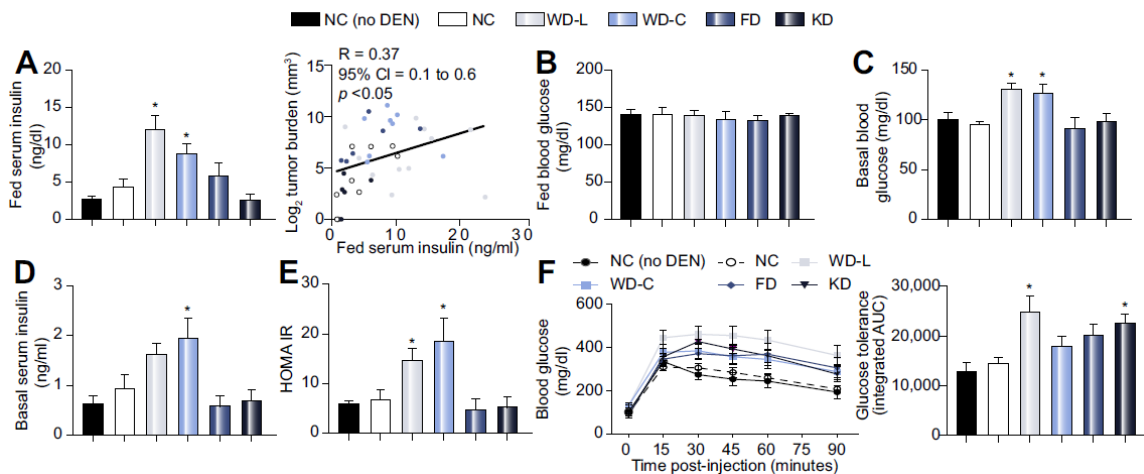


Figure 29. Liver tumor burden is associated with post-prandial insulin, but not other parameters of whole-body glucose metabolism in males.

A) Fed serum insulin and (B) glucose levels, and (C) fasted serum insulin and (D) glucose levels after 16 weeks of study diet. (E) HOMA-IR derived from basal blood glucose and insulin levels. (F) Blood glucose levels in mice over time and integrated area under the curve (AUC) for glucose tolerance. Data in bar graphs and line graphs presented as mean \pm SEM. * indicates a significant difference compared to NC, $p < 0.05$ ($n = 5-11$).

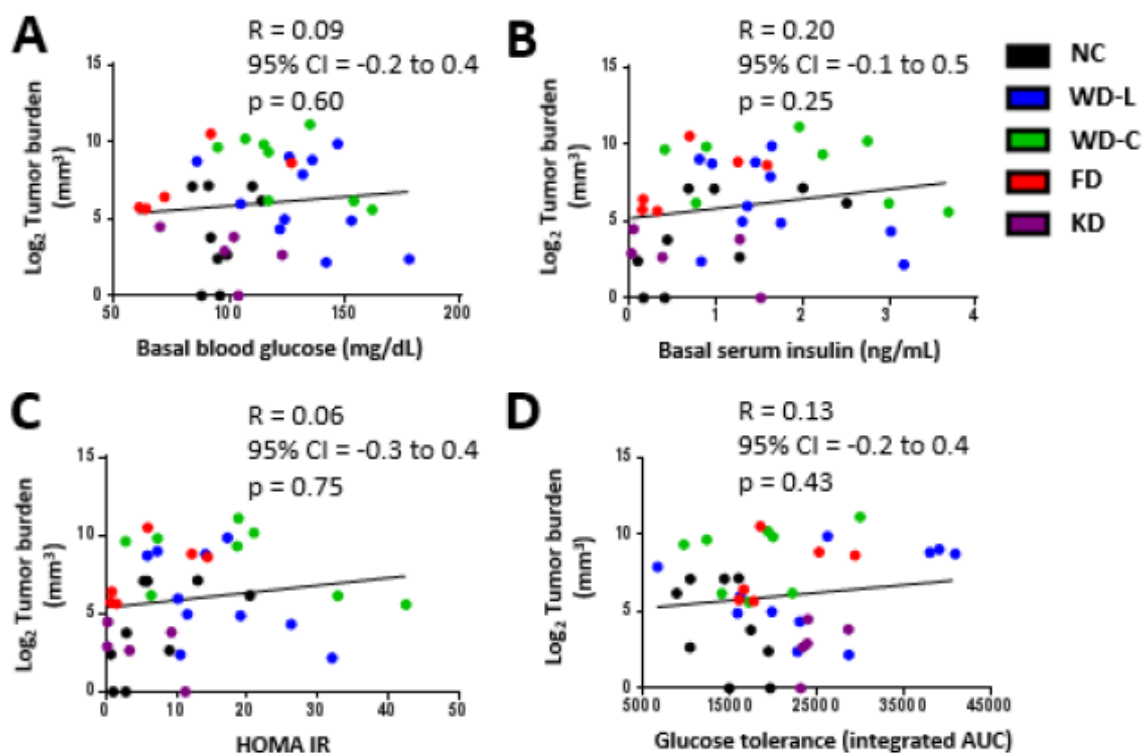


Figure 30. Association of liver tumor burden with parameters of whole-body glucose metabolism in males.

Correlation analyses of tumor burden and fasted serum insulin (A), basal blood glucose (B), HOMA-IR (C), and glucose tolerance (integrated AUC) (D) after 16 weeks of study diet. Linear regression and Pearson correlation analyses were used to test for correlation with tumor burden (n=5-11).

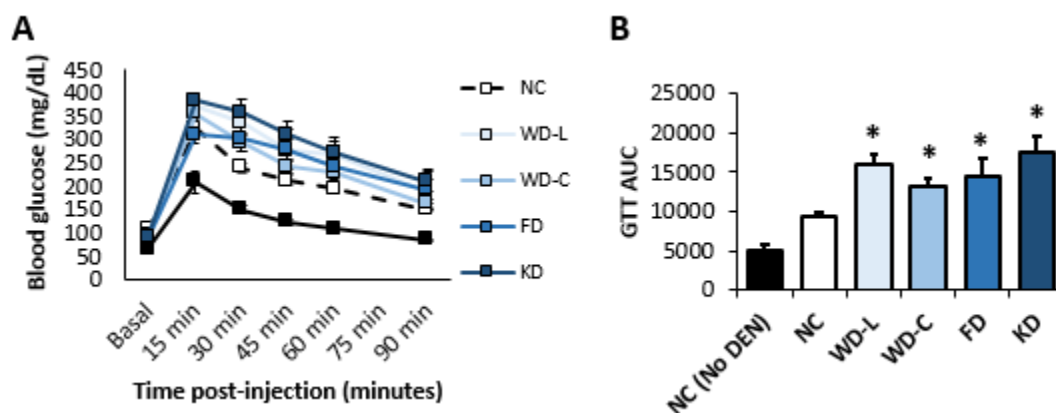


Figure 31. Glucose tolerance in females.

A) Blood glucose levels in mice over time and **(B)** integrated area under the curve (AUC) during a glucose tolerance test in 22-week-old female C57BL/6N mice. * indicates significant difference from NC, $p < 0.05$ ($n=5-9$). Error bars represent mean \pm SEM.

4.1.5 Inflammation

To examine whether diet-induced inflammation was associated with liver tumor burden, we measured mRNA expression of IL-6, IL-1 β , and TNF α as markers of inflammation in non-tumor involved liver tissue. Although no individual diet significantly increased liver IL-6 expression, there was a significant positive association between tumor burden and liver IL-6 expression at the level of individual mice (Figure 32A, right panel). In contrast, while mice fed the WD-C had significantly increased IL-1 β and TNF α expression, neither IL-1 β nor TNF α were independently associated with tumor burden (Figure 33A and B). Furthermore, serum inflammatory markers IL-6 or TNF α were not related to tumor burden (Figure 34A and B). Collectively, of the liver and serum inflammatory markers measured, only liver IL-6 mRNA expression significantly correlated with tumor burden across diet groups.

4.1.6 Serum adipokines

Leptin and adiponectin are adipokines altered with obesity and both hormones are linked to insulin sensitivity and cancer. Serum analysis of each mouse identified an inverse correlation between serum adiponectin and both dietary sugar intake (WD-L, WD-C, and FD) and tumor burden (Figure 34B). In contrast, leptin was not independently associated with tumor burden despite significantly higher concentrations in mice fed Western diets (WD-L and WD-C) (Figure 34C).

4.1.7 Liver protein expression

To examine potential mechanisms by which diet affects liver tumor burden, we performed Western blot analysis of proteins in both tumor tissue and non-tumor liver tissue. We first examined expression and activation of proteins involved in genotoxic stress response, growth and survival. AMP-activated protein kinase (AMPK) is known to be phosphorylated and activated under conditions of genotoxic stress²³⁰. Consistent with this, we observed that AMPK was hyper-phosphorylated in liver tissue of mice treated with DEN compared to non-DEN-treated mice (Figure 32A and C). However, we did not detect any cancer-specific difference in the regulation of AMPK targets including p53 expression²³¹ or mTORC1 activity (as determined by p70S6K phosphorylation at T389) (Figure 32C and Figure 35A, B, and D). In summary, DEN increased both AMPK and mTORC1 activity, but their activity was not correlated to diet or tumor burden in the DEN model of liver cancer.

SIRT1 is an NAD⁺-dependent deacetylase that can also be activated under genotoxic stress. Active SIRT1 can deacetylate p53 at K379, resulting in reduced p53 activity as well as degradation²³². SIRT1 was not differentially expressed between groups (Figure 35A and F); however, DEN treatment led to decreased acetylated p53 at K379 in all diet groups except KD (Figure 35A and E).

We next examined the expression of proteins involved in cell cycle regulation and apoptosis. Compared to mice fed low-sugar diets (NC and KD), mice fed the high-sugar diets (WD-L, WD-C, and FD) had lower p21 protein expression (Figure 32C and D) and less cleaved caspase-3 (CASP3) (Figure 32C and E). Together, these data indicate that high sugar diets are associated with anti-apoptosis (reduced CASP3 cleavage) and increased cell cycle progression (reduced p21 expression).

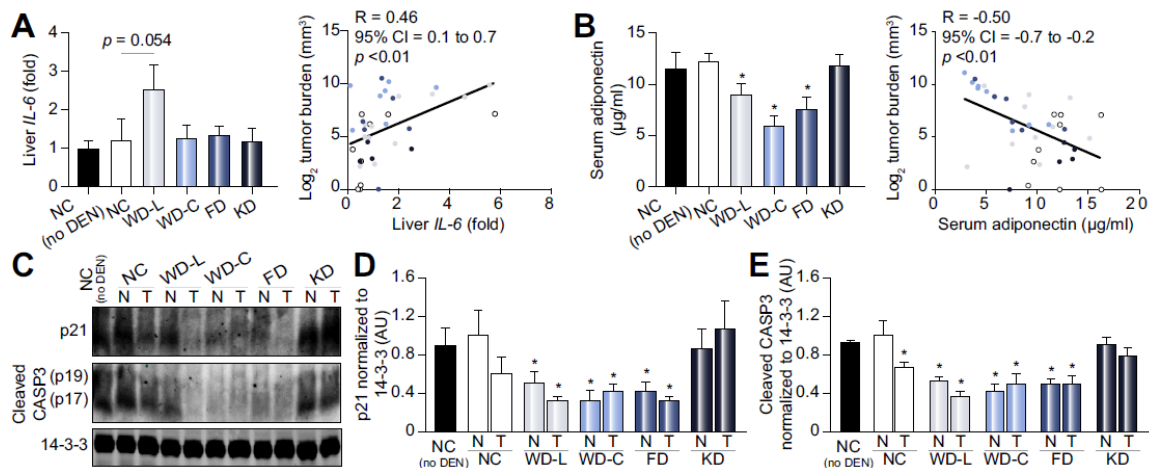


Figure 32. Liver tumor burden is positively correlated with liver IL-6, but negatively associated with serum adiponectin and apoptosis in males.

A) Fold-change in mRNA expression of IL-6 in non-tumor-involved liver tissue. (Left panel); IL-6 expression level averaged by diet. (Right panel) IL-6 expression compared to tumor burden for each mouse in the study. (B) Adiponectin concentration in serum collected from mice at 32 weeks of age, averaged per diet (left panel) and compared to tumor burden in each mouse (right panel) (for A and B. $n = 5-11$). (C) Protein expression in tumor tissue and non-tumor-involved liver tissue from mice at final harvest. 14-3-3 was used as a loading control. Protein expression was measured in at least three independent mice for each group; one representative set is shown. Quantitation of Western blot band densities for (D) p21 and (E) cleaved CASP3 (for D and E, $n = 3$). Data in bar graphs are presented as mean \pm SEM. * indicates a significant difference compared to NC, $p < 0.05$.

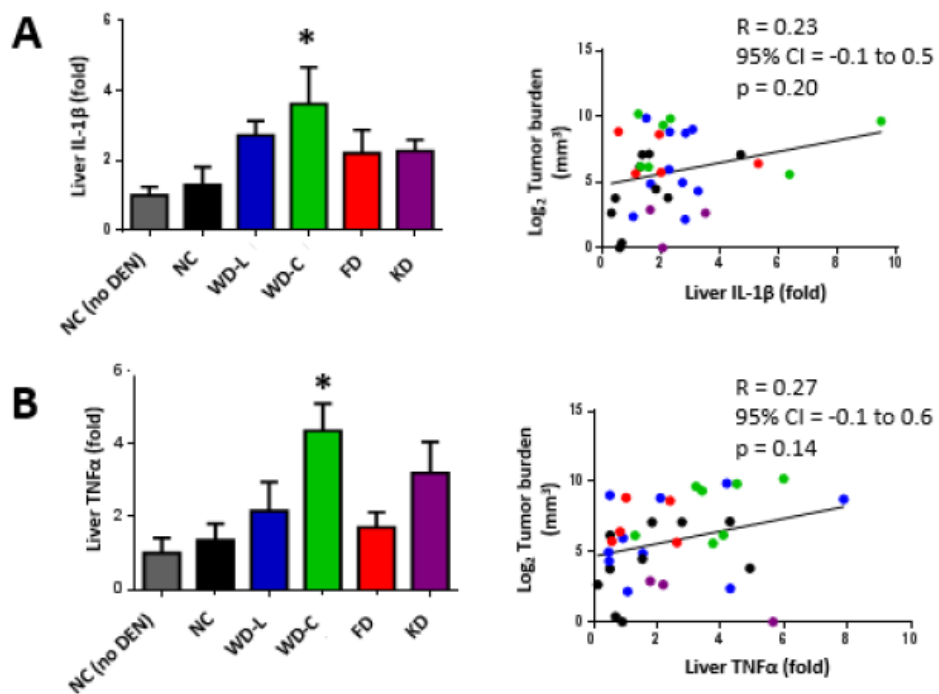


Figure 33. Liver inflammatory markers in males.

Fold change in mRNA expression of IL-1 β (A) and TNF α (B) in non-tumor-involved liver tissue. Data in bar graphs presented as mean \pm SEM. * indicates a significant difference compared to NC, $p < 0.05$ ($n = 5-11$).

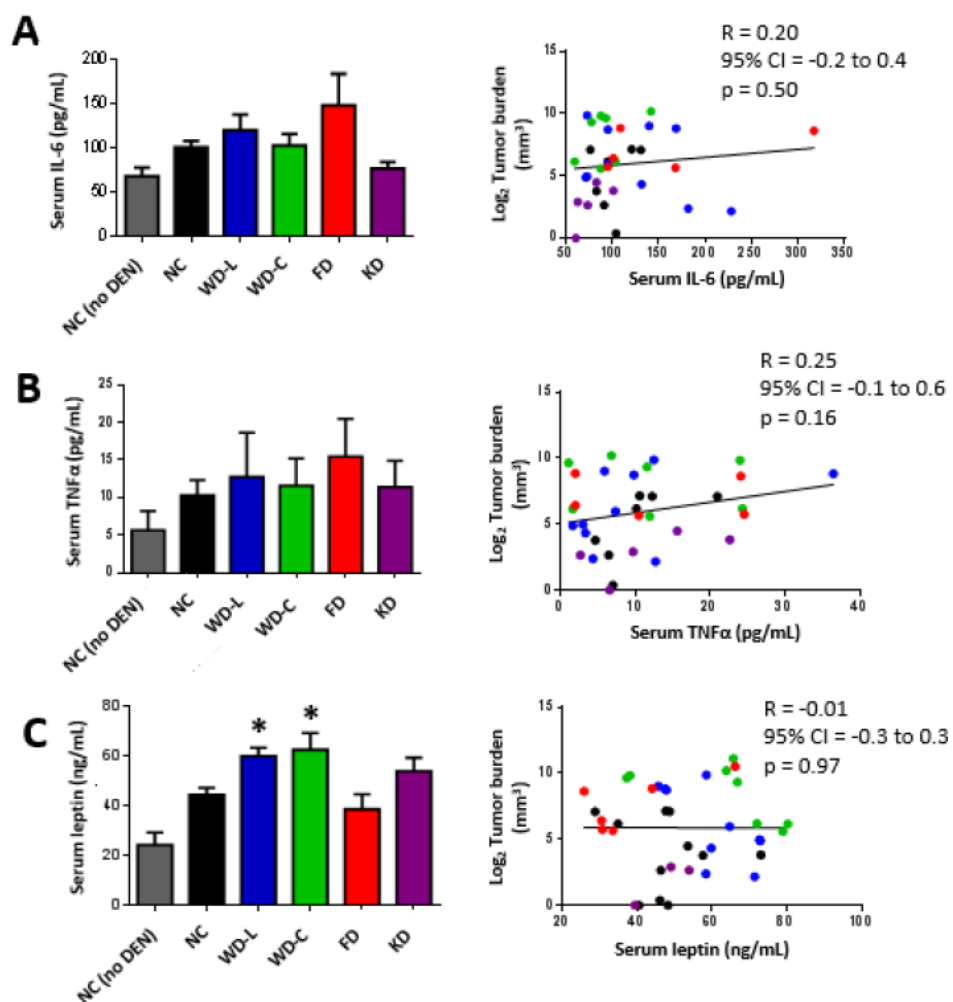


Figure 34. Serum inflammatory markers in males.

Serum concentrations of IL-6 (A), TNFα (B), and leptin (C). Data in bar graphs presented as mean±SEM. * indicates a significant difference compared to NC, p<0.05 (n=5-11).

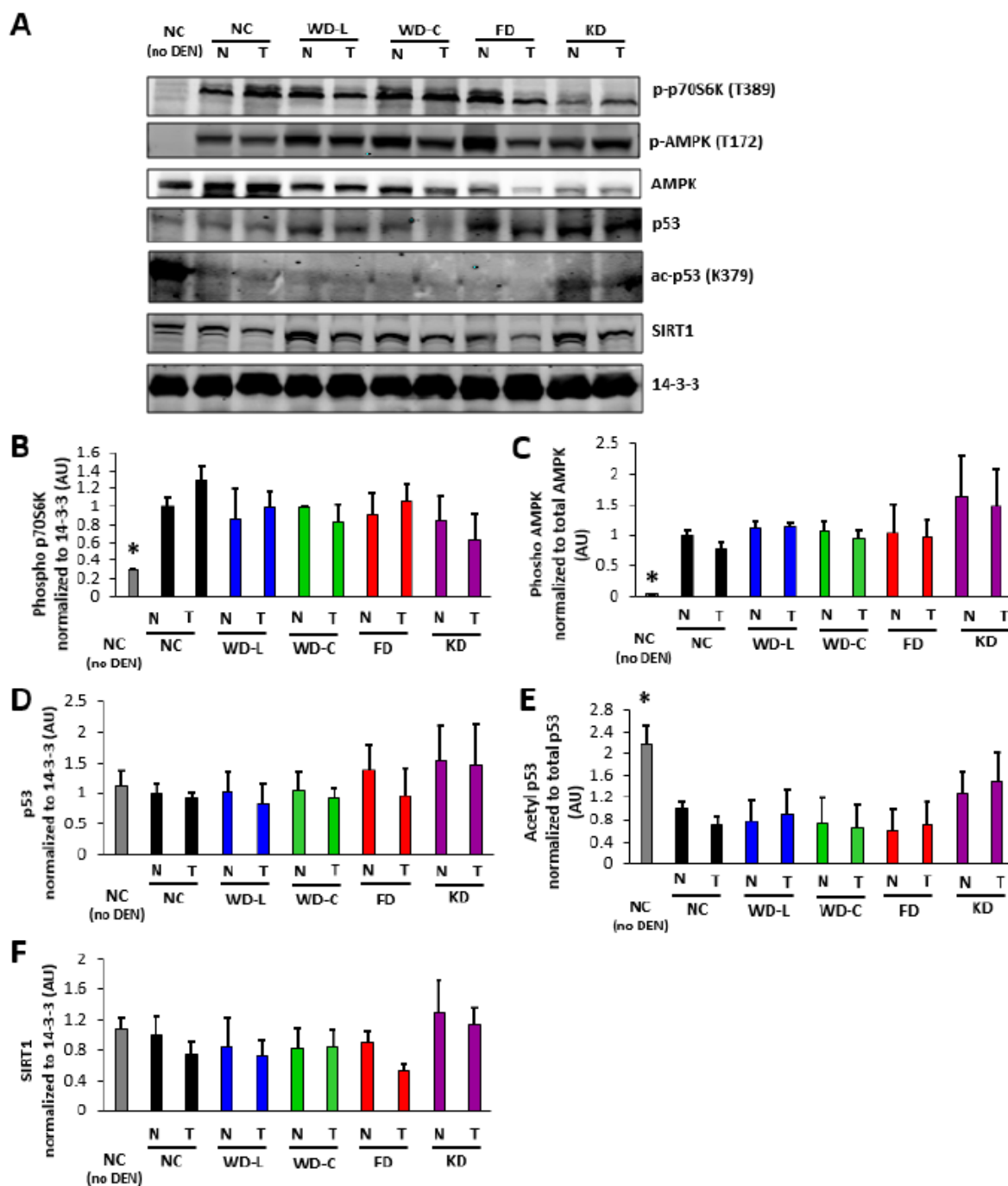


Figure 35. Liver protein expression.

A) Protein expression in non-tumor-involved and tumor liver tissue from mice at final harvest. 14-3-3 was used as a loading control. Protein expression was measured in at least three independent mice for each group; one representative set is shown. Quantitation of Western blot band densities for phosphorylated p70S6K (B), phosphorylated AMPK (C), p53 (D), acetylated p53 (E), and SIRT1 (D). For B-F, data presented as mean \pm SEM. * indicates a significant difference compared to NC, $p < 0.05$ (n=3).

4.1.8 Discussion

The etiology of obesity-related primary liver cancer is thought to evolve through stages of non-alcoholic fatty liver disease (NAFLD), non-alcoholic steatohepatitis (NASH), fibrosis and cryptogenic cirrhosis²³³. Obesity is a risk factor for NAFLD; therefore, it is considered to be a proximal contributor to the progression of liver cancer²³⁴⁻²³⁶. However, it remains unclear whether obesity per se or the chronic intake of obesigenic macronutrients is most important in promoting liver cancer tumor growth^{237,238}. The purpose of this study was to investigate the interplay between dietary nutrients under controlled and well-defined conditions using the DEN model of murine liver cancer.

Of the 5 diets tested in this study, 2 diets served as known controls. The lard-based Western diet is known to increase liver tumor burden compared to a normal chow diet^{183,239}, and the mechanism is widely thought to be a consequence of obesity-related metabolic disturbances. However, the other 3 test diets (coconut oil-based Western diet, lipogenic high fructose diet, and ketogenic diet) have not previously been evaluated in a mouse model of liver cancer. By comparing these diets, we observed that adiposity can be uncoupled from primary liver tumor burden. For example, mice fed a ketogenic diet rich in lard had low tumor burden despite marked adiposity. In addition, mice fed a lipogenic fructose diet were lean but had considerable tumor burden compared to mice fed NC diet. The NC and FD diets had equivalent fat and carbohydrate compositions, but the majority of carbohydrates in FD were from sugars (sucrose and fructose), whereas the carbohydrates in NC were from uncooked starch (complex glucose polysaccharides).

Importantly, mice fed FD developed considerable tumor burden despite being the leanest group. In addition, FD feeding did not increase other cancer-related phenotypes including liver inflammation or glucose intolerance compared to normal chow-fed controls. It is notable that the DEN-treated C57BL/6N mice fed Western diets gained increased adiposity, but did not gain significantly more body mass compared to mice fed NC. In other studies, DEN-treated C57BL/6J mice fed Western diets have a more robust increase in both body mass and adiposity; e.g., Park et al.¹⁸³. The reason for the lack of a large fold-change in body mass in this study is related to the fact that C57BL/6N mice fed NC diet are larger than baseline C57BL/6J mice fed NC diet. For example, the NC-fed mice in this study weighed on average 41 grams, which is a higher body mass compared to adult C57BL/6J mice in similar studies¹⁸³. This body weight phenotype difference is consistent with recent studies comparing the C57BL/6J and C57BL/6N strains, wherein C57BL/6N mice gained more body weight over time than C57BL/6J mice fed NC diet^{240,241}. Because the C57BL/6N mice in our study gained considerable body weight with chow feeding, the high calorie diets did not have pronounced obesigenic effects. This result strongly supports a role for dietary sugar intake in tumor burden that is independent of obesity and obesity-related phenotypes.

We also investigated whether altering only the type of dietary fat could affect tumor burden. Lard fat is composed of 95% long chain fatty acids. Consumption of high-fat high-sucrose lard-based diets results in impaired whole-body glucose tolerance. In contrast, coconut oil is composed of 63% medium-chain fatty acids that are highly saturated, have less deleterious effects on whole-body glucose tolerance than lard-based

diets (Figure 29F), but exacerbate liver fat accumulation²²⁵. We observed that both WD-L and WD-C had increased tumor burden compared to NC; however, mice fed WD-C had the greatest tumor burden and tumor multiplicity of all diets. One possibility is that the lipogenic nature of medium chain fat diets contributes to worsening disease progression. These findings may have implications for dietary consideration in Southeast Asian populations that readily consume coconut oil and also have among the greatest incidence of hepatitis and liver cancer worldwide^{242,243}.

Numerous studies have linked the pro-inflammatory cytokines IL-6, IL-1 β , and TNF α to liver cancer. Liver inflammation accompanies steatosis in the development of NASH^{233,244} and liver cancer in humans^{234,245,246}. We observed that liver IL-6 expression was positively associated with tumor burden. Recently, a study by Park et al. demonstrated that IL-6 knockout mice treated with DEN and fed a lard-based Western diet had less liver tumor burden than wild type controls fed the same diet¹⁸³. Although this study demonstrates that loss of IL-6 is protective against liver cancer, it should be noted that the IL-6 mutant mice were leaner than controls, had lower liver triglycerides, and had lower serum insulin levels¹⁸³. Thus, one possibility is that the beneficial alterations in serum insulin or liver fat content in IL-6 knockout mice confer this protection from liver cancer.

In the present study, liver steatosis was highly associated with liver tumor development. Compared to mice fed NC, mice fed diets with the highest sugar content (WD-L, WD-C, and FD) had the greatest liver lipid content and tumor burden. Since insulin and IL-6 are potent activators of lipogenesis^{247,248}, one possible scenario is that

high sugar consumption, coupled with elevated postprandial insulin and IL-6 expression, provides the stimuli to promote tumor growth. The concept that lipogenesis is an important driver of cancer progression has been suggested previously^{191,197,249}. Consistent with this concept is our observation that mice fed diets low in sugar (NC and KD) had the lowest postprandial insulin, IL-6 expression, liver lipid content and lowest tumor burden. Importantly, our data is in line with a recent prospective human study that identified hyperinsulinemia as a more prominent risk factor for HCC than obesity²⁵⁰.

Adiponectin inhibits the proliferation of liver cancer cells by increasing apoptosis, and low serum adiponectin is linked with poor-prognosis HCC in patients²⁵¹. Previous studies have shown that excess sugar consumption is sufficient to decrease serum adiponectin levels in rats²⁵² and humans²⁵³. In the present study, we observed that serum adiponectin levels were decreased in mice fed diets containing high sugar. We also identified that lower serum adiponectin levels were associated with less cleaved caspase-3 and a decrease in p21 expression in liver tissue. Together, these data support a possible scenario whereby excess sugar intake leads to a reduction in serum adiponectin that consequently impairs apoptosis and/or enables cell cycle progression. The findings of this study are summarized in Figure 36.

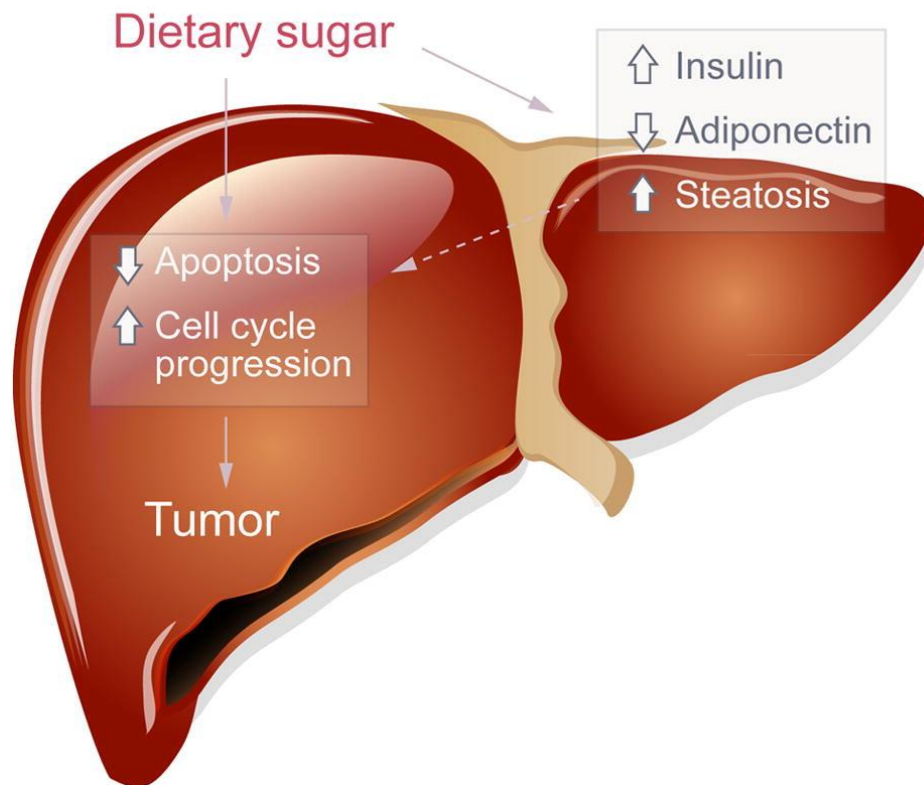


Figure 36. Summary figure of dietary effects on liver tumor burden in mice treated with DEN

Dietary sugar was associated with decreased apoptosis and increased cell cycle progression, leading to higher liver tumor burden. Dietary sugar also increased post-prandial insulin, decreased serum adiponectin, and caused liver steatosis, which may be linked to alterations in cell survival, cell cycle progression, and tumor progression.

4.1.9 Summary

In summary, this study demonstrates the powerful influence of nutrition on primary liver cancer growth and progression. The matrix of diets used in this study provides strong evidence that dietary sugar consumption is more significant for tumor growth than over-nutrition (e.g., excess dietary fat), adiposity, and/or insulin resistance. These data reduce the complexity of the metabolic milieu associated with liver tumor growth and narrow attention on roles for adiponectin, post-prandial hyperinsulinemia, and liver lipogenesis. Future nutritional studies in mice are necessary to determine whether established liver tumor growth can be stalled or reversed if sugar is removed from the diet. If so, these data would provide pre-clinical evidence to support testing dietary intervention in patients diagnosed with primary liver cancer.

4.2 Effect of ACC inhibition on hepatocellular carcinoma development

4.2.1 Background

Hepatocellular carcinoma (HCC) is one of the deadliest cancers in the world. In spite of aggressive screening, less than 25% of patients are eligible for potentially curative surgical resection or liver transplantation owing to the presence of advanced-stage cancer or fibrotic liver disease. There are currently no curative pharmacological interventions for HCC. Sorafenib, a multi kinase inhibitor, is approved for unresectable HCC, but only a minority of patients are responsive and the survival benefits are often limited to just a few months²⁵⁴. For many patients, only palliative care can be offered, especially in advanced cases²⁵⁵. These sobering facts illustrate the need to identify new therapeutic targets for the treatment or prevention of liver cancer.

A well-known metabolic phenotype of HCC is increased lipogenesis^{190–192,256}, but whether this alteration has a functional role in HCC etiology remains unclear. Acetyl-CoA carboxylase (ACC) enzymes are required for lipogenesis, and we have previously validated that mice lacking hepatic ACC activity are completely deficient in lipogenesis²¹². There is strong rationale for targeting ACC enzymes in liver cancer. First, Calvisi and colleagues reported an increase in ACC1 enzyme expression in HCC tumor tissue that correlated with decreased survival¹⁹¹. Second, in the same study, the knockdown of ACC1 was sufficient to increase apoptosis and reduce the viability of human HCC cells *in vitro*¹⁹¹. Third, Yahagi and colleagues¹⁹⁰ evaluated ten HCC cases and observed increased ACC1 expression in tumor tissue compared to adjacent non-cancerous liver tissue of all cases. Finally, ACC enzymes are druggable targets. Based on

this evidence, there is considerable interest in testing whether ACC enzymes represents therapeutic drug targets for the prevention or treatment of HCC. In the present study we investigated the role of lipogenesis in liver tumor development using mice that lack ACC activity in the liver.

4.2.2 Results

HCC has a distinct lipogenic phenotype compared to non-cancerous liver

To better understand the relationship between ACC expression and HCC in a broad patient population, we used the Oncomine database to evaluate ACC expression in more than 300 HCC and non-cancerous liver specimens. These data showed that ACC1 (*ACACA*) gene expression was elevated by 2-fold in HCC compared to non-cancerous liver (Figure 37A). Of the HCC cases that had associated clinical data, *ACACA* expression was positively associated with tumor grade (Figure 37B). In contrast, ACC2 gene (*ACACB*) expression was significantly decreased by 25% in HCC tumor tissue compared to non-cancerous liver tissue, and was not associated with tumor grade (Figure 38A-B).

We next compared these results in humans with mouse liver tumors caused by the hepatocellular carcinogen diethylnitrosamine (DEN). DEN is the most commonly-used mouse model of liver tumorigenesis and DEN-induced tumors are known to have genetic signatures related to poor prognosis in humans¹⁶⁹. Furthermore, the DEN model demonstrates similarities to human HCC in the context of gender bias and mechanisms of

tumor initiation involving oxidative damage²²²⁻²²⁴. Herein, we show that DEN-induced liver tumors had a 2-fold increase in *Acaca* expression compared to non-tumor tissue of DEN-treated mice, and nearly 3-fold increase compared to normal liver of age-matched control mice that were naïve to DEN (Figure 37C). In contrast, hepatic *Acacb* expression was decreased by 50% in tumor tissue compared to non-cancerous tissue in DEN-treated mice (Figure 38C). These data show that DEN-induced liver tumors in mice closely resemble human HCC with respect to changes in ACC gene expression.

To determine whether the lipogenic program of liver cancer is maintained outside of the tumor environment in mouse and human liver cancer cells, we measured rates of lipogenesis in human HCC cells (HepG2 and HuH7), murine hepatoma cell lines (Hepa1-6 and Hepa1c1c7), primary non-cancerous murine hepatocytes (hepatocytes), and human immortalized non-cancerous liver cells (PH5CH8). Compared to non-cancer cells, all cancer cells had significantly higher rates of lipogenesis irrespective of whether they were derived from mouse or human tissue (Figure 37D). In contrast, these cell lines had no cancer-specific alterations in any other parameter of cellular bioenergetics including basal oxygen consumption rate (OCR), extracellular acidification rate (ECAR), or spare respiratory capacity (Figure 39A-F).

The ultimate goal of chemotherapeutics is to cause selective cytotoxicity to malignant cells without toxicity to non-cancerous cells. Therefore, we investigated whether the inhibition of lipogenesis differentially affected the viability of cancer cells compared to non-cancer cells by treatment with the pan-ACC inhibitor Sorafenib A (SorA). SorA was maximally effective at inhibiting lipogenesis when used at 100 nM

(Figure 38D), and this concentration reduced the viability of the HepG2, Hepa1-6, and Hepa1c1c7 cancer cells, but did not affect viability of the HuH7 cancer cells or the two non-cancerous cells (Figure 37E). These results demonstrate that ACC inhibition has some selectivity for killing cancerous liver cells compared to non-cancerous cells, but not all malignant cells are sensitive to SorA.

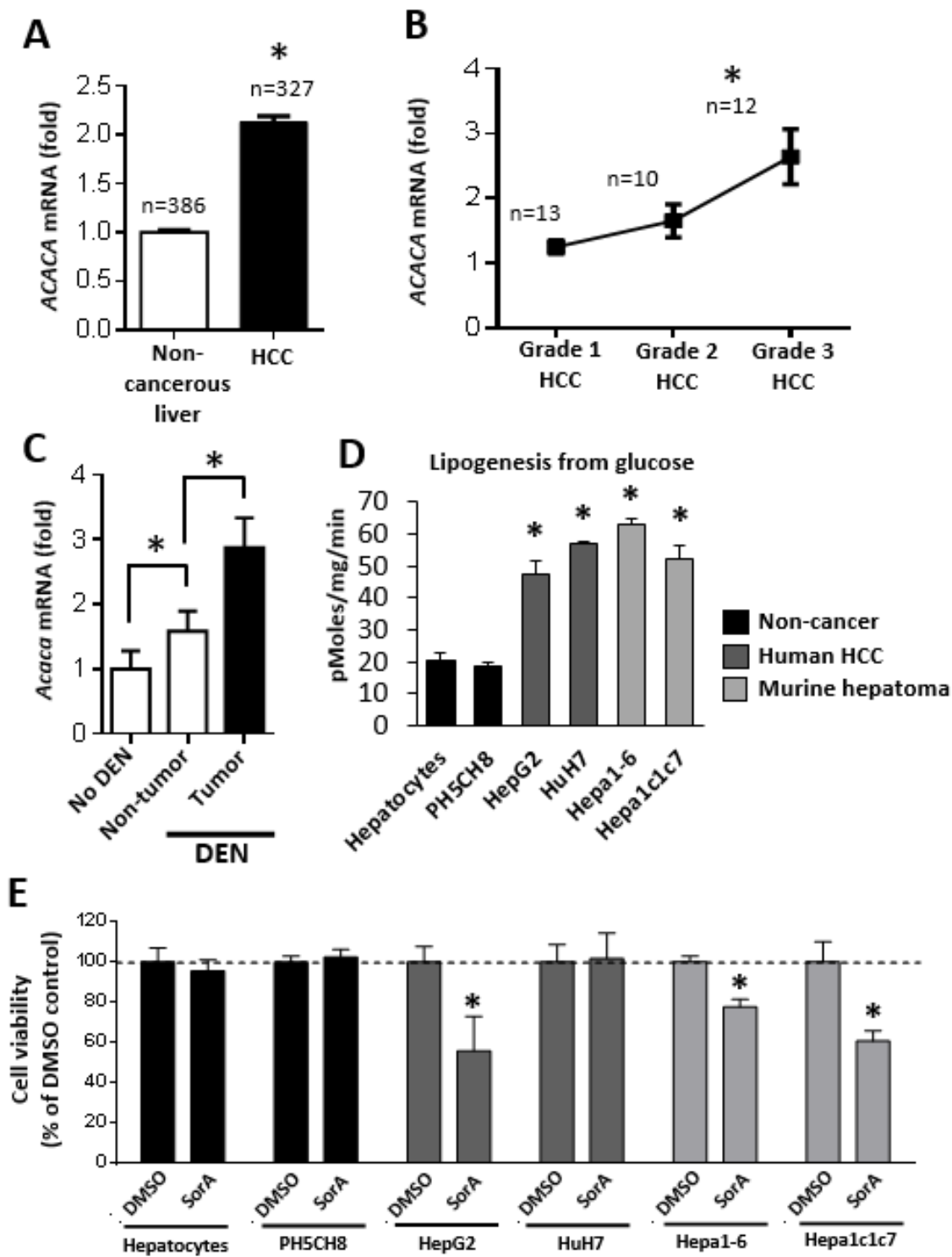


Figure 37. Liver cancer displays a lipogenic phenotype and liver cancer cells are programmed for dependency on lipogenesis.

(A) Fold *ACACA* mRNA expression in human non-cancerous liver and HCC. (B) Fold *ACACA* mRNA expression by HCC grade. * indicates significant difference from Grade 1 HCC. (C) Fold *Acaca* mRNA expression in non-tumor or tumor liver tissue of C57BL/6N mice untreated or treated with DEN at 2w of age and harvested at 32w of age (n=4-9). Rates of (D) lipogenesis in non-cancerous cells (murine hepatocytes and human PH5CH8), and liver cancer cells lines from human (HepG2 and HuH7) and murine origin (Hepa1-6 and Hepa1c1c7). For D, * indicates significant difference from hepatocytes, $p < 0.05$ (n=3-4). (E) Cell viability after treatment with 100nM SorA or DMSO vehicle in the presence of 10% fetal bovine serum for 120h. * indicates significant difference from DMSO, $p < 0.05$ (n=3-4). (B-E) were analyzed by one-way ANOVA. Data are represented as mean \pm SEM.

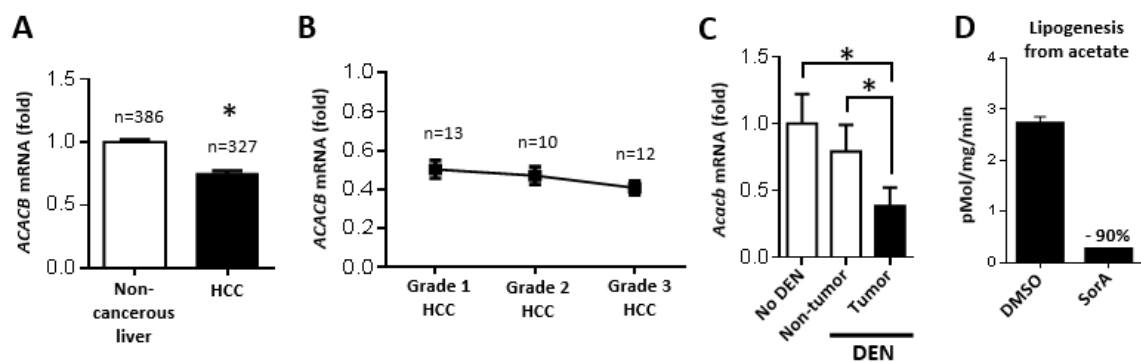


Figure 38. ACC2 mRNA expression in HCC and inhibition of lipogenesis by SorA.

(A) Relative fold *ACACB* mRNA expression in human non-cancerous liver and HCC. (B) Relative fold *ACACB* mRNA expression by HCC grade. (C) Relative fold *Acacb* mRNA expression in non-tumor or tumor liver tissue of C57Bl/6N mice untreated or treated with DEN at 2w of age and harvested at 32w of age (n=4-9). (D) Rates of lipogenesis in primary murine hepatocytes in the presence of 100nM SorA or DMSO vehicle (n=3). B and C were analyzed by one-way ANOVA. * indicates significant difference, $p < 0.05$. Data are represented as mean \pm SEM.

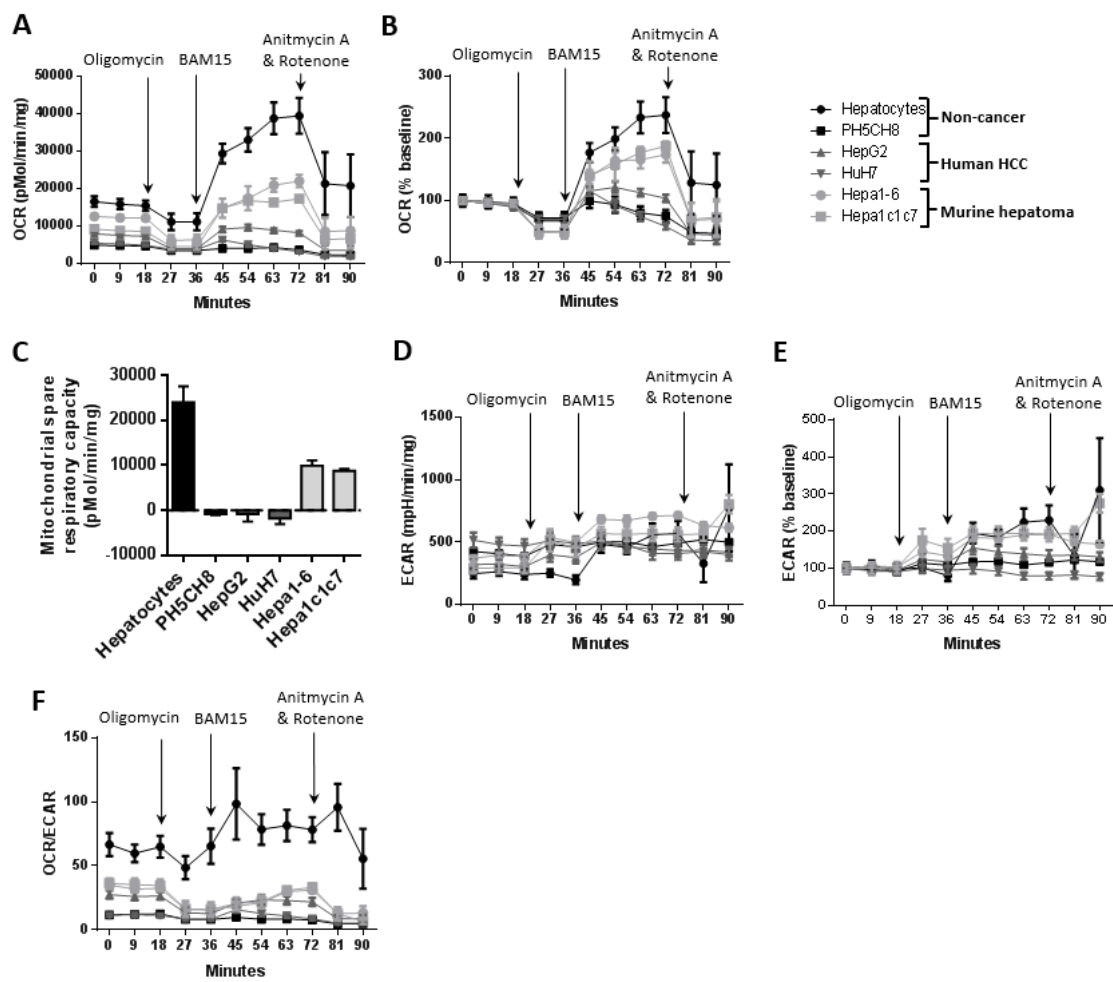


Figure 39. Mitochondrial function in liver non-cancer and cancer cells.

Mitochondrial stress test in whole cells using oligomycin (2 μ M), BAM15 (2 μ M), Antimycin A (10 μ M), and Rotenone (1 μ M) as indicated. Oxygen consumption rate (OCR) (A) normalized to protein or (B) normalized to basal OCR and (C) mitochondrial spare respiratory capacity in non-cancerous cells (primary murine hepatocytes and the immortalized human liver cell line PH5CH8), human liver cancer cell lines (HepG2 and Huh7), and murine liver cancer cell lines (Hepa1-6 and Hepa1c1c7). Extra-cellular acidification rate (ECAR) (D) normalized to protein or (E) normalized to basal ECAR. (F) Ratio of OCR to ECAR (OCR/ECAR) (n=3). Data are represented as mean \pm SEM.

ACC inhibition increases liver tumor incidence and multiplicity in mice

Based on the data shown in Figure 37 and a published study showing that HCC viability is decreased upon knockdown of ACC1¹⁹¹, we hypothesized that ACC activity may be important for the initiation and/or growth of liver tumors. Therefore, we next tested whether liver lipogenesis is necessary for liver tumor development *in vivo* using liver-specific ACC1 and ACC2 double knockout (LDKO) mice²¹². Double knockout mice were used instead of an ACC1-specific knockout because ACC2 can compensate for the loss of ACC1 to catalyze lipid synthesis¹³⁶. Thus, in order to evaluate the role of lipogenesis, it was necessary to inhibit both ACC1 and ACC2. As outlined in Figure 40A, LDKO mice and floxed littermate (Flox) controls were treated with DEN at 2 weeks of age and fed a lipogenic Western diet from 6 weeks until final tumor analysis at 40 weeks of age.

As shown in Figure 40B-D, LDKO mice had a greater than 2-fold increase in tumor incidence than Flox controls. Furthermore, of the mice that developed liver tumors, LDKO mice had significantly higher tumor multiplicity. LDKO livers had higher expression of the liver tumor marker *alphafetoprotein (Afp)* in both tumor tissue and nearby tissue where no macroscopically visible tumors were observed (Figure 423A). Consistent with results in Figure 1C, Flox control mice had higher *Acaca* expression in tumor tissue compared to non-tumor tissue (Figure 42B), while LDKO mice completely lacked gene expression of *Acaca* and *Acacb*, as expected (Figure 42B-C). The lack of ACC expression in LKDO tumor tissue confirms that the tumors did not arise from another cell type. Furthermore, evaluation of a spontaneously immortalized cell line

generated from a LDKO tumor also confirmed the lack of ACC1 or ACC2 expression (Figure 42D) and complete deficiency in *de novo* lipogenesis (Figure 42E) despite continued proliferation in culture. Because hyperproliferation is an important step in the transformation of hepatocytes to HCC²⁵⁷, we performed histological analysis of proliferation in H&E stained liver tissue. LDKO mice had a greater abundance of hyperplastic foci in compared to Flox controls (Figure 40E-F). This result is consistent with the increased *Afp* observed in non-tumor tissue of LDKO mice (Figure 42A), indicating the presence of more preneoplastic foci. This hyperproliferative phenotype was validated by immunohistochemical staining for Ki67, a marker of cell proliferation (Figure 40G-H). In contrast, cleaved caspase 3 (CASP3), a marker of apoptosis, was not significantly different between LDKO and Flox controls (Figure 41A-B).

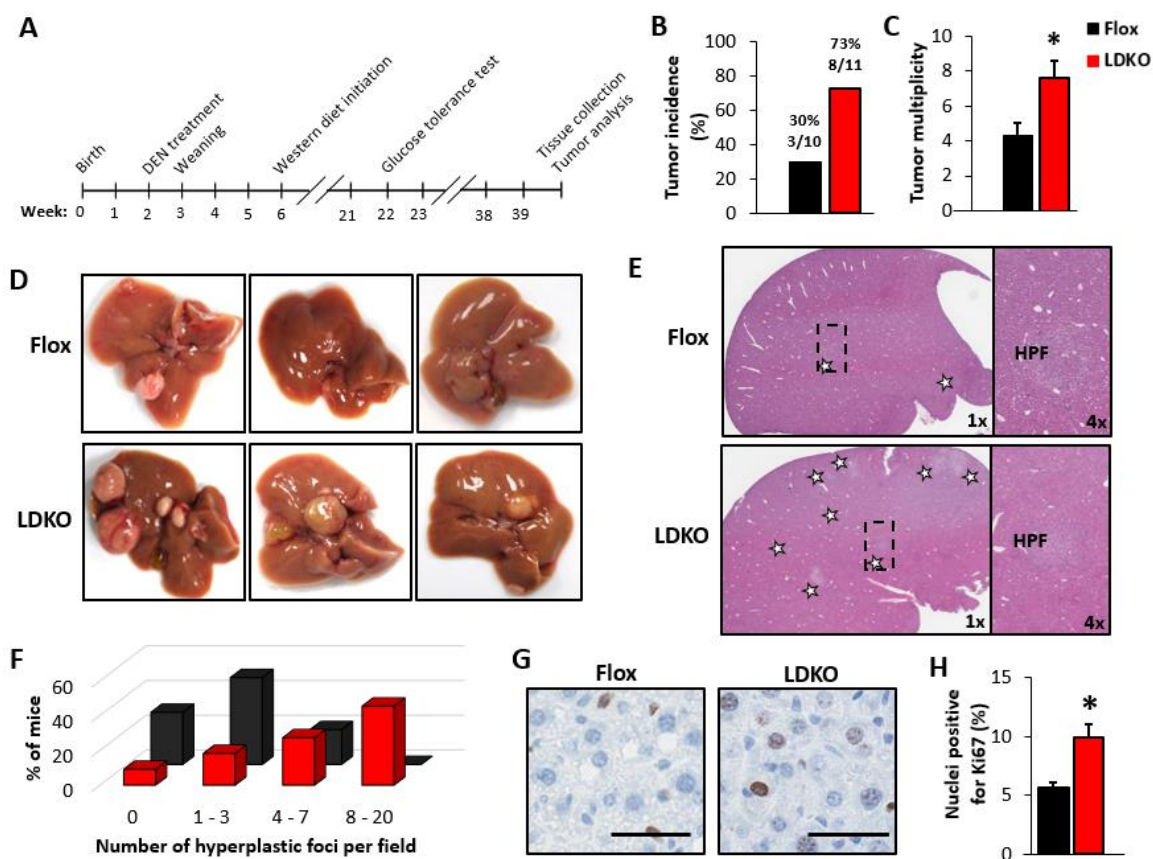


Figure 40. Liver ACC deletion increases diethylnitrosamine-induced tumorigenesis and liver cell proliferation in mice.

(A) Diagram of study timeline. Liver tumor (B) incidence and (C) multiplicity in Flox and LDKO mice treated DEN at 2w of age and harvested at 40w of age. (D) Representative images of livers of DEN-treated LDKO and Flox mice at 40w of age. (E) Representative H&E staining of liver sections of DEN-treated LDKO and Flox mice at 40w of age and (F) quantitation of hyperplastic foci (HPF) per field (white stars indicate hyperplastic foci). (G) Representative images and (H) quantitation of Ki67 IHC. Scale bars=50 μ m. * indicates significant difference, $p < 0.05$ ($n=10-11$). Data are represented as mean \pm SEM.

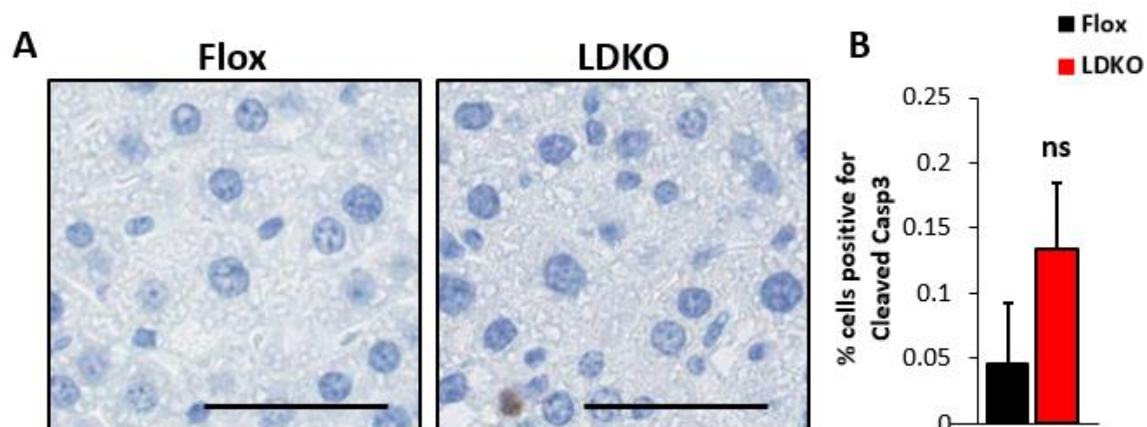


Figure 41. Cleaved CASP3 staining in livers of DEN-treated Flox and LDKO mice.

(A) Representative images and (B) quantitation of Cleaved CASP3 IHC staining of DEN-treated Flox and LDKO mice at 40w of age. Scale bars=50 μ m. Data are represented as mean \pm SEM.

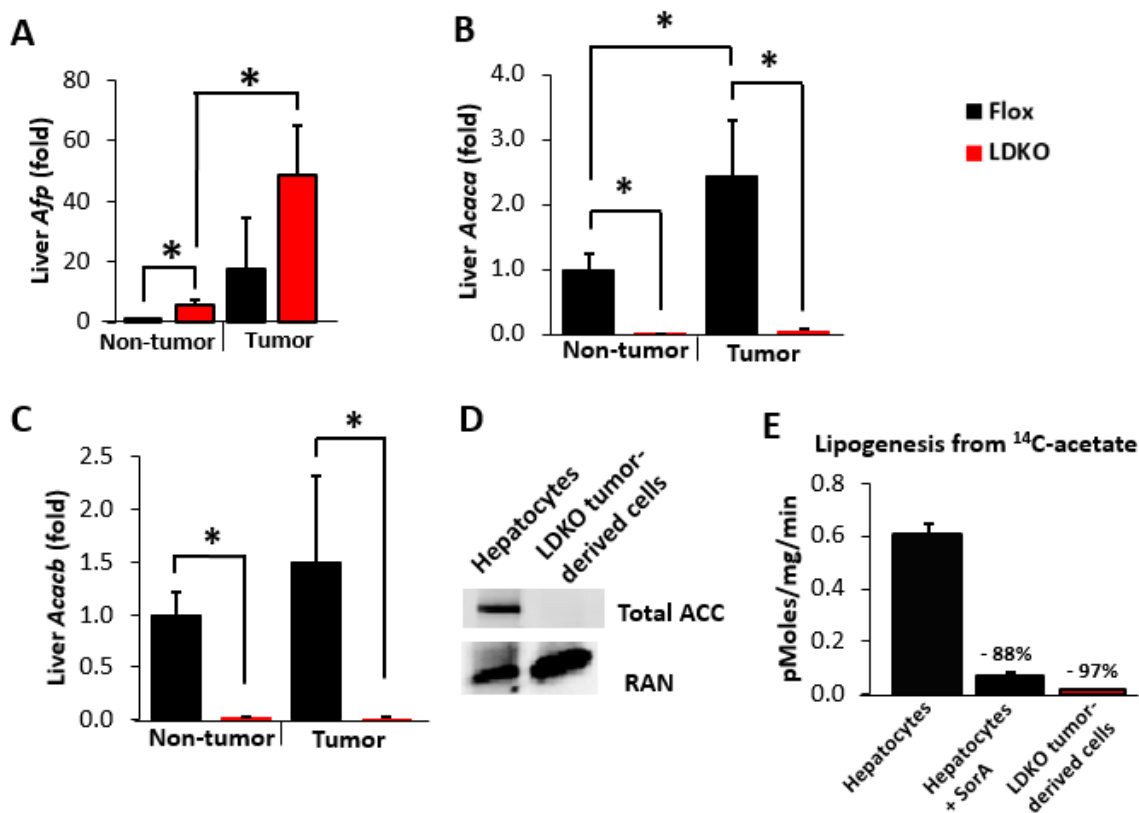


Figure 42. Livers and tumors of LDKO mice are completely deficient in lipogenesis.

Fold mRNA expression of (A) *Afp*, (B) *Acaca* and (C) *Acacb* in non-tumor and tumor liver tissue of DEN-treated Flox and LDKO mice at 40w of age (n=10-11 for non-tumor tissue; n=3-6 for tumor tissue). (D) Protein expression of total ACC1 and ACC2 in isolated primary murine hepatocytes and cells derived from a tumor of a DEN-treated LDKO mouse (LDKO tumor-derived cells). RAN was used as a loading control. (E) Rate of lipogenesis in hepatocytes with or without 100nM SorA, or in LDKO tumor-derived cells (n=3). For F, percent change indicates difference from untreated hepatocytes. * indicates significant difference, $p < 0.05$. A-C were analyzed by one-way ANOVA. Data are represented as mean \pm SEM.

ACC inhibition reprograms hepatocyte metabolism to support survival and proliferation

HCC commonly develops in the setting of obesity, fatty liver, glucose intolerance, and hyperinsulinemia, and these physiological parameters are thought to contribute to risk of developing HCC. Therefore, we next investigated whether differences in physiology or nutrient metabolism may have contributed to increased tumorigenesis in LDKO mice. While LDKO mice had no significant differences in body weight, adiposity, liver triglyceride or cholesterol content, glucose tolerance, or serum insulin levels (Figure 43A-F), there was evidence of considerable metabolic reprogramming in the liver. Genes involved in fatty acid transport (e.g. *Fatp5* and *Cd36*) and their associated transcription factor *Pparg*²⁵⁸ were upregulated in LDKO liver tissue (Figure 44A and C), while genes responsible for mitochondrial fat oxidation (e.g. *Cpt1a* and *Mcad*) and their associated transcription factor *Ppargc1a*²⁵⁹⁻²⁶¹ were decreased (Figure 44B-C). Furthermore, metabolomics analysis showed that succinylcarnitine, a metabolite of mitochondrial fatty acid oxidation, was lower by 50% in LDKO liver tissue (Figure 44D). In contrast, gene expression of other transcription factors involved in lipid metabolism was unchanged, including SREBP1c and PPAR α (Figure 44C). These data suggest that LDKO liver tissue compensates for the lack of lipogenesis to maintain normal triglyceride levels by increasing fat uptake and decreasing fat oxidation. Since hepatic ACC inhibition did not affect physiological parameters associated with HCC, we hypothesized that the increased tumor development in LDKO mice was related to liver-intrinsic metabolic compensations.

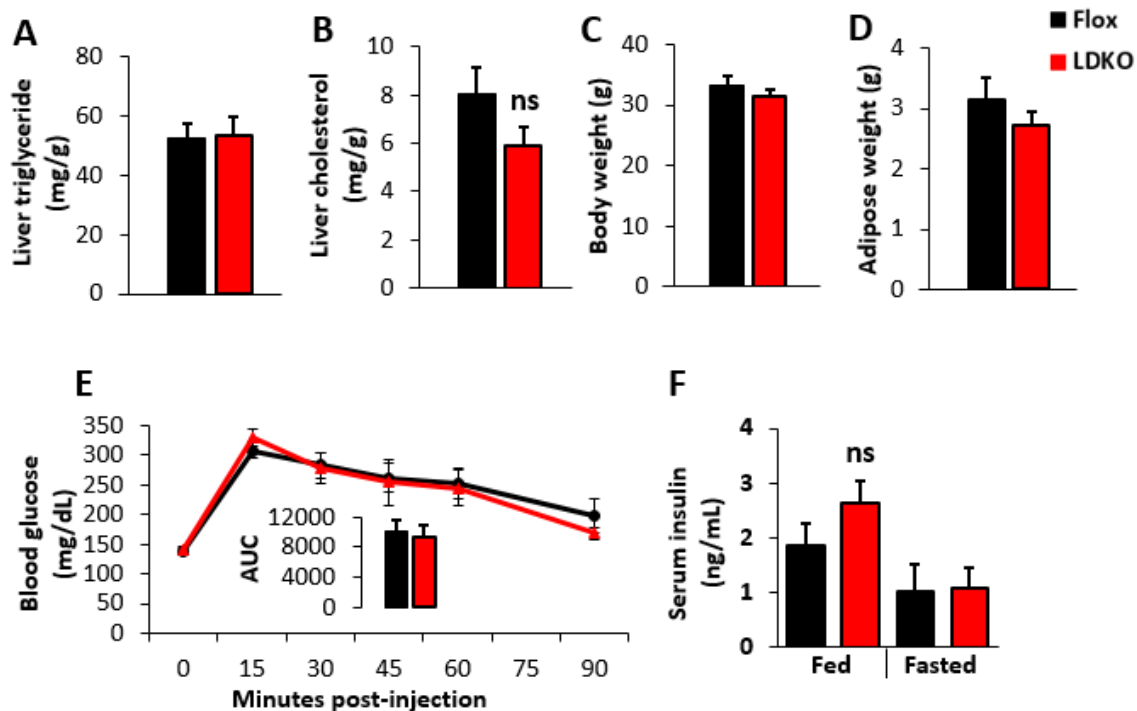


Figure 43. LDKO mice have no alterations in liver fat levels or whole-body physiology.

Liver (A) triglyceride and (B) cholesterol content, and (C) body weight and (D) adipose weight of DEN-treated LDKO and Flox mice at 40w of age. (E) Blood glucose concentrations over time and area under the curve (AUC) during a glucose tolerance test in DEN-treated LDKO and Flox mice at 22w of age. (F) Serum insulin levels in random-fed or 12 hour-fasted Flox and LDKO mice at 22w of age. * indicates significant difference, $p < 0.05$ ($n=10-11$). Data are represented as mean \pm SEM.

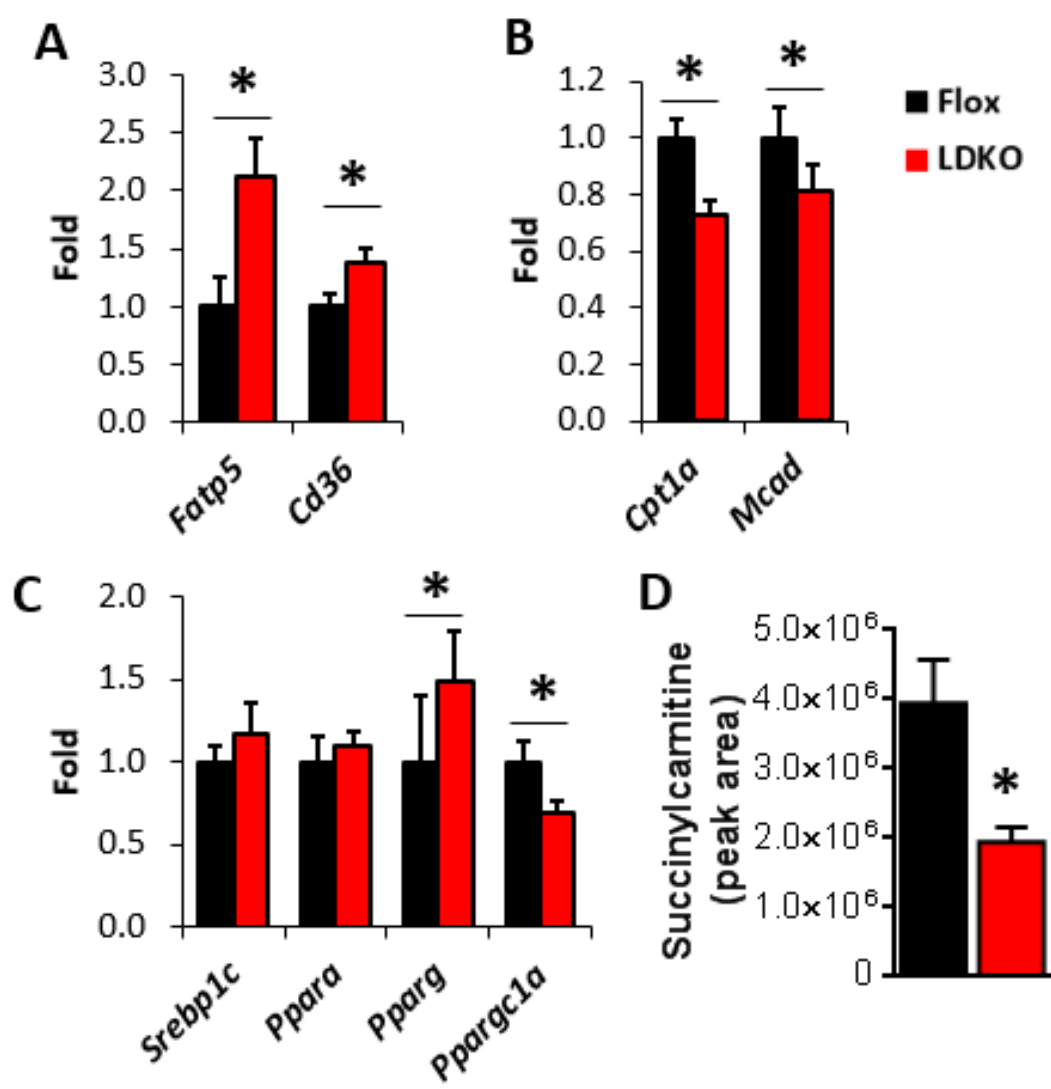


Figure 44. Metabolic gene expression and succinylcarnitine levels in livers of DEN-treated Flox and LDKO mice.

Fold mRNA expression in liver tissue of DEN-treated Flox and LDKO mice at 40w of age for metabolic genes involved in (A) lipid transport and metabolism: Fatty acid transport protein 5 (*Fatp5*) and fatty acid translocase (*Cd36*) and (B) mitochondrial fatty acid metabolism: carnitine palmitoyltransferase (*Cpt1a*) and medium chain acyl-CoA dehydrogenase (*Mcad*); and (C) transcription factors: sterol regulatory element-binding protein 1c (*Srebp1c*), peroxisome proliferator-activated receptors *Ppara* and *Pparg*, and PPAR γ coactivator 1 α (*Ppargc1a*). (D) Levels of succinylcarnitine measured by metabolomics in livers of Flox and LDKO mice at 40w of age. For A-C, n=10-11. For D, n=5-7. * indicates significant difference, $p < 0.05$. Data are represented as mean \pm SEM.

To gain a better understanding of the metabolic changes in LDKO liver tissue that could contribute to proliferation and tumorigenesis, global metabolomics analyses were performed on non-tumor liver tissue from 40 week-old LDKO and control mice that were treated with DEN at 14 days of age (not shown). These data revealed upregulation of the pentose phosphate pathway (PPP) and associated antioxidant systems. Gene expression of glucose-6-phosphate dehydrogenase (*G6pd*) (Figure 45A), the rate-limiting enzyme of the PPP, as well as its products, 6-phosphogluconate and NADPH, were both highly elevated in LDKO livers (Figure 45B-C). NADPH is an important molecule for antioxidant defense and is used as a substrate by antioxidant enzymes such as glutathione reductase to reduce oxidized glutathione (GSSG) to glutathione (GSH). Consistent with the increase in NADPH, the glutathione pathway was highly enriched in the metabolomics data (Figure 45D), and the ratio of GSH:GSSG was higher in LDKO liver tissue from both 40 week-old mice and 15 day old mice compared to Flox controls (Figure 45E and Figure 46B-C). Additionally, gene expression of glucokinase (*Gk*), the enzyme that converts glucose to glucose-6-phosphate, was significantly increased in LDKO liver tissue (Figure 46A).

DEN-induced tumor initiation involves ROS production and genotoxic damage²²². Since LDKO mice had evidence of increased antioxidant status, we investigated whether DNA damage was altered in livers of mice exposed to DEN. Following 24 hours of DEN exposure, LDKO mice had less DEN-induced DNA damage than controls as evidenced by less 8-hydroxydeoxyguanosine (8-OHdG) and less γ H2A.X expression, a marker of DNA double-strand breaks (Figure 45F-H). To determine whether antioxidant defenses

protect hepatocytes from DEN-induced genotoxic damage, primary cells were pre-treated with the cell-permeable glutathione precursor γ -glutamyl monoethyl ester (GEE) prior to DEN exposure. These data show that GEE pre-treatment decreased DEN-induced γ H2A.X, which was accompanied by reduced cleaved CASP3 expression (Figure 45I-K). Importantly, DEN treatment of Flox mice resulted in an acute increase in apoptosis and reduction in proliferation, as evidenced by cleaved CASP3 and reduced Ki67 staining (Figure 47A-D). However, DEN had no effect on Ki67-positive nuclei in LDKO liver tissue and resulted in nearly half as much cleaved CASP3 compared to Flox control tissue (0.6% of LDKO cells stained for cleaved CASP3 vs 1.1% of Flox control cells) (Figure 47A-D), indicating that the increased antioxidant status induced by ACC enzyme inhibition ultimately protected hepatocytes from the apoptotic effects of DEN, enabling continued proliferation.

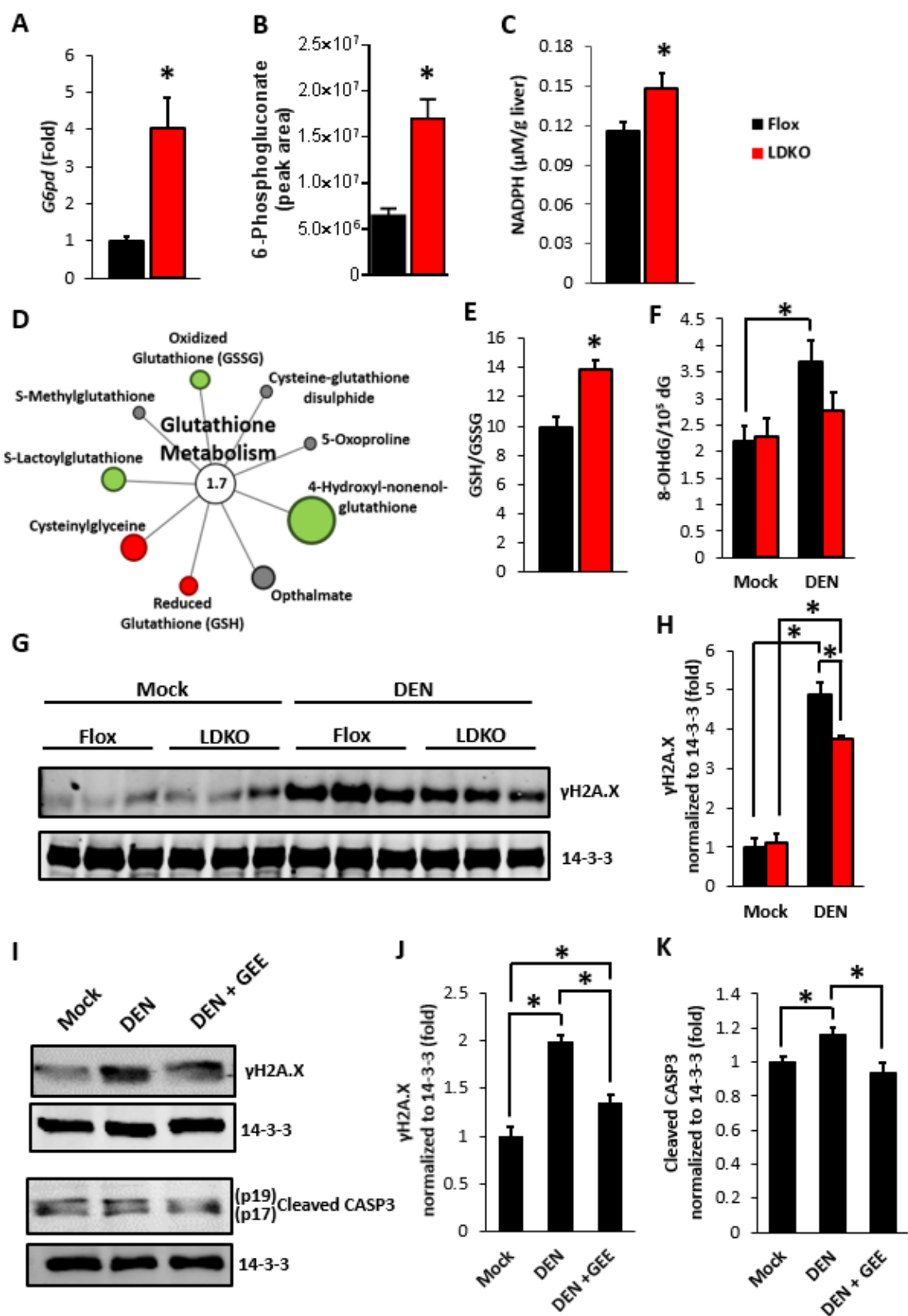


Figure 45. Increased liver antioxidant status is a potential mechanism for increased cell proliferation and tumorigenesis in LDKO mice.

(A) Fold *G6pd* mRNA expression, (B) 6-phosphogluconate levels, and (C) NADPH levels of DEN-treated LDKO and Flox mice at 40w of age. (D) Overall fold-enrichment and individual metabolite levels of glutathione metabolism in DEN-treated livers of LDKO mice relative to livers of Flox mice at 40w of age. Red indicates a significant increase in metabolite levels, green indicates a significant decrease in metabolite levels, and gray indicates no significant difference in levels between LDKO and Flox. Circle size corresponds with the relative magnitude of difference between LDKO/Flox levels. Liver (E) GSH:GSSG ratio levels of DEN-treated LDKO and Flox mice at 40w of age. (F) 8-OHdG levels of DNA isolated from Flox and LDKO liver tissue 24h after DEN treatment. (G) Representative Western blots and (H) quantitation of γ H2A.X protein expression in liver tissue from Flox and LDKO mice 24h after DEN treatment. (I) γ H2A.X and cleaved CASP3 protein expression of primary hepatocytes isolated from 2 week-old Flox mice then pretreated with vehicle or 1 mM γ -glutamyl monoethyl ester (GEE) for 1 hour, followed by the addition of vehicle or 50 μ M DEN, then harvested 24 hours after DEN treatment. Quantitation of protein expression for (J) γ H2A.X and (K) cleaved CASP3. For G and I, 14-3-3 was used as a loading control. For A, C and E, n=10-11. For B and D, n=5-7. For F-H, n=3-4. I-K show one experiment representing three independent experiments. * indicates significant difference, $p < 0.05$. F, H, J and K were analyzed by one-way ANOVA. Data are represented as mean \pm SEM.

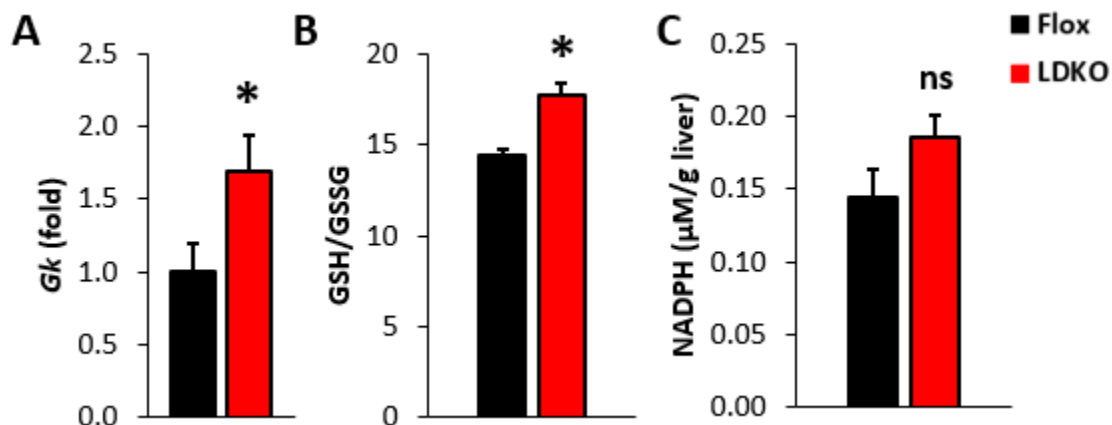


Figure 46. LDKO mice have higher liver glucokinase expression and antioxidant status.

(A) Fold change in *Gk* mRNA expression of DEN-treated Flox and LDKO mice at 40w of age. (B) GSH:GSSG ratio and (C) NADPH levels in liver tissue of Flox and LDKO mice 24h after DEN treatment. For A, n=10-11. For B and C, n=4. * indicates significant difference, $p < 0.05$. Data are represented as mean \pm SEM.

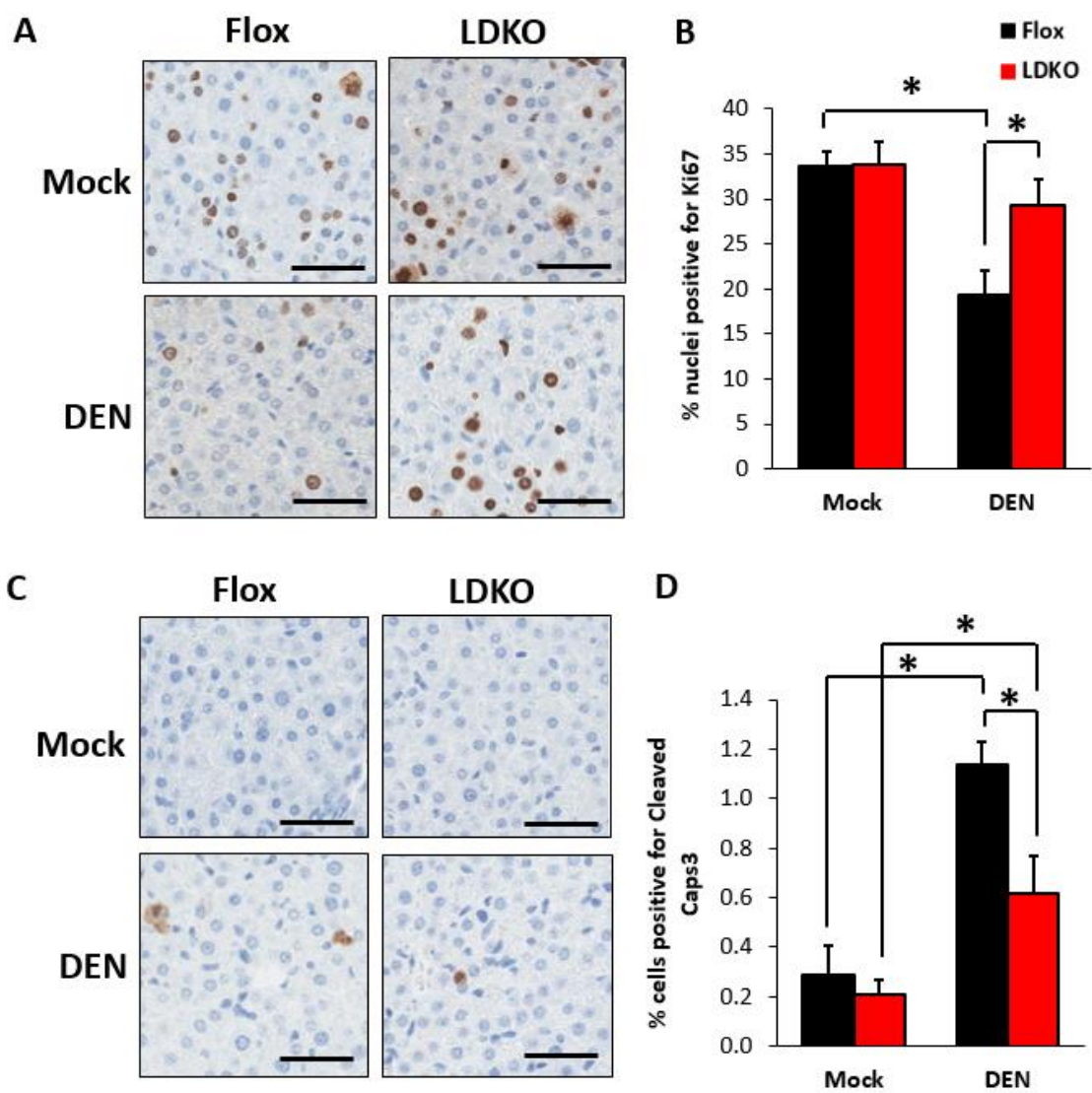


Figure 47. LDKO livers maintain proliferation and are resistant to apoptosis acutely in response to DEN treatment.

IHC in liver sections of LDKO and Flox mice treated with vehicle (Mock) or DEN at 2w of age and harvested 24h after treatment. (A) Representative images and (B) quantitation of Ki67 staining. (C) Representative images and (D) quantitation of Cleaved CASP3 staining. Scale bars=50 μ m. * indicates significant difference, $p < 0.05$ (n=4), analyzed by one-way ANOVA. Data are represented as mean \pm SEM.

Discussion

Lipogenesis is a metabolic pathway that is upregulated in many types of cancer including liver cancer. Lipogenesis is thought to be advantageous to cancer cells because this pathway supplies new lipids for the synthesis of membranes, it produces saturated lipids that are not subject to oxidation and may increase lipid raft signaling domains, and *de novo* synthesized lipids may serve as ligands for transcription factors^{189,193,197}. The role of lipogenesis in cancer has been tested primarily in the context of cell-based systems or pharmacologic approaches, where the data consistently show that blocking lipogenesis impairs cancer cell viability²⁶². However, the role of lipogenesis in cancer has not been studied using mouse models lacking lipogenesis. To test the role of lipogenesis in primary liver cancer, we used mice lacking ACC enzyme activity specifically in hepatocytes and subjected them to the hepatocellular carcinogen DEN. Unexpectedly, the loss of ACC activity resulted in an increase in tumorigenesis. Although lipogenesis may assist cancer cells in some contexts, the present findings clearly demonstrate that *de novo* synthesized lipids are not essential for liver tumor formation or progression.

It is curious that inhibiting ACC activity exacerbated liver tumorigenesis. The mechanism whereby ACC enzyme inhibition contributes to increased tumorigenesis was not associated with most of the hallmark risk factors for liver cancer including hepatic steatosis, obesity, or glucose intolerance. However, global metabolomics data revealed that ACC-deficient liver tissues had increased PPP metabolites. Since the PPP produces NADPH and the lipogenesis pathway consumes NADPH, it was not surprising that intracellular NADPH levels were increased in ACC-deficient liver. NADPH is a

substrate for antioxidant defense enzymes including glutathione reductase, and accordingly we observed an increase in the ratio of reduced:oxidized glutathione (GSH:GSSG). These data demonstrate that the lack of ACC activity resulted in an environment with strong antioxidant defense. It is likely that this antioxidant environment contributed to increased tumorigenesis by increasing the survival of hepatocytes injured by DEN treatment. In support of this hypothesis, GEE treatment alone was sufficient to reduce DEN-induced caspase 3 cleavage. Notably, despite being partially protected from the genotoxic effects of DEN, the LDKO mice developed more tumors. This suggests that DNA damage, although blunted, was sufficient for hepatocyte transformation. These data reveal a role for ACC enzymes in cell antioxidant status and survival in the context of cancer. This result is consistent with the observation by Hay and colleagues wherein AMPK activation promoted cancer cell survival and proliferation by inhibiting ACC enzymes¹². In the Hay study, NADPH levels and the GSH:GSSG ratios were increased; however, PPP activity was not evaluated.

4.2.3 Summary

The current study demonstrates an important role for hepatic ACC activity in regulating antioxidant defense and susceptibility to tumor development. Because the mice used in this study had a perinatal deletion of the ACC enzymes and compensatory pathways were established prior to carcinogen exposure, future studies should determine how inhibition of lipogenesis in established tumors may affect their growth or progression. In light of the present data, clinical interventions targeting ACC activity should be approached with caution, as ACC inhibition may exacerbate tumorigenesis.

CONCLUDING REMARKS AND FUTURE DIRECTIONS

The liver carries out many responsibilities on behalf of the body including detoxification, cholesterol synthesis, fatty acid synthesis, and nutrient storage and export. Aberrations in these processes have been linked to a myriad of diseases including type II diabetes, atherosclerosis, fatty liver disease, and liver cancer. Therefore, understanding the molecular basis of these processes is of great consequence to human health.

The major storage form of excess nutrients in the liver is fat; however, excess fat deposition in the liver can be problematic, as it is associated with metabolic disorders including fatty liver disease, type II diabetes, and liver cancer. The ACC enzymes are major regulators of liver lipid content by catalyzing the conversion of excess glucose in the liver to fat, and by inhibiting mitochondrial fat oxidation. Thus, inhibition of the ACC enzymes was expected to prevent the development of fatty liver. To better understand the role of ACC activity in normal liver metabolism and in the context of metabolic disease we developed liver-specific ACC1 and ACC2 double knockout (LDKO) mice that completely lacked hepatocyte lipogenesis.

Characterization of LDKO mice on a normal chow diet revealed unexpected phenotypes of increased hepatic triglyceride and decreased fat oxidation. We also observed that chronic ACC inhibition led to hyper-acetylation of proteins in the extra-mitochondrial space. These data reveal the existence of a sensory pathway that detects acetyl-CoA availability and adapts lipid metabolism to increase hepatic fat stores. Further work is required to understand the metabolic processes affected by ACC inhibition, and

to elucidate the functional consequences of these alterations in liver and whole-body metabolism.

Liver lipogenesis is thought to be important for storing excess glucose in the context of high-carbohydrate feeding, thus the lack of glucose disposal into lipid was expected to increase blood glucose levels. However, we demonstrated that inhibition of liver lipogenesis paradoxically increased glucose disposal into the liver and improved whole-body glucose tolerance. ACC inhibition caused a depletion of liver triglycerides after 3 weeks of high-carbohydrate fat-free diet, accompanied by decreased adipose tissue. This indicates that the liver communicates its need for lipid to the adipose tissue, resulting in adipose tissue compensation, emphasizing the importance of liver signals in whole-body nutrient homeostasis. The factor(s) release by the liver to communicate its nutritional status to the adipose tissue has yet to be identified, and may represent promising points of therapeutic intervention in the context of whole-body glucose intolerance.

We found that liver ACC inhibition protected mice from diet-induced fatty liver. However, a decrease in liver fat was not sufficient to ameliorate diet-induced glucose intolerance. Future studies should test whether inhibition of lipogenesis in other tissues such as adipose tissue or skeletal muscle is sufficient to improve whole-body glucose tolerance in the context of a Western diet, and whether reduction of liver fat levels is required for such an effect.

Our studies of liver ACC inhibition have revealed that ACC activity regulates the intracellular acetyl-CoA pool, causing global alterations in metabolic protein acetylation

and expression. A consequence of this metabolic reprogramming was reduced fatty acid oxidation in hepatocytes, in conjunction with decreased expression of the rate-limiting enzyme in fatty acid oxidation, CPT1a. A major regulator of CPT1 expression, PGC-1 α , is known to be highly regulated by acetylation. We confirmed that PGC-1 α was hyperacetylated in LDKO livers, and inhibition of PGC-1 α acetylation in LDKO hepatocytes was sufficient to restore normal rates of oxygen consumption. This work demonstrates that ACC activity controls metabolic flexibility at least in part by regulating PGC-1 α acetylation. Many metabolic proteins are known to be regulated by acetylation; therefore, it is possible that ACC regulates a host of proteins to coordinate metabolic flux based on cellular nutrient availability. Understanding the full extent of metabolic regulation by the ACC enzymes will require considerable effort, but may reveal potential points of therapeutic intervention for metabolic disease.

Liver cancer is an especially fatal disease that is highly influenced by environmental factors such as obesity, insulin resistance, and fatty liver. Previous studies have demonstrated that an obesigenic Western diet promotes liver tumor development, but whether obesity was required for this effect was unclear. In mice predisposed to developing liver tumor by a liver carcinogen, we found that dietary sugar promoted liver tumor regardless of dietary fat content and obesity. Tumor burden was, however, positively correlated with liver fat accumulation, postprandial insulin, liver inflammation, and negatively correlated with adiponectin. Furthermore, livers of mice fed high sugar diets had indications of less apoptosis and more progression through cell cycle. This

study revealed that dietary sugar can drive liver tumor progression, and opens the door for future studies to test the specific role of sugar metabolism in liver cancer.

Very little is currently understood about the molecular etiology of liver cancer. Lipogenesis is a hallmark metabolic phenotype of liver cancer and may represent a connection between dietary sugar and liver cancer, however its role in liver cancer development or progression was unclear. Unexpectedly, we found that LDKO mice treated with a liver carcinogen had increased susceptibility to carcinogen-induced liver tumor. This was associated with a robust antioxidant defense that was secondary to decreased NADPH consumption via lipogenesis and increased NADPH production from the pentose phosphate pathway. Increased NADPH maintained glutathione in a more reduced state, and administration of glutathione precursors was sufficient to reduce DEN-induced DNA damage in hepatocytes. This study demonstrates that lipogenesis is not necessary for liver tumor growth, and identifies a protective role for ACC enzymes against tumorigenesis by modulating antioxidant defense. It remains to be tested whether blocking ACC activity in tumor cells that have upregulated lipogenesis is an effective strategy to prevent tumor growth and progression.

This present work helps to clarify the role of liver nutrient metabolism and lipogenesis in normal liver function and metabolic disease (summarized in Figure 48). We have identified a broad role for the ACC enzymes as nutritional rheostats, regulators of metabolic protein activity, and modulators of cellular antioxidant status and growth. Although ACC appeared as an appealing therapeutic target in fatty liver disease, we have learned that hepatic ACC inhibition is not sufficient to prevent diet-induced glucose

intolerance. Furthermore, our studies warrant caution when targeting ACC enzyme activity, due to metabolic compensations that promote liver tumor development.

Additional research in liver nutrient metabolism and the role of the ACC enzymes is needed to continue to unravel these complex regulatory mechanisms and to identify potential points of therapeutic intervention for diseases such as type II diabetes and liver cancer.

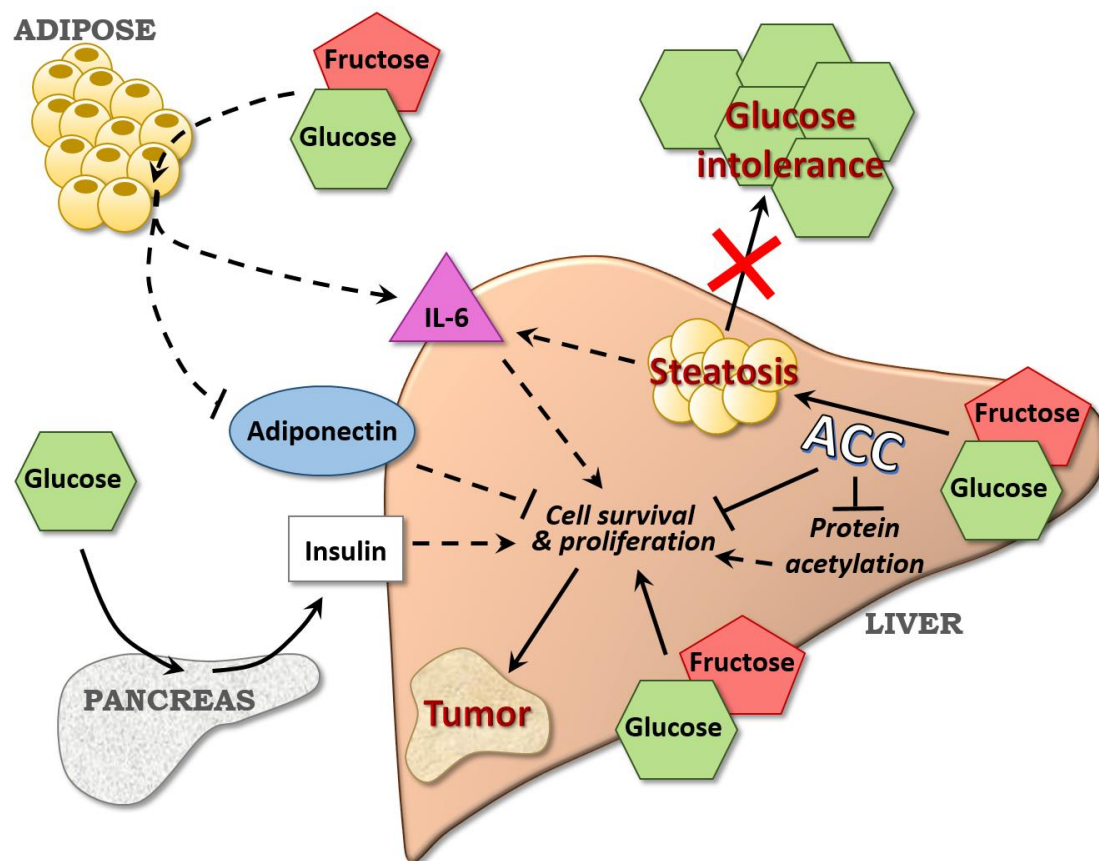


Figure 48. Model for the role of sugars and acetyl-CoA carboxylase activity in liver and whole-body pathophysiology.

ACC enzyme activity inhibits protein acetylation. Protein acetylation has broad effects on liver metabolism which may collectively promote cell survival and proliferation. Thus, the ability of ACC enzyme activity to block cell survival and proliferation may involve regulation of protein acetylation. Dietary intake of sugar (i.e. glucose and fructose) promotes liver steatosis via a mechanism dependent on ACC enzyme activity; however, liver steatosis is not sufficient to cause whole-body glucose intolerance in the context of a high-sugar Western diet. Liver steatosis is linked to production of the inflammatory cytokine IL-6 in the liver. IL-6 production by adipose-resident immune cells may be stimulated by high-sugar feeding. High-sugar feeding decreases adipose-derived adiponectin. Adiponectin signaling prevents cell survival and proliferation. Circulating glucose causes the pancreas to release insulin. IL-6 and insulin signaling promote cell survival and proliferation, whereas adiponectin signaling prevents cell survival and proliferation. Thus, increased IL-6 and insulin and decreased adiponectin may be mechanisms by which dietary sugar intake promotes liver cell survival and proliferation to increase liver tumor development.

PUBLICATIONS RESULTING FROM THIS WORK

1. **Marin E. Healy**, Jenny D.Y. Chow, Frances L. Byrne, David S. Breen, Norbert Leitinger, Chien Li, Stephen H. Caldwell, Carolin Lackner, and Kyle L. Hoehn. Dietary effects on liver tumor burden in mice treated with the hepatocellular carcinogen diethylnitrosamine. *Journal of Hepatology*, 62(3):99-606, 2015.

2. Jenny D.Y. Chow, Robert T. Lawrence, **Marin E. Healy**, John E. Dominy, Jason A. Liao, David S. Breen, Frances L. Byrne, Brandon M. Kenwood, Carolin Lackner, Saeko Okutsu, Valeria R. Mas, Stephen H. Caldwell, Jose L. Tomsig, Gregory J. Cooney, Pere B. Puigserver, Nigel Turner, David E. James, Judit Villén, and Kyle L. Hoehn. Genetic inhibition of hepatic acetyl-CoA carboxylase activity increases liver fat and alters global protein acetylation. *Molecular Metabolism*, 3(4):419-31, 2014.

3. **Marin E. Healy**, Jenny D.Y. Chow, Frances L. Byrne, Sujoy Lahiri, Stefan R. Hargett, David S. Breen, David E. James, Jill K. Slack-Davis, Carolin Lackner, Stephen Caldwell, and Kyle L. Hoehn. Lipogenesis is not required for tumorigenesis. *Under review as of July 13, 2015*.

METHODS

General mouse husbandry

Mice were housed and bred in a temperature-controlled room (22°C) on a 12-hour light-dark cycle in filter-top cages with ad libitum access to food and water. Mice were fed a standard chow diet (7912 Teklad LM-485 from Harlan Laboratories; 25 kcal% protein, 17 kcal% fat and 58 kcal% carbohydrates) unless otherwise specified. All animal experiments were performed according to standard operating procedures approved by the Institutional Animal Care and Use Committee at University of Virginia.

Generation of LDKO and Flox mice

Ozgene Australia (Murdoch, Australia) was contracted to generate Acc1 and Acc2 floxed mice described previously^{201,263}. Mice were produced on a pure C57BL/6 background using Bruce4 embryonic stem cells. Acc1 and Acc2 floxed mice were bred with C57BL/6 FLPe mice to delete the neomycin selection cassettes. To generate liver-specific deletions, female Acc1lox/lox/Acc2lox/lox mice were bred with male Acc1lox/lox/Acc2lox/lox mice expressing liver-specific albumin-Cre. Offspring from this cross produced a 1:1 ratio of LDKO (liver-specific double ACC knockout) to floxed control (Flox) offspring.

Breeding of wildtype C57BL/6N mice

Male and female C57BL/6NHsd mice were purchased from Harlan Laboratories.

The C57BL/6N strain was chosen over C57BL/6J because the latter has a gene mutation in nicotinamide nucleotide transhydrogenase (Nnt) that contributes to glucose intolerance

and reduced insulin secretion²⁶⁴. Mice were time-mated to produce litters simultaneously.

Offspring male and female C57BL/6N mice were treated with DEN

Diets for study of metabolic effects in LDKO and Flox mice

To study the effects of liver ACC deletion in the context of a high-carbohydrate fat-free diet, Flox and LDKO mice were fed a diet that contained (w/w) <1% fat (03314, Harlan Teklad) from 20 weeks of age for 3 weeks. To study the effects of liver ACC deletion in the context of a high-fat diet, Flox and LDKO mice were fed a diet that contained (w/w) 21% lard and 20% sucrose (D12451, Research Diets) from 28 weeks of age for 12 weeks.

Diets for liver cancer studies

From 6 weeks of age, mice were fed one of five experimental diets. Food was provided ad libitum in order to prevent alterations in food-seeking behavior and disruptions in normal set-points for food intake. Dietary intervention was delayed until 4 weeks after treatment with the carcinogen, to distinguish tumor initiation by the carcinogen from promotion of lesion growth by the diets. Weight of food consumed per cage was measured bi-weekly from diet initiation until study completion. kCals consumed were calculated based on kCal content per gram of food for each diet. kCals consumed per cage were then divided by the number of mice in the cage to estimate kCals consumed per mouse.

Diets for DEN-treated wildtype mice

Diets were prepared in-house according to methods previously established in our laboratory²⁰¹, with modifications to macronutrient (i.e., fat and carbohydrate) content. All diets contained (w/w): 4% Mineral Mix AIN-76 (Harlan Teklad), 1% Vitamin Mix AIN-76 (Harlan Teklad), 0.4% choline bitartrate, 0.3% methionine, and 2% gelatine. NC contained (w/w): 6% wheat bran, 67% uncooked corn starch, 17% casein, and 3% safflower oil. FD contained (w/w): 6% wheat bran, 21% uncooked corn starch, 31% sucrose, 15% fructose, 17% casein, and 3% safflower oil. WD-L and WD-C contained (w/w): 18% uncooked corn starch, 5% wheat bran, 21% sucrose, either 23% lard or coconut oil, 18% casein, and 3% safflower oil. KD contained (w/w): 71% lard, 16% casein, and 6% safflower oil. Sample size sufficient to detect a 20% change in tumor number was estimated a priori, using a power analysis based on group means and standard deviations previously reported¹⁸³ (n = 6–12 mice per diet group). Only 6 of 8 mice in the male KD group completed the study, as 2 mice were euthanized before study completion due to wounds incurred from fighting. The euthanized mice did not show evidence of tumor burden.

Diet for DEN-treated LDKO and Flox mice

Starting at 6 weeks of age, mice were fed a Western diet (D12451, Research Diets) which contained (w/w) 21% lard and 20% sucrose.

Respirometry

Oxygen consumption rate (VO_2) and respiratory exchange ratio (RER) were measured under consistent environmental temperature (20-22°C) using an indirect calorimetry system (Oxymax series, Columbus Instruments, Columbus, OH), as described¹⁵. Studies were commenced after acclimation to the metabolic chamber with airflow of 0.5 L/min. Gas samples were measured at 16-min intervals over a 24-hour period with food and water provided ad libitum unless indicated otherwise.

Serum collection and preparation

Submandibular whole blood was sampled from mice in the random-fed (postprandial) state (21:00 hours) or after a 12-hour overnight fast. Serum was isolated by allowing coagulation for 30 minutes at room temperature followed by centrifugation at 2,000 x g for 15 min at 4°C, then stored at -80°C until further analysis.

Serum metabolite measurements

Metabolites were determined according to manufacturers' protocols: Triglyceride assay (Pointe Scientific); Cholesterol assay (Infinity Cholesterol Liquid Reagent, Thermo Scientific); Free fatty acid assay (BioVision); Ketone assay (Cayman); NAD^+ assay (BioAssay System). In DEN-treated male C57BL/6 mice, serum cytokines were measured by ELISA colorimetric assay kits in serum collected at the time of harvest (IL-6 and $\text{TNF}\alpha$, Cayman Chemical; leptin and adiponectin, Boster Biosciences).

Histology and immunohistochemistry

Liver samples were fixed in 10% neutral buffered formalin and paraffin-embedded for microtome sectioning (5 μm thick) and hematoxyline&eosin staining. Frozen-sections from OCT-embedded liver samples were used for Oil-Red-O staining as previously described²⁶⁵. Microscopy was performed and analyzed on a ScanScope.

DEN treatment of mice

Mice were treated with diethylnitrosamine (DEN) (25 mg/kg) at 14 days of age via intraperitoneal (i.p.) injection as described^{183,266}. Mice were weaned at 21 days of age and randomly allocated to cages. All weaned mice were fed a standard chow diet until 6 weeks of age.

Metabolic tolerance testing and insulin sensitivity.

Tolerance testing was performed in LDKO and Flox mice fasted for 6 hours, or C57BL/6 mice fasted overnight for 12 hours. Mice were injected with glucose (1.5 g/kg i.p.), insulin (1 U/kg), or pyruvate (2 g/kg) and tail vein blood glucose levels were monitored over time. Insulin and glucose measurements were collected in the random-fed state at 19:00 hours, or in the basal state after a 12-hour overnight fast. Glucose was measured in whole blood using an Accu-Chek glucometer (Roche Diagnostics) and insulin was measured in serum using an ELISA colorimetric assay kit (Crystal Chem) according to the manufacturer's protocol. Insulin sensitivity was estimated using the HOMA-IR

method²⁶⁷, calculated using the formula: $basal\ insulin \left(\frac{mU}{L} \right) * \frac{basal\ glucose \left(\frac{mg}{dl} \right)}{405}$.

Triglyceride production and oral triglyceride tolerance assays

To measure hepatic triglyceride production rate, female mice (12 wks of age) were injected i.p. with 1 g/kg body weight Poloxamer 407²⁶⁸ and serum triglyceride levels were measured over 24 h. Mice were fasted from 08:00 to 12:00 hours, and tail vein whole blood was sampled prior to injection then at 1, 2, 6, and 24 h after injection. To determine oral triglyceride tolerance, mice were fasted from 08:00 to 12:00 hours prior to receiving safflower oil by oral gavage (10 mL/g body weight). Tail vein blood was sampled prior to gavage then hourly for 6 hours. Serum was isolated and stored at 20°C until triglyceride assay (Pointe Scientific).

Tissue collection of DEN-treated mice and tumor analysis

Male mice were euthanized at 32 weeks of age (26 weeks of study diet) and female mice were euthanized at 40 weeks of age (34 weeks of study diet). All mice were euthanized in the random-fed state between 09:00 and 11:00 hours. Tumor multiplicity, which represents the number of surface-hemorrhaging tumors per liver, was counted. The diameter of each visible tumor (≥ 0.5 mm in diameter) was used to calculate tumor volume using the formula: $\frac{4}{3}\pi radius^3$. Individual tumor volumes were summed to calculate total liver tumor burden per animal. For male C57BL/6 mice, tumor burden values were used throughout the study to test for correlations with diet-related parameters as a representation of both tumor size and number. Mice without visible tumors were excluded from tumor burden, multiplicity, and all other analyses (n = 1–2 per group). For all mice, the large lobe of the liver was kept for histology, and the remaining liver was divided into non-tumor-involved and tumor-involved tissue, snap-frozen in liquid

nitrogen, and stored at -80°C until further biochemical analyses. The weights of both gonadal and subcutaneous fat pads were summed and represented as combined adipose weight per animal. To study the effect of liver ACC1 and ACC2 genetic deletion in mice, liver ACC1 and ACC2 double knockout (LDKO) mice were generated on a C57BL/6J background as we have previously described¹¹ and compared with floxed (Flox) littermate controls. To determine whether loss of ACC expression could decrease or increase tumor incidence, we used female mice for this study because tumor incidence is approximately 30%, whereas for males tumor incidence is approximately 90%^{183,266}. Offspring female LDKO and Flox mice were treated with 25 mg/kg DEN at 14 days of age via *i.p.* injection. For the long-term DEN study, mice were genotyped and paired with littermates and weaned to cages at 21 days of age, $n=10-11$ per genotype. Starting at 6 weeks of age, mice were fed a Western diet (D12451, Research Diets) which contained (w/w) 21% lard and 20% sucrose. Tumor burden analysis and final tissue collection was performed at 40 weeks of age. For the acute DEN study, mice were genotyped at 12 days of age, treated with DEN at 14 days of age according to our standard protocol, and then tissues were collected 24 hours after DEN treatment for analysis.

Liver histology and immunohistochemistry

The large lobe of the liver was paraffin-embedded for microtome sectioning (5 μm thick) and hematoxylin & eosin (H&E) staining or immunohistochemistry (IHC). Slides were digitally scanned using an Aperio ScanScope (SC System) to produce high-resolution images (resolution: 0.25 μm per pixel). Histological analysis and IHC quantitation was performed in a blinded manner. Hyperplastic foci (HPF) were identified by the presence

of focal basophilia. HCA was characterized by the presence of basophilic cells and cells containing glycogen and fat, resembling human HCA. HCC was distinguished from pre-neoplastic lesions if three or more of the standard criteria were met: undifferentiated trabecular structure; enlarged, mild-moderately polymorphic hyperchromatic nuclei with enlarged nucleoli; presence of basophilia; increased abundance of mitotic figures; and invasive growth²⁶⁹⁻²⁷¹. HCC that developed within HCA was classified as HCC foci, and HCC that arose from hepatic tissue was classified as bona fide HCC. IHC quantitation was performed on 6 randomly-selected 3cm² areas for each animal.

Protein isolation and Western blotting

Liver tissue was homogenized in RIPA buffer (10 mM TRIS pH 8.0, 0.5 mM EGTA, 1% Triton X-100, 0.2% SDS, 100 mM NaCl) with protease inhibitors cocktail (Roche) and phosphatase inhibitors (2 mM sodium orthovanadate, 1 mM sodium pyrophosphate, 10 mM sodium fluoride, 250 nM microcystin). Liver ACC proteins were analyzed using avidin-pulldown as described previously^{201,212}. For acetyl-lysine immunoblotting, liver tissue or cells were lysed in RIPA buffer (50 mM TRIS pH 8.0, 100 mM NaCl, 0.5 mM EGTA pH 7.0, 0.4% v/v Triton X-100, 10 mM nicotinamide), with protease inhibitors cocktail (Roche) and phosphatase inhibitors (2 mM sodium orthovanadate, 1 mM sodium pyrophosphate, 10 mM sodium fluoride, 250 nM microcystin LR), and immunoblotted with an antiacetyl-lysine antibody (Cell Signaling 9441). Cells were lysed in HES-SDS lysis buffer (250 mM sucrose, 20 mM HEPES, pH 7.4, 1 mM EDTA, 2% SDS). Antibodies used for immunoblotting were: phospho-Akt (S473) (587F11; Cell Signaling 4051), pan Akt (C67E7, Cell Signaling 4691), pan 14-3-3

(H-8, Santa Cruz, sc-1657), Mitomix rodent OXPHOS cocktail (Mitosciences MS604), CPT1 (H-40, Santa Cruz, sc-98834) and alpha-tubulin (H-300, Santa Cruz, sc-5546), phospho-p70S6K (T389) (Cell Signaling 9206S), phospho-AMPK (T172) (Cell Signaling 2535P), AMPK (Cell Signaling 2793S), p53 (Santa Cruz 6243), acetyl-p53 (K379) (Cell Signaling 2570S), SIRT1 (Millipore 07-131), p21 (Abcam 7960), cleaved CASP3 (Cell Signaling 9661), Cyclin D1 (Santa Cruz 753), pan ACC (Cell Signaling 3676), RAN (Cell Signaling 4462), Ki-67 (Epitomics 4203), and γ H2A.X (Cell Signaling 9718S). Line scan analysis was performed using Image J.

RNA isolation and qPCR

Liver (2 mg, Trizol) or cells (1 mg, Direct-zol) total RNA was semiquantitated by standard two-step RT-PCR (High Capacity cDNA synthesis kit, Roche; Sensifast SYBR Green mix, Bioline) using genespecific primers (Integrated DNA Technologies). Relative fold expression was calculated using the delta-delta Ct method with *Cyclophilin A* as a housekeeping gene. Primer sequences are listed in Table 2.

Liver fat content

Lipid was extracted from frozen liver tissue based on the method from Folch²⁷². Colorimetric assay kits were used to measure triglyceride (Pointe Scientific) and cholesterol (Infinity, Thermo Scientific) content of the lipid extracts according to the manufacturers' protocols.

NADPH and NADH assays

NADPH and NADH was measured in liver using enzyme cycling assay kits (Abcam 65349 and Promega G9071, respectively) according to the manufacturers' protocols.

GSH:GSSG assay

GSH and GSSG were measured in liver samples using a fluorescent detection kit (BioVision K264) according to the manufacturer's protocol. Prior to the assay spin columns (EMD Millipore 10kDa) were used to eliminate interfering proteins.

8-OHdG assay

Genomic DNA was extracted from frozen liver tissue using a purification spin column followed by DNA elution according to manufacturer's instructions (Qiagen AllPrep® DNA/RNA/Protein Mini). Extracted DNA was converted to single-stranded DNA by incubation at 95°C for 5 minutes then rapidly chilled on ice. Single-stranded DNA was then digested to nucleosides in 20 mM sodium acetate buffer pH 5.2 containing nuclease P1 (Sigma N8630) at a final pH of 5.2 at 37°C for 2 hours, followed by incubation in 100 mM Tris buffer containing alkaline phosphatase (Sigma P6774) at a final pH of 7.5 at 37°C for 1 hour. The nucleoside-containing mixture was centrifuged at 6000 x g for 5 minutes and the supernatant was used for the 8-OHdG assay. 8-OHdG was quantitated using an ELISA assay according to the manufacturer's protocol (Cell Biolabs STA-320).

Metabolomics in liver tissue of DEN-treated LDKO and Flox mice

Metabolomics was performed by Metabolon, Inc. (Durham, North Carolina, USA).

Samples were prepared using the automated MicroLab STAR® system from Hamilton Company. A recovery standard was added prior to the first step in the extraction process for QC purposes. To remove protein, dissociate small molecules bound to protein or trapped in the precipitated protein matrix, and to recover chemically diverse metabolites, proteins were precipitated with methanol under vigorous shaking for 2 min (Glen Mills GenoGrinder 2000) followed by centrifugation. The resulting extract was divided into five fractions: one for analysis by UPLC-MS/MS with positive ion mode electrospray ionization, one for analysis by UPLC-MS/MS with negative ion mode electrospray ionization, one for LC polar platform, one for analysis by GC-MS, and one sample was reserved for backup. Samples were placed briefly on a TurboVap® (Zymark) to remove the organic solvent. Instrument variability was determined by calculating the median relative standard deviation (RSD) for the standards that were added to each sample prior to injection into the mass spectrometers. Overall process variability was determined by calculating the median RSD for all endogenous metabolites (i.e., non-instrument standards) present in 100% of the pooled matrix samples. The LC/MS portion of the platform was based on a Waters ACQUITY ultra-performance liquid chromatography (UPLC) and a Thermo Scientific Q-Exactive high resolution/accurate mass spectrometer interfaced with a heated electrospray ionization (HESI-II) source and Orbitrap mass analyzer operated at 35,000 mass resolution. The sample extract was dried then reconstituted in acidic or basic LC-compatible solvents, each of which contained 8 or more injection standards at fixed concentrations to ensure injection and chromatographic

consistency. One aliquot was analyzed using acidic positive ion optimized conditions and the other using basic negative ion optimized conditions in two independent injections using separate dedicated columns (Waters UPLC BEH C18-2.1x100 mm, 1.7 μ m). Extracts reconstituted in acidic conditions were gradient eluted from a C18 column using water and methanol containing 0.1% formic acid. The basic extracts were similarly eluted from C18 using methanol and water, however with 6.5mM Ammonium Bicarbonate. The third aliquot was analyzed via negative ionization following elution from a HILIC column (Waters UPLC BEH Amide 2.1x150 mm, 1.7 μ m) using a gradient consisting of water and acetonitrile with 10mM Ammonium Formate. The MS analysis alternated between MS and data-dependent MS2 scans using dynamic exclusion, and the scan range was from 80-1000 m/z. The samples destined for analysis by GC-MS were dried under vacuum for a minimum of 18 h prior to being derivatized under dried nitrogen using bistrimethyl-silyltrifluoroacetamide. Derivatized samples were separated on a 5% diphenyl / 95% dimethyl polysiloxane fused silica column (20 m x 0.18 mm ID; 0.18 μ m film thickness) with helium as carrier gas and a temperature ramp from 60° to 340°C in a 17.5 min period. Samples were analyzed on a Thermo-Finnigan Trace DSQ fast-scanning single-quadrupole mass spectrometer using electron impact ionization (EI) and operated at unit mass resolving power. The scan range was from 50–750 m/z. Raw data was extracted, peak-identified and QC processed using Metabolon hardware and software foundations for informatics components were the LAN backbone, and a database server running Oracle 10.2.0.1 Enterprise Edition. Compounds were identified by comparison to library entries of purified standards or recurrent unknown entities based on authenticated

standards that contains the retention time/index (RI), mass to charge ratio (m/z), and chromatographic data (including MS/MS spectral data). Following log transformation with the minimum observed value for each compound, Welch's two-sample t-test was used to identify biochemicals that differed significantly between experimental groups.

Evaluating mRNA expression using Oncomine.

A search was conducted within Oncomine™ (www.oncomine.com) for "Hepatocellular Carcinoma". A filter for studies that reported expression of ACC1 (*ACACA*) and ACC2 (*ACACB*) was then applied. Studies that reported mRNA expression data for both HCC and non-cancerous liver tissue were identified, resulting in 3 independent studies which encompassed data from a total of 327 HCC and 386 non-cancerous liver samples. One study contained clinical data for HCC grade for each sample, so this data was also used in a separate analysis to compare mRNA expression by tumor grade. All mRNA expression values were converted from Log_2 to linear scale, then mRNA expression of HCC tissue was expressed as fold-difference from the non-cancerous liver within each individual study. Linear fold-expression values from the individual studies were pooled to allow overall comparison of mRNA expression in HCC compared to non-cancerous tissue.

Cell culture

Primary mouse hepatocytes were isolated according to an established protocol²⁷³, seeded in Dulbecco's modified Eagle's medium (DMEM) supplemented with 4.5 g/L glucose, 10% fetal bovine serum, 1 μM dexamethasone, and 100 nM insulin for 4 h, and cultured overnight prior to experiment in DMEM with 4.5 g/L glucose and 10% fetal bovine

serum. For protein acetylation experiments, primary hepatocytes were treated with nicotinamide (NAM) at 5 mM for 24 h. For insulin stimulation experiments, hepatocytes were cultured in serum-free DMEM with 1 g/L glucose, 0.2% bovine serum albumin, 100 nM dexamethasone and no insulin for 3 h prior to addition of insulin for 10 min. DMSO was used as vehicle control. For metabolic characterization experiments, hepatocytes isolated from an adult wildtype C57BL/6J mouse and cell lines were cultured overnight prior to experiment in DMEM with 4.5 g/L glucose and 10% fetal bovine serum. For cell viability assays, cells were seeded at 2000 cells/well in 96-well plates. After 120 hours of treatment with compounds, viability was measured by addition of thiazoyl blue tetrazolium bromide (MTT) reagent. Formazan crystals were solubilized in 0.1% NP40 in acidified isopropanol and absorbance read at 590/620nm²⁷⁴. For experiments testing the effects of DEN *in vitro*, primary hepatocytes were isolated from 2 week-old Flox and LDKO mice and seeded at 3x10⁵ cells/mL. Four hours after isolation, the media was changed to DMEM supplemented with 1 g/L glucose, 0.2% bovine serum albumin, 100 nM dexamethasone, and 1 nM insulin. The next day, the cells were treated with vehicle or 1 mM glutathione monoethyl ester (GEE; cell-permeable glutathione precursor) (Bachem H-1298) for 1 hour, then vehicle or 50 uM diethylnitrosamine (DEN) was added. Cells were harvested 24 hours after DEN treatment for Western blotting.

In vitro metabolic substrate competition assays and enzyme activity assays

Substrate competition assays were performed on monolayered hepatocytes (20,000 cells/cm²) in Krebs-Ringer Phosphate buffer (1.2 M NaCl, 6 mM Na₂HPO₄, 60 mM KCl, 4 mM NaH₂PO₄, 12 mM MgSO₄, 125 mM HEPES pH7.4, 10 mM CaCl₂)

supplemented with non-labeled substrates: 50 μM acetate, 5mM glucose, 0.5mM glutamine, 125 μM palmitate and 1 mM carnitine, and one of the following radioactive labeled substrates: 10 $\mu\text{Ci/mL}$ ^{14}C -acetate (de novo lipogenesis), 10 $\mu\text{Ci/mL}$ ^3H -glucose (glycolysis) or 2 $\mu\text{Ci/mL}$ ^{14}C -palmitate (fatty acid oxidation). Cells were incubated in sealed wells at 37°C for 1.5 h. Lipids were extracted by the Folch method³⁷ and analyzed by scintillation counting or thin-layer chromatography to measure de novo lipogenesis. Palmitate oxidation was determined by acidifying each well with 2 M perchloric acid and trapping carbon dioxide in 2 M NaOH in a small tube placed in the well. Acid soluble ^{14}C -labeled metabolites were extracted by centrifugation to determine incomplete palmitate oxidation. Glycolysis was measured by scintillation counting ^3H -glucose that was converted to ^3H -H₂O using the diffusion equilibrium method. Measurements of the activity of oxidative enzymes involved in metabolism and mitochondrial function were performed as described previously²¹².

Seahorse Extracellular Flux assays

Measurement of oxygen consumption rate (OCR) and extracellular acidification rate (ECAR) of cells during a mitochondrial stress test was performed using a Seahorse XF-24 Flux Analyzer (Seahorse Biosciences) as we have previously described^{274,275}.

Mitochondrial spare respiratory capacity represents the difference between the maximal oxygen consumption rate upon addition of the mitochondrial uncoupler BAM15²⁹ and the basal oxygen consumption rate at minute 18 before addition of Oligomycin.

Acetyl-CoA measurements

Acetyl-CoA levels were measured by mass spectrometry using methods described in Refs. ^{276,277}. For quantification in mouse liver, tissue pieces (40 mg) were homogenized in 500 μ L ice-cold isolation media (250 mM sucrose, 10 mM Tris-HCl and 1 mM EGTA), and centrifuged at 800 x g for 5 min at 4°C to pellet cell debris and nuclei.

Cleared cell lysate was centrifuged at 10,000 x g for 10 min at 4°C to obtain a pellet enriched in mitochondria. Pellets were resuspended in 1 mL of 6% perchloric acid, and the supernatant (cytoplasm and microsome) fraction was mixed with an equal volume of 12% perchloric acid. ¹³C-3-malonyl-CoA (0.5 μ M final) was added as a recovery standard. After centrifugation and ultracentrifugation of extract, supernatant was applied to a solid-phase extraction column (Oasis HLB 1 cc-30 mg, Waters) preconditioned with acetonitrile then milliQ water. Bound acyl-CoAs were washed with milliQ water, eluted with acetonitrile, dried under nitrogen gas at 37°C, and resuspended in 120 μ L of solvent A (2% ACN, 10 mM ammonium acetate, 5 mM acetic acid, 10 mM DIPEA) and analyzed by HPLC-MS. Analyses were performed using a triple quadrupole mass spectrometer (AB-Sciex 4000 Q-Trap) coupled to a Shimadzu LC-20AD LC system equipped with a Supelco Discovery C18 column (50 mm 2.1 mm 5 μ m bead size) integrated with a precolumn (4 x 4 mm). A binary solvent system (total flow 0.25 mL/min) was used that consisted of the following solvents, A: 98.6% H₂O, 2% acetonitrile, 5 mM acetic acid, 10 mM N,N-Diisopropylethylamine, 10 mM ammonium acetate; B: 75% acetonitrile, 25% solvent A. Chromatographic runs started at 100% A for 1 min, a linear gradient to reach 100% at 3.5 min, then 100% B for 2 min, and finally 100% solvent A for 2.5 min (8 min total). Column temperature was set to 30°C and the

flow rate was 0.5 mL/min. Measurements were carried out in positive mode using previously published transitions for acetyl-CoA (m/z 857.2 \rightarrow m/z 350.2) and ^{13}C -malonyl-CoA (m/z 810.4 \rightarrow m/z 303.2)^{276,277} using the following settings (DP, EP, CE, CXP, in volts: 91, 10, 43, 8; 106, 10, 41, 10; 116, 10, 43, 10). Quantification was carried out by measuring peak areas using the software Analyst 1.5.1 that were corrected for recovery using ^{13}C -malonyl-CoA as an internal standard.

Acetylation proteomics

Sample preparation

Liver tissue was dounce homogenized in 9 M Urea with addition of complete EDTA-free protease inhibitor cocktail (Roche), 10 mM nicotinamide, and 50 mM butyric acid. After sonication on ice for 30 seconds, lysates were centrifuged at 10,000 x g and assayed for protein content using the BCA method. Protein extracts were reduced with 5 mM DTT and alkylated with 15 mM iodoacetamide. A 2.5 mg aliquot of protein from each sample was diluted 5-fold with 50 mM Tris pH 8.2 and digested overnight with trypsin (Promega) at 37°C. The resulting peptides were acidified to pH 2 with trifluoroacetic acid (TFA) and desalted (but not eluted) using a tC18 SepPak cartridge (Waters) prior to on-column isotopic labeling of primary amines by reductive demethylation²⁷⁸. After desalting, 5 mL of labeling reagent (light: 0.4% CH_2O , 60 mM NaCNBH_3 in 0.5 M MES pH 5.5, heavy: 0.4% CD_2O , 60 mM NaCNBD_3 in 0.5 M MES pH 5.5) was passed through the column at approximately 0.5 mL/min. The reaction was quenched by 15 column volumes of 1% TFA, washed with 0.5% acetic acid. Labeled peptides were eluted and mixed in a 1:1 ratio for further analysis. Immediately after mixing heavy (+34.0689

Da) and light (+28.0313 Da) peptides, a 100 µg aliquot was removed for quantitative analysis of the unmodified proteome and dried by vacuum centrifugation. Peptides were resuspended in 0.1% NH₄OH and fractionated in step-wise format with increasing concentrations of acetonitrile on microfilters constructed in-house using pH-resistant SDB-XC reverse phase chromatography material (3M Empore)²⁷⁹. Eluates were dried by vacuum centrifugation and stored at -20°C prior to further analysis. Labeled peptides containing acetylated lysines were enriched after mixing by immunoaffinity purification. Briefly, 4.9 mg of dried peptides were resuspended in 50 mM MOPSSNaOH pH 7.2, 10 mM Na₂HPO₄, 50 mM NaCl and incubated overnight at 4°C with pre-conjugated acetyl-lysine antibody (Immunechem). Immunoprecipitates were washed four times and eluted with 0.15% TFA. Acetylated peptides were desalted and fractionated in a stepwise format with increasing concentrations of NH₄HCO₃ using microfilters constructed in-house using SCX material (3M Empore). Eluates were desalted, dried, and stored at -20°C prior to further analysis.

LC-MS/MS and data processing

Samples were subjected to reverse phase liquid chromatography on an EASY nLC (Thermo) equipped with a 40 cm x 75 µm column packed in-house with 1.9 mM Repronil C18 particles (Dr. Maisch) and online analyzed by tandem mass spectrometry in a Q-Exactive (for unmodified peptides, 90 min gradients) or an LTQ Orbitrap Velos (for acetylated peptides, 120 min gradients). Mass spectra were acquired using a data dependent acquisition method (twenty most intense precursors selected for

fragmentation) with dynamic exclusion (30 seconds). Raw spectra were converted to mzXML open data format and searched using Sequest against a concatenated forward and reverse version of the Uniprot mouse protein sequence database (v11/29/2012), digested with trypsin and allowing for up to two missed cleavages. Peptide mass tolerance was 50 ppm. Fragment ion tolerance was 0.36 for LTQ-Orbitrap-Velos data and 0.01 for Q-Exactive data. Carbamidomethylated cysteine (+57.021464), dimethylated lysine (+28.0313), and dimethylated peptide N-terminus (+28.0313) were searched as fixed modifications. Oxidized methionine (+15.994915), heavy dimethylated lysine (+6.03766), and heavy dimethylated peptide N-terminus (+6.03766) were searched as variable modifications in all cases. For acetyl-lysine enriched samples, an additional variable lysine modification was used: +13.97926, which corresponds to the difference between an acetyl group (+42.0105) and the fixed dimethyl group (+28.0313). This accounts for the fact that a lysine can be acetylated or dimethylated, but not both. Identified peptides were filtered to a false discovery rate of <1% and allowing only peptides that were correctly labeled and a minimum of 7 amino acids in length. For protein analysis, peptides were additionally filtered to a protein level FDR of <1%. In general, because acetylation events cause missed cleavages to occur yielding only one possible lysine candidate, site localization was not an issue. Nevertheless, localization scores and site refinement were performed using an in-house implementation of the Ascore algorithm²⁸⁰ where an Ascore >13 equates to $p < 0.05$. Maximum peak intensities and heavy-to-light (H/L) ratios for identified peptides were calculated using an in-house peptide quantification algorithm. To be considered for quantitation, we required a peptide

signal to noise ratio >5 . For most peptides ($>90\%$), both light and heavy isotope intensities were measured. If only one isotope was measured, a ratio was calculated between peptide intensity and local noise. When more than one peptide was measured, the average H/L ratio was computed. For protein quantitation, H/L ratios for peptides mapping to the same protein were averaged. Similarly, for acetylation site quantitation, H/L ratios for peptides mapping to the same site were averaged. Resulting datasets were \log_2 transformed. To control for mixing error, both the acetylation site data and protein data were normalized to the median protein ratio. Finally, acetylation site quantifications were individually corrected for changes in its respective protein by subtracting the \log_2 ratio of the parent protein from the acetylation site ratio.

Bioinformatics

Statistical analysis was performed in R version 2.15.2. For subcellular compartment analysis, protein identifications were mapped to Gene Ontology Cellular Component terms using gene sets from the Molecular Signatures Database MsigDB²⁸¹. For mitochondrial protein analysis, the mouse MitoCarta database²⁸² was converted to Uniprot identifiers and used to assign high confidence mitochondrial proteins to the datasets. Metabolic pathways and proteins were manually curated from IUBMB-Nicholson metabolic pathway diagrams (<http://www.iubmb-nicholson.org>), and plotted according to \log_2 fold change using Cytoscape v2.8.3²⁸³. Functional enrichment analysis was performed using DAVID bioinformatics resources v6.7²⁸⁴.

Acetylated proteins were queried for enrichment against a background containing all proteins found in the proteome dataset.

Statistical analyses

Results are presented as mean \pm standard error of the mean (SEM) and compared by two-tailed parametric student's t-test unless otherwise indicated. For male DEN-treated C57BL/6 mice, group results are presented as mean \pm standard error of the mean (SEM) and compared by one-way ANOVA followed by Fisher's PLSD post-hoc test. Tumor burden (mm^3) and multiplicity values were \log_2 -transformed to stabilize group variance, which is appropriate when standard error is proportional to changes in the mean. One-way ANOVA and Fisher's PLSD post-hoc tests were performed on the \log_2 -transformed data. Scatter plots were analyzed by linear regression to determine line of best-fit, followed by Pearson's correlation analysis to measure the correlation coefficient between two variables. Statistical significance was accepted at $p < 0.05$. Statistical analyses were performed using GraphPad Prism v6.00.

Table 2. Primer sequences

Gene	Forward (5'-3')	Reverse (5'-3')
<i>Acaca</i>	GTCTGCTGGGAAGTTAATCCAG	TCCTGCAGCTCTAGCAGAGG
<i>Acacb</i>	ACAGAGATTTACCGTCGCGT	CGCAGCGATGCCATTGT
<i>Afp</i>	CCCGCTTCCCTCATCC	GAAGCTATCCCAAACCTCATTTTCG
<i>Cd36</i>	GATGACGTGGCAAAGAACAG	TCCTCGGGGTCTGAGTTAT
<i>Cpt1a</i>	TTGGGCCGGTTGCTGAT	GTCTCAGGGCTAGAGAACTTGAA
<i>CypA</i>	CGATGACGAGCCCTTGG	TCTGCTGTCTTTGGAACCTTGTG
<i>Fatp5</i>	GCACCTTCTGACCCAGTACC	GTAAGCAGCCAAGGAATCCA
<i>G6pc</i>	CCGGATCTACCTTGCTGCTCACTTT	TAGCAGGTAGAATCCAAGCGCGAAAC
<i>G6pd</i>	AAGAAGCCTGGCATGTTCTT	GAAGCCCACTCTCTTCATCA
<i>Gk</i>	CCCTGAGTGGCTTACAGTTC	ACGGATGTGAGTGTTGAAGC
<i>Mcad</i>	GCAGGTTTCAAGATCGCAATG	TGAAACTCCTTGGTGCTCCACT
<i>Pdk4</i>	CACATGCTCTTCGAACTCTTCAAG	TGATTGTAAGGTCTTCTTTTCCCAAG
<i>Ppargc1a</i>	CCCTGCCATTGTTAAGAC	TGCTGCTGTTCTCTGTTTT
<i>Ppara</i>	TGCAAACCTGGACTTGAACG	AGGAGGACAGCATCGTGAAG
<i>Pparg</i>	GATGCAAGGGTTTTTCCGAAG	CAAGGCACTTCTGAAACCGACA
<i>Srebp1c</i>	CGTCTGCACGCCCTAGG	CTGGAGCATGTCTTCAAATGTG

REFERENCES

1. Niwa, T., Murayama, N. & Yamazaki, H. Oxidation of endobiotics mediated by xenobiotic-metabolizing forms of human cytochrome. *Curr Drug Metab* **10**, 700–12 (2009).
2. Cao, J., Beisker, W., Schraner, T. I. & Nusse, M. Flow cytometric analysis of in vitro micronucleus induction in hepatocytes treated with carcinogens. **7**, 447–451 (1993).
3. Liska, D. J. The detoxification enzyme systems. *Altern. Med. Rev.* **3**, 187–198 (1998).
4. Denison, M. S. & Whitlock, J. P. Xenobiotic-inducible transcription of cytochrome P450 genes. *J. Biol. Chem.* **270**, 18175–18178 (1995).
5. McGraw, J. & Waller, D. Cytochrome P450 variations in different ethnic populations. *Expert Opin. Drug Metab. Toxic.* **8**, 371–82 (2012).
6. Bondy, S. C. & Naderi, S. Contribution of hepatic cytochrome P450 systems to the generation of reactive oxygen species. *Biochem Pharmacol* **48**, 155–9 (1994).
7. Lu, S. C. Regulation of hepatic glutathione synthesis: current concepts and controversies. *FASEB J.* **13**, 1169–83 (1999).
8. Zamek-Gliszczynski, M. J., Hoffmaster, K. a., Nezasa, K. I., Tallman, M. N. & Brouwer, K. L. R. Integration of hepatic drug transporters and phase II metabolizing enzymes: Mechanisms of hepatic excretion of sulfate, glucuronide, and glutathione metabolites. *Eur. J. Pharm. Sci.* **27**, 447–486 (2006).
9. Winkler, B. S., DeSantis, N. & Solomon, F. Multiple NADPH-producing pathways control glutathione (GSH) content in retina. *Exp Eye Res.* **43**, 829–47 (1986).
10. Chow, C. K. & Tappel, A. L. Activities of pentose shunt and glycolytic enzymes in lungs of ozone-exposed rats. *Arch Env. Heal.* **26**, 205–8 (1973).
11. Shi, Z. Z. *et al.* Glutathione synthesis is essential for mouse development but not for cell growth in culture. *Proc. Natl. Acad. Sci. U. S. A.* **97**, 5101–5106 (2000).
12. Jeon, S., Chandel, N. & Hay, N. AMPK regulates NADPH homeostasis to promote tumour cell survival during energy stress. *Nature* **485**, 661–65 (2012).

13. Schnelldorfer, T. *et al.* Glutathione depletion causes cell growth inhibition and enhanced apoptosis in pancreatic cancer cells. *Cancer* **89**, 1440–7 (2000).
14. König, J., Nies, A. T., Cui, Y., Leier, I. & Keppler, D. Conjugate export pumps of the multidrug resistance protein (MRP) family: Localization, substrate specificity, and MRP2-mediated drug resistance. *Biochim. Biophys. Acta - Biomembr.* **1461**, 377–394 (1999).
15. Cole, S. P. *et al.* Overexpression of a glucose transporter gene in a multidrug-resistant human lung cancer cell line. *Science (80-.)*. **258**, 1650–4 (1992).
16. Unger, R. H., Aguilar-Parada, E., Müller, W. a & Eisentraut, a M. Studies of pancreatic alpha cell function in normal and diabetic subjects. *J. Clin. Invest.* **49**, 837–848 (1970).
17. Exton, J. H., Jefferson, L. S., Butcher, R. W. & Park, C. R. Gluconeogenesis in the perfused liver. The effects of fasting, alloxan diabetes, glucagon, epinephrine, adenosine 3', 5'-monophosphate and insulin. *Am. J. Med.* **40**, 709–15 (1966).
18. Owen, O. E., Felig, P., Morgan, a. P., Wahren, J. & Cahill, G. F. Liver and kidney metabolism during prolonged starvation. *J. Clin. Invest.* **48**, 574–583 (1969).
19. Bolli, G. *et al.* Mechanisms of glucagon secretion during insulin-induced hypoglycemia in man.. Role of the beta cell and arterial hyperinsulinemia. *J. Clin. Invest.* **73**, 917–922 (1984).
20. Kaneko, K. *et al.* Insulin inhibits glucagon secretion by the activation of PI3-kinase in In-R1-G9 cells. *Diabetes Res. Clin. Pract.* **44**, 83–92 (1999).
21. Puigserver, P. *et al.* Insulin-regulated hepatic gluconeogenesis through FOXO1 – PGC-1 a interaction. *Nature* **423**, 550–555 (2003).
22. Li, S., Brown, M. S. & Goldstein, J. L. Bifurcation of insulin signaling pathway in rat liver: mTORC1 required for stimulation of lipogenesis, but not inhibition of gluconeogenesis. *Proc. Natl. Acad. Sci. U. S. A.* **107**, 3441–3446 (2010).
23. James, D. E., Strube, M., Muedler, M. & Mueckler, M. Molecular cloning and characterization of an insulin-regulatable glucose transporter. *Nature* **338**, 83–87 (1989).
24. Olson, a L. & Pessin, J. E. Structure, function, and regulation of the mammalian facilitative glucose transporter gene family. *Annu. Rev. Nutr.* **16**, 235–256 (1996).

25. Rand, E. B., Depaoli, A. M., Davidson, N. O., Bell, G. I. & Burant, C. F. Sequence, tissue distribution, and functional characterization of the rat fructose transporter GLUT5. *Am. J. Physiol.* **264**, G1169–76 (1993).
26. Barzilai, N. & Rossetti, L. Role of glucokinase and glucose-6-phosphatase in the acute and chronic regulation of hepatic glucose fluxes by insulin. *J. Biol. Chem.* **268**, 25019–25025 (1993).
27. Cori, C. F., Schmidt, G. & Cori, G. T. The synthesis of a polysaccharide from glucose-1-phosphate in muscle extract. *Science (80-.)*. **89**, 464–65 (1939).
28. Leloir, L. F., Olavarria, J. M., Goldmerg, S. H. & Carminatti, H. Biosynthesis of glycogen from uridine diphosphate glucose. *Arch. Biochem. Biophys.* **81**, 508–20 (1959).
29. Kruger, N. J. & Von Schaewen, A. The oxidative pentose phosphate pathway: Structure and organisation. *Curr. Opin. Plant Biol.* **6**, 236–246 (2003).
30. Pandolfi, P. P. *et al.* Targeted disruption of the housekeeping gene encoding glucose 6-phosphate dehydrogenase (G6PD): G6PD is dispensable for pentose synthesis but essential for defense against oxidative stress. *EMBO J.* **14**, 5209–5215 (1995).
31. Juhnke, H., Krems, B., Kotter, P. & Entian, K. D. Mutants that show increased sensitivity to hydrogen peroxide reveal an important role for the pentose phosphate pathway in protection of yeast against oxidative stress. *Mol Gen Genet* **252**, 456–64 (1996).
32. Shefer, S., Hauser, S., Lapar, V. & Mosbach, E. H. HMG CoA reductase of intestinal mucosa and liver of the rat. *J. Lipid Res.* **13**, 402–412 (1972).
33. Harlan, W. R. & Wakil, S. J. Synthesis of fatty acids in animal tissues. I. Incorporation of C¹⁴-acetyl coenzyme A into a variety of long chain fatty acids by subcellular particles. *J Biol Chem* **238**, 3216–23 (1963).
34. Polgar, L. The mechanism of action of glyceraldehyde-3-phosphate dehydrogenase. *Experientia* **20**, 408–13 (1964).
35. Chance, B., Garfinkel, D., Higgins, J. & Hess, B. Metabolic control mechanisms. 5. A solution for the equations representing the interaction between glycolysis and respiration in ascites tumor cells. *J Biol Chem* **235**, 2426–39 (1960).
36. Douard, V. & Ferraris, R. P. Regulation of the fructose transporter GLUT5 in health and disease. *Am. J. Physiol. Endocrinol. Metab.* **295**, E227–E237 (2008).

37. Kiefer, P., Heinzle, E., Zelder, O., Wittmann, C. & Icrobiol, a P. P. L. E. N. M. Comparative Metabolic Flux Analysis of Lysine-Producing *Corynebacterium glutamicum* Cultured on Glucose or Fructose. *Appl. Environ. Microbiol.* **70**, 229–239 (2004).
38. Garland, P. B., Shepherd, D. & Yates, D. W. Steady-state concentrations of coenzyme A, acetyl-coenzyme A and long-chain fatty acyl-coenzyme A in rat-liver mitochondria oxidizing palmitate. *Biochem. J.* **97**, 587–594 (1965).
39. Krebs, H. a. The citric acid cycle and the Szent-Györgyi cycle in pigeon breast muscle. *Biochem. J.* **34**, 775–779 (1940).
40. Hatefi, Y. The mitochondrial electron transport and oxidative phosphorylation system. *Annu. Rev. Biochem.* **1985**, 1015–69
41. Itoh, H., Takahashi, A., Adachi, K. & Noji, H. Mechanically driven ATP synthesis by F₁-ATPase. *Nature* **427**, 465–468 (2004).
42. Owen, O. E., Kalhan, S. C. & Hanson, R. W. The key role of anaplerosis and cataplerosis for citric acid cycle function. *J. Biol. Chem.* **277**, 30409–30412 (2002).
43. Seubert, W. & Huth, W. On the mechanism of gluconeogenesis and its regulation. II. The mechanism of gluconeogenesis from pyruvate and fumarate. *Biochem Z* **343**, 176–91 (1965).
44. Spencer, a, Corman, L. & Lowenstein, J. M. Citrate and the conversion of carbohydrate into fat. A comparison of citrate and acetate incorporation into fatty acids. *Biochem. J.* **93**, 378–388 (1964).
45. Zhang, Y. *et al.* Liver LXR α expression is crucial for whole body cholesterol homeostasis and reverse cholesterol transport in mice. *J. Clin. Invest.* **122**, 1688–1699 (2012).
46. Repa, J. J. & Mangelsdorf, D. J. The role of orphan nuclear receptors in the regulation of cholesterol homeostasis. *Annu. Rev. Cell Dev. Biol.* **16**, 459–81 (2000).
47. Bensch, W. R. & Rodwell, V. W. Purification and properties of 3-hydroxy-3-methylglutaryl coenzyme A reductase from *Pseudomonas*. *J. Biol. Chem.* **245**, 3755–3762 (1970).

48. Chin, D. J. *et al.* Molecular cloning of 3-hydroxy-3-methylglutaryl coenzyme a reductase and evidence for regulation of its mRNA. *Proc. Natl. Acad. Sci. U. S. A.* **79**, 7704–7708 (1982).
49. Chun, K. T., Bar, N. S. & Simoni, R. D. The regulated degradation of 3-hydroxy-3-methylglutaryl CoA reductase requires a short lived protein and occurs in the endoplasmic reticulum. *J. Biol. Chem.* **265**, 22004–22010 (1990).
50. Luong, A., Hannah, V. C., Brown, M. S. & Goldstein, J. L. Molecular characterization of human acetyl-CoA synthetase, an enzyme regulated by sterol regulatory element-binding proteins. *J. Biol. Chem.* **275**, 26458–26466 (2000).
51. Espenshade, P. J. & Hughes, A. L. Regulation of sterol synthesis in eukaryotes. *Annu. Rev. Genet.* **41**, 401–427 (2007).
52. Brown, M. S. & Goldstein, J. L. The SREBP Pathway: Regulation Review of Cholesterol Metabolism by Proteolysis of a Membrane-Bound Transcription Factor. **89**, 1–10 (2009).
53. Deykin, D. & Goodman, D. S. The hydrolysis of long-chain fatty acid esters of cholesterol with rat liver enzymes. *J. Biol. Chem.* **237**, 3649–3656 (1962).
54. Gordon, H., Lewis, B., Eales, L. & Brock, J. Dietary fat and cholesterol metabolism; faecal elimination of bile acids and other lipids. *Lancet* **273**, 1299–306 (1957).
55. Morgan, R. & Hoffman, N. The interaction of lipase, lipase cofactor and bile salts in triglyceride hydrolysis. *Biochim Biophys Acta* **248**, 143–8 (1971).
56. Mitropoulos, K. a & Balasubramaniam, S. Cholesterol 7 -hydroxylase in rat liver microsomal preparations. *Biochem. J.* **128**, 1–9 (1972).
57. Rush, W., Gibson, G. & Parke, D. The purification and reconstitution of cytochrome P-450-dependent cholesterol 7 alpha-hydroxylase activity from rat liver microsomal fractions [proceedings]. *Biochem Soc Trans* **8**, 102–3 (1980).
58. Stroup, D., Crestani, M. & Chiang, J. Identification of a bile acid response element in the cholesterol 7 alpha-hydroxylase gene CYP7A. *Am. J. Physiol.* **273**, G508–17 (1997).
59. Yao, Z. & McLeod, R. S. Synthesis and secretion of hepatic apolipoprotein B-containing lipoproteins. *Biochim. Biophys. Acta - Lipids Lipid Metab.* **1212**, 152–166 (1994).

60. Yang, C. Y. *et al.* Human very low density lipoprotein structure: interaction of the C apolipoproteins with apolipoprotein B-100. *J. Lipid Res.* **34**, 1311–1321 (1993).
61. Brown, M. S., Faust, J. R. & Goldstein, J. L. Role of the low density lipoprotein receptor in regulating the content of free and esterified cholesterol in human fibroblasts. *J. Clin. Invest.* **78**, 783 (1975).
62. Denis, J. & Foster, W. The Role of Malonyl-CoA in the Coordination of Fatty Acid Synthesis and Oxidation in Isolated Rat Hepatocytes. *J Biol Chem* **253**, 8294–8300 (1978).
63. Jachson, K. & Schutz, Y. Glycogen storage capacity and de novo lipogenesis massive carbohydrate overfeeding in man. *Am J Clin Nutr* **48**, 240–247 (1988).
64. Polakis, S. E., Guchhait, R. B., Zwergel, E. E., Lane, M. D. & Cooper, T. G. Acetyl Coenzyme A Carboxylase system of *Escherichia coli*. Studies on the mechanisms of the biotin carboxylase- and carboxyltransferase-catalyzed reactions. *J Biol Chem* **249**, 6657–67 (1974).
65. Gregolin, C., Ryder, E., Kleinschmidt, A. K., Warner, R. C. & Lane, M. D. Molecular characteristics of liver acetyl-CoA carboxylase. *Biochemistry* **56**, 148–155 (1966).
66. Abu-Elheiga, L. *et al.* The subcellular localization of acetyl-CoA carboxylase 2. *Proc. Natl. Acad. Sci. U. S. A.* **97**, 1444–1449 (2000).
67. Saddik, M., Gamble, J., Witters, L. a & Lopaschuk, G. D. Acetyl-CoA carboxylase regulation of fatty acid oxidation in the heart. *J. Biol. Chem.* **268**, 25836–25845 (1993).
68. Munday, M. R., Campbell, D. G., Carling, D. & Hardie, D. G. Identification by amino acid sequencing of three major regulatory phosphorylation sites on rat acetyl-CoA carboxylase. *Eur. J. Biochem.* **175**, 331–338 (1988).
69. Ahmad, F., Ahmad, P. M., Pieretti, L. & Watters, G. T. Purification and subunit structure of rat mammary gland acetyl coenzyme A carboxylase. *J. Biol. Chem.* **253**, 1733–1737 (1978).
70. Ha, J., Daniel, S., Broyles, S. S. & Kim, K. H. Critical phosphorylation sites for acetyl-CoA carboxylase activity. *J. Biol. Chem.* **269**, 22162–8 (1994).
71. Katsurada, a *et al.* Effects of nutrients and hormones on transcriptional and post-transcriptional regulation of fatty acid synthase in rat liver. *Eur. J. Biochem.* **190**, 427–433 (1990).

72. Foretz, M., Guichard, C., Ferré, P. & Foufelle, F. Sterol regulatory element binding protein-1c is a major mediator of insulin action on the hepatic expression of glucokinase and lipogenesis-related genes. *Proc. Natl. Acad. Sci. U. S. A.* **96**, 12737–12742 (1999).
73. Osborne, T. F. Sterol regulatory element-binding proteins (SREBPS): Key regulators of nutritional homeostasis and insulin action. *J. Biol. Chem.* **275**, 32379–32382 (2000).
74. Schultz, J. R. *et al.* Role of LXRs in control of lipogenesis. *Genes Dev.* **14**, 2831–2838 (2000).
75. Yoshikawa, T. *et al.* Polyunsaturated fatty acids suppress sterol regulatory element-binding protein 1c promoter activity by inhibition of liver X receptor (LXR) binding to LXR response elements. *J. Biol. Chem.* **277**, 1705–1711 (2002).
76. Hwang, S. H., Ki, S. H., Bae, E. J., Kim, H. E. & Kim, S. G. Role of adenosine monophosphate-activated protein kinase-p70 ribosomal S6 kinase-1 pathway in repression of liver X receptor-alpha-dependent lipogenic gene induction and hepatic steatosis by a novel class of dithiolethiones. *Hepatology* **49**, 1913–1925 (2009).
77. Owen, J. L. *et al.* From the Cover: Insulin stimulation of SREBP-1c processing in transgenic rat hepatocytes requires p70 S6-kinase. *Proc. Natl. Acad. Sci.* **109**, 16184–16189 (2012).
78. Sheng, Z., Otani, H., Brown, M. S. & Goldstein, J. L. Independent regulation of sterol regulatory element-binding proteins 1 and 2 in hamster liver. *Proc. Natl. Acad. Sci. U. S. A.* **92**, 935–938 (1995).
79. Hegarty, B. D. *et al.* Distinct roles of insulin and liver X receptor in the induction and cleavage of sterol regulatory element-binding protein-1c. *Proc. Natl. Acad. Sci. U. S. A.* **102**, 791–796 (2005).
80. Dentin, R., Girard, J. & Postic, C. Carbohydrate responsive element binding protein (ChREBP) and sterol regulatory element binding protein-1c (SREBP-1c): Two key regulators of glucose metabolism and lipid synthesis in liver. *Biochimie* **87**, 81–86 (2005).
81. Koo, S. H., Dutcher, A. K. & Towle, H. C. Glucose and Insulin Function through Two Distinct Transcription Factors to Stimulate Expression of Lipogenic Enzyme Genes in Liver. *J. Biol. Chem.* **276**, 9437–9445 (2001).

82. Yamashita, H. *et al.* A glucose-responsive transcription factor that regulates carbohydrate metabolism in the liver. *Proc. Natl. Acad. Sci. U. S. A.* **98**, 9116–9121 (2001).
83. Dentin, R. *et al.* Glucose 6-phosphate, rather than xylulose 5-phosphate, is required for the activation of ChREBP in response to glucose in the liver. *J. Hepatol.* **56**, 199–209 (2012).
84. Smith, S. The animal fatty acid synthase: one gene, one polypeptide, seven enzymes. *FASEB J.* **8**, 1248–1259 (1994).
85. McKeon, T. a. & Stumpf, P. K. Purification and characterization of the stearyl-acyl carrier protein desaturase and the acyl-acyl carrier protein thioesterase from maturing seeds of safflower. *J. Biol. Chem.* **257**, 12141–12147 (1982).
86. Collins, J. M. *et al.* De novo lipogenesis in the differentiating human adipocyte can provide all fatty acids necessary for maturation. *J. Lipid Res.* **52**, 1683–1692 (2011).
87. Schrijver, E. De, Brusselmans, K., Heyns, W. & Cells, C. RNA Interference-mediated Silencing of the Fatty Acid Synthase Gene Attenuates Growth and Induces Morphological Changes and Apoptosis of LNCaP Prostate Cancer Cells RNA Interference-mediated Silencing of the Fatty Acid Synthase Gene Attenuates Growth and . 3799–3804 (2003).
88. Thiam, A. R., Farese, R. V & Walther, T. C. The biophysics and cell biology of lipid droplets. *Nat. Rev. Mol. Cell Biol.* **14**, 775–86 (2013).
89. Hebbes, T. R., Thorne, a W. & Crane-Robinson, C. A direct link between core histone acetylation and transcriptionally active chromatin. *EMBO J.* **7**, 1395–1402 (1988).
90. Hong, L., Schroth, G. P., Matthews, H. R., Yau, P. & Bradbury, E. M. Studies of the DNA binding properties of histone H4 amino terminus. Thermal denaturation studies reveal that acetylation markedly reduces the binding constant of the H4 ‘tail’ to DNA. *J. Biol. Chem.* **268**, 305–314 (1993).
91. Zhang, M., Galdieri, L. & Vancura, A. The yeast AMPK homolog SNF1 regulates acetyl coenzyme A homeostasis and histone acetylation. *Mol. Cell. Biol.* **33**, 4701–4717 (2013).
92. Zhao, S. *et al.* Regulation of cellular metabolism by protein lysine acetylation. *Science (80-)*. **327**, 1000–4 (2010).

93. Hallows, W. C., Yu, W. & Denu, J. M. Regulation of glycolytic enzyme phosphoglycerate mutase-1 by Sirt1 protein-mediated deacetylation. *J. Biol. Chem.* **287**, 3850–3858 (2012).
94. Lerin, C. *et al.* GCN5 acetyltransferase complex controls glucose metabolism through transcriptional repression of PGC-1 α . *Cell Metab.* **3**, 429–438 (2006).
95. Puigserver, P. *et al.* A cold-inducible coactivator of nuclear receptors linked to adaptive thermogenesis. *Cell* **92**, 829–839 (1998).
96. Yoon, J. C. *et al.* Control of hepatic gluconeogenesis through the transcriptional coactivator PGC-1. *Nature* **413**, 131–138 (2001).
97. Gerhart-Hines, Z. *et al.* Metabolic control of muscle mitochondrial function and fatty acid oxidation through SIRT1/PGC-1 α . *EMBO J.* **26**, 1913–1923 (2007).
98. Chakravarthy, M. V. *et al.* ‘New’ hepatic fat activates PPAR α to maintain glucose, lipid, and cholesterol homeostasis. *Cell Metab.* **1**, 309–322 (2005).
99. Nohara, H., Takahashi, T. & Kikuo, O. Enzymatic acetylation of histones and some characters of their acetyl groups. *Biochim Biophys Acta* **154**, 529–39 (1967).
100. Paik, W. K., Pearson, D., Lee, H. W. & Kim, S. Nonenzymatic acetylation of histones with acetyl-CoA. *Biochim Biophys Acta* **213**, 513–22 (1970).
101. Brownell, J. E. *et al.* Tetrahymena histone acetyltransferase A: A homolog to yeast Gcn5p linking histone acetylation to gene activation. *Cell* **84**, 843–851 (1996).
102. Takahashi, H., McCaffery, J. M., Irizarry, R. a. & Boeke, J. D. Nucleocytosolic Acetyl-Coenzyme A Synthetase Is Required for Histone Acetylation and Global Transcription. *Mol. Cell* **23**, 207–217 (2006).
103. Cai, L., Sutter, B. M., Li, B. & Tu, B. P. Acetyl-CoA Induces Cell Growth and Proliferation by Promoting the Acetylation of Histones at Growth Genes. *Mol. Cell* **42**, 426–437 (2011).
104. Galdieri, L. & Vancura, A. Acetyl-CoA carboxylase regulates global histone acetylation. *J. Biol. Chem.* **287**, 23865–23876 (2012).
105. Pietrocola, F., Galluzzi, L., Bravo-San Pedro, J. M., Madeo, F. & Kroemer, G. Acetyl Coenzyme A: A Central Metabolite and Second Messenger. *Cell Metab.* **21**, 805–821 (2015).

106. Angulo, P. GI epidemiology: nonalcoholic fatty liver disease. *Aliment. Pharmacol. Ther.* **25**, 883–889 (2007).
107. Williams, C. D. *et al.* Prevalence of nonalcoholic fatty liver disease and nonalcoholic steatohepatitis among a largely middle-aged population utilizing ultrasound and liver biopsy: A prospective study. *Gastroenterology* **140**, 124–131 (2011).
108. Powell, E. E. *et al.* The natural history of nonalcoholic steatohepatitis: a follow-up study of forty-two patients for up to 21 years. *Hepatology* **11**, 74–80 (1990).
109. Angulo, P. & Lindor, K. D. Non-alcoholic fatty liver disease. *J. Gastroenterol. Hepatol.* **17 Suppl**, S186–S190 (2002).
110. Alder, M. & Schaffner, F. Fatty liver hepatitis and cirrhosis in obese patients. *Am J Med* **67**, 811–6 (1979).
111. Lee, R. G. Nonalcoholic steatohepatitis: a study of 49 patients. *Hum. Pathol.* **20**, 594–598 (1989).
112. Pinto, H. C. *et al.* Nonalcoholic steatohepatitis. Clinicopathological comparison with alcoholic hepatitis in ambulatory and hospitalized patients. *Dig Dis Sci* **41**, 172–9 (1996).
113. Angulo, P., Keach, J. C., Batts, K. & Lindor, K. D. Independent Predictors of Liver Fibrosis in Patients With Nonalcoholic Steatohepatitis. *Hepatology* **30**, 1356–1362 (1999).
114. Lonardo, A., Ballestri, S., Marchesini, G., Angulo, P. & Loria, P. Nonalcoholic fatty liver disease: A precursor of the metabolic syndrome. *Dig. Liver Dis.* **47**, 181–90 (2015).
115. King, I. B. *et al.* Prospective association of fatty acids in the de novo lipogenesis pathway with risk of type 2 diabetes : the Cardiovascular Health Study 1 – 5. 153–163 (2015). doi:10.3945/ajcn.114.092601.De
116. Assy, N. *et al.* Fatty infiltration of liver in hyperlipidemic patients. *Dig Dis Sci* **45**, 1929–34 (2000).
117. Targher, G. & Arcaro, G. Non-alcoholic fatty liver disease and increased risk of cardiovascular disease. *Atherosclerosis* **191**, 235–240 (2007).
118. Chitturi, S. *et al.* NASH and insulin resistance: Insulin hypersecretion and specific association with the insulin resistance syndrome. *Hepatology* **35**, 373–379 (2002).

119. Pagano, G. *et al.* Nonalcoholic steatohepatitis, insulin resistance, and metabolic syndrome: further evidence for an etiologic association. *Hepatology* **35**, 367–72 (2002).
120. Marchesini, G., Brizi, M. & Bianchi, G. Nonalcoholic fatty liver disease: a feature of the metabolic syndrome. *Diabetes* **50**, 1844–1850 (2001).
121. Marchesini, G. *et al.* Association of nonalcoholic fatty liver disease with insulin resistance. *Am. J. Med.* **107**, 450–455 (1999).
122. Abdul-Ghani, M. a., Matsuda, M., Balas, B. & DeFronzo, R. a. Muscle and liver insulin resistance indexes derived from the oral glucose tolerance test. *Diabetes Care* **30**, 89–94 (2007).
123. Perry, R. J., Samuel, V. T., Petersen, K. F. & Shulman, G. I. The role of hepatic lipids in hepatic insulin resistance and type 2 diabetes. *Nature* **510**, 84–91 (2014).
124. Ontko, J. a & Wang, C. S. Elevation of liver diacylglycerols and molecular species of diacylglycerols in rats fed a lipogenic diet. *J. Lipid Res.* **30**, 691–699 (1989).
125. Meshkani, R. & Adeli, K. Hepatic insulin resistance, metabolic syndrome and cardiovascular disease. *Clin. Biochem.* **42**, 1331–1346 (2009).
126. Fullerton, M. D. *et al.* Single phosphorylation sites in Acc1 and Acc2 regulate lipid homeostasis and the insulin-sensitizing effects of metformin. *Nat. Med.* **19**, 1649–1654 (2013).
127. Reboucas, G. & Isselbacher, K. J. Studies on the pathogenesis of the ethanol-induced fatty liver. I. Synthesis and oxidation of fatty acids by the liver. *J Clin Invest* **40**, 1355–62 (1961).
128. Timlin, M. T. & Parks, E. J. Temporal pattern of de novo lipogenesis in the postprandial state in healthy men. *Am. J. Clin. Nutr.* **81**, 35–42 (2005).
129. Donnelly, K. L. *et al.* Sources of fatty acids stored in liver and secreted via lipoproteins in patients with nonalcoholic fatty liver disease. *J. Clin. Invest.* **115**, 1343–1351 (2005).
130. Diraison, F., Moulin, P. & Beylot, M. Contribution of hepatic de novo lipogenesis and reesterification of plasma non esterified fatty acids to plasma triglyceride synthesis during non-alcoholic fatty liver disease. *Diabetes Metab* **29**, 478–85 (2003).

131. Nakamuta, M. *et al.* Evaluation of fatty acid metabolism-related gene expression in nonalcoholic fatty liver disease. *Int J Mol Med* **16**, 631–5 (2005).
132. Kohjima, M. *et al.* Re-evaluation of fatty acid metabolism-related gene expression in nonalcoholic fatty liver disease. *Int J Mol Med* **20**, 351–358 (2007).
133. Araya, J. *et al.* Increase in long-chain polyunsaturated fatty acid n - 6/n - 3 ratio in relation to hepatic steatosis in patients with non-alcoholic fatty liver disease. *Clin Sci* **106**, 635–43 (2004).
134. Abu-Elheiga, L. *et al.* Mutant mice lacking acetyl-CoA carboxylase 1 are embryonically lethal. *Proc. Natl. Acad. Sci. U. S. A.* **102**, 12011–12016 (2005).
135. Chirala, S. S. *et al.* Fatty acid synthesis is essential in embryonic development: fatty acid synthase null mutants and most of the heterozygotes die in utero. *Proc. Natl. Acad. Sci. U. S. A.* **100**, 6358–6363 (2003).
136. Harada, N. *et al.* Hepatic de novo lipogenesis is present in liver-specific ACC1-deficient mice. *Mol. Cell. Biol.* **27**, 1881–1888 (2007).
137. Mao, J. *et al.* Liver-specific deletion of acetyl-CoA carboxylase 1 reduces hepatic triglyceride accumulation without affecting glucose homeostasis. *Proc. Natl. Acad. Sci. U. S. A.* **103**, 8552–8557 (2006).
138. Savage, D. B. *et al.* Reversal of diet-induced hepatic steatosis and hepatic insulin resistance by antisense oligonucleotide inhibitors of acetyl-CoA carboxylases 1 and 2. *J. Clin. Invest.* **116**, 817–824 (2006).
139. Torre, L. a *et al.* Global Cancer Statistics, 2012. **00**, 1–22 (2015).
140. El-Serag, H. B., White, D. L. & Nurgalieva, Z. Epidemiology of Hepatocellular Carcinoma. *Gastrointest. Oncol. A Crit. Multidiscip. Team Approach* **24**, 409–420 (2009).
141. Bosch, F. X., Ribes, J., Díaz, M. & Cléries, R. Primary liver cancer: Worldwide incidence and trends. *Gastroenterology* **127**, 5–16 (2004).
142. Daniele, B., Bencivenga, A., Megna, A. S. & Tinessa, V. Alpha-Fetoprotein and Ultrasonography Screening for Hepatocellular Carcinoma. *Gastroenterology* **127**, 108–112 (2004).
143. Snowberger, N. *et al.* Alpha fetoprotein, ultrasound, computerized tomography and magnetic resonance imaging for detection of hepatocellular carcinoma in patients with advanced cirrhosis. *Aliment. Pharmacol. Ther.* **26**, 1187–1194 (2007).

144. Ho, C.-L., Yu, S. C. H. & Yeung, D. W. C. 11C-acetate PET imaging in hepatocellular carcinoma and other liver masses. *J. Nucl. Med.* **44**, 213–221 (2003).
145. Roncalli, M., Park, Y. N. & Di Tommaso, L. Histopathological classification of hepatocellular carcinoma. *Dig. Liver Dis.* **42**, 228–234 (2010).
146. Bruix, J. & Sherman, M. Management of hepatocellular carcinoma: An update. *Hepatology* **53**, 1020–1022 (2011).
147. Amsden, G. W. Hepatitis C and liver transplantation. *Gut* **44**, 1–6 (1999).
148. Ahmad, J., Dodson, S. F., Demetris, a. J., Fung, J. J. & Shakil, a. O. Recurrent hepatitis C after liver transplantation: A nonrandomized trial of interferon alfa alone versus interferon alfa and ribavirin. *Liver Transplant.* **7**, 863–869 (2001).
149. Ghobrial, R. M. *et al.* A 10-year experience of liver transplantation for hepatitis C: analysis of factors determining outcome in over 500 patients. *Ann. Surg.* **234**, 384–393; discussion 393–394 (2001).
150. Berenguer, M. *et al.* Contribution of donor age to the recent decrease in patient survival among HCV-infected liver transplant recipients. *Hepatology* **36**, 202–210 (2002).
151. Forman, L. M., Lewis, J. D., Berlin, J. a, Feldman, H. I. & Lucey, M. R. The association between hepatitis C infection and survival after orthotopic liver transplantation. *Gastroenterology* **122**, 889–896 (2002).
152. Vogl, T. J. *et al.* Review on transarterial chemoembolization in hepatocellular carcinoma: Palliative, combined, neoadjuvant, bridging, and symptomatic indications. *Eur. J. Radiol.* **72**, 505–516 (2009).
153. Takayasu, K. *et al.* Prospective Cohort Study of Transarterial Chemoembolization for Unresectable Hepatocellular Carcinoma in 8510 Patients. *Gastroenterology* **131**, 461–469 (2006).
154. Hilgard, P. *et al.* Sorafenib in advanced hepatocellular carcinoma. *N. Engl. J. Med.* **359**, 378–390 (2008).
155. Zeng, Z. C. *et al.* A comparison of treatment combinations with and without radiotherapy for hepatocellular carcinoma with portal vein and/or inferior vena cava tumor thrombus. *Int. J. Radiat. Oncol. Biol. Phys.* **61**, 432–443 (2005).

156. Marrero, J. A., Fontana, R. J., Conjeevaram, H. S., Emick, D. M. & Lok, A. S. NAFLD may be a common underlying liver disease in patients with hepatocellular carcinoma in the United States. *Hepatology* **36**, 1349–54 (2002).
157. Bugianesi, E. *et al.* Expanding the natural history of nonalcoholic steatohepatitis: From cryptogenic cirrhosis to hepatocellular carcinoma. *Gastroenterology* **123**, 134–140 (2002).
158. Tsubouchi, H. *et al.* Levels of the human hepatocyte growth factor in serum of patients with various liver diseases determined by an enzyme-linked immunosorbent assay. *Hepatology* **13**, 1–5 (1991).
159. Matsuzaki, K. *et al.* Chronic inflammation associated with hepatitis C virus infection perturbs hepatic transforming growth factor beta signaling, promoting cirrhosis and hepatocellular carcinoma. *Hepatology* **46**, 48–57 (2007).
160. Wiemann, S. U. *et al.* Hepatocyte telomere shortening and senescence are general markers of human liver cirrhosis. *FASEB J.* **16**, 935–942 (2002).
161. Farazi, P. a *et al.* Differential Impact of Telomere Dysfunction on Initiation and Progression of Hepatocellular Carcinoma Differential Impact of Telomere Dysfunction on Initiation and Progression of. **4**, 5021–5027 (2003).
162. Petrosillo, G. *et al.* Mitochondrial dysfunction in rat with nonalcoholic fatty liver Involvement of complex I, reactive oxygen species and cardiolipin. *Biochim. Biophys. Acta* **1767**, 1260–1267 (2007).
163. Knudsen, E. S., Gopal, P. & Singal, A. G. The changing landscape of hepatocellular carcinoma: Etiology, genetics, and therapy. *Am. J. Pathol.* **184**, 574–583 (2014).
164. Guichard, C. *et al.* Integrated analysis of somatic mutations and focal copy-number changes identifies key genes and pathways in hepatocellular carcinoma. *Nat. Genet.* **44**, 694–698 (2012).
165. Huang, J. *et al.* Exome sequencing of hepatitis B virus–associated hepatocellular carcinoma. *Nat. Genet.* **44**, 1117–1121 (2012).
166. Fujimoto, A. *et al.* Whole-genome sequencing of liver cancers identifies etiological influences on mutation patterns and recurrent mutations in chromatin regulators. *Nat. Genet.* **44**, 760–764 (2012).

167. Kan, Z. *et al.* Whole-genome sequencing identifies recurrent mutations in hepatocellular carcinoma Whole-genome sequencing identifies recurrent mutations in hepatocellular carcinoma. 1422–1433 (2013). doi:10.1101/gr.154492.113
168. McClendon, a. K. *et al.* RB and p53 cooperate to prevent liver tumorigenesis in response to tissue damage. *Gastroenterology* **141**, 1439–1450 (2011).
169. Lee, J.-S. *et al.* Application of comparative functional genomics to identify best-fit mouse models to study human cancer. *Nat. Genet.* **36**, 1306–1311 (2004).
170. Bakiri, L. & Wagner, E. F. Mouse models for liver cancer. *Mol. Oncol.* **7**, 206–223 (2013).
171. Li, Z., Tuteja, G., Schug, J. & Kaestner, K. H. Foxa1 and Foxa2 are essential for sexual dimorphism in liver cancer. *Cell* **148**, 72–83 (2012).
172. Kelland, L. R. ‘Of mice and men’: Values and liabilities of the athymic nude mouse model in anticancer drug development. *Eur. J. Cancer* **40**, 827–836 (2004).
173. Chisari, F. V *et al.* Molecular pathogenesis of hepatocellular carcinoma in hepatitis B virus transgenic mice. *Cell* **59**, 1145–1156 (1989).
174. Dubois, N. *et al.* Time-course development of differentiated hepatocarcinoma and lung metastasis in transgenic mice. *J Hepatol* **13**, 227–39 (1991).
175. Sandgren, E. P., Quaife, C. J., Pinkert, C. A., Pamiter, R. D. & Brinster, R. L. Oncogene-induced liver neoplasia in transgenic mice. *Oncogene* **4**, 715–24 (1989).
176. Sepulveda, a. R. *et al.* Development of a transgenic mouse system for the analysis of stages in liver carcinogenesis using tissue-specific expression of SV40 large T-antigen controlled by regulatory elements of the human α -1-antitrypsin gene. *Cancer Res.* **49**, 6108–6117 (1989).
177. Michalopoulos, G. K. Liver regeneration after partial hepatectomy: critical analysis of mechanistic dilemmas. *Am. J. Pathol.* **176**, 2–13 (2010).
178. Bralet, M. P., Pichard, V. & Ferry, N. Demonstration of direct lineage between hepatocytes and hepatocellular carcinoma in diethylnitrosamine-treated rats. *Hepatology* **36**, 623–630 (2002).
179. Maeda, S., Kamata, H., Luo, J. L., Leffert, H. & Karin, M. IKKbeta couples hepatocyte death to cytokine-driven compensatory proliferation that promotes chemical hepatocarcinogenesis. *Cell* **121**, 977–990 (2005).

180. Bhaskaran, K. *et al.* Body-mass index and risk of 22 specific cancers: a population-based cohort study of 5.24 million UK adults. *Lancet* **384**, 755–765 (2014).
181. Calle, E. E., Rodriguez, C., Walker-thurmond, K. & Thun, M. J. Overweight, obesity, and mortality from cancer in a prospectively studied cohort of U.S. adults. *N. Engl. J. Med.* **349**, 1625–1638 (2003).
182. Wolk, A. *et al.* A prospective study of obesity and cancer risk (Sweden). *Cancer Causes Control* **12**, 13–21 (2001).
183. Park, E. J. *et al.* Dietary and genetic obesity promote liver inflammation and tumorigenesis by enhancing IL-6 and TNF expression. *Cell* **140**, 197–208 (2010).
184. Yoshimoto, S. *et al.* Obesity-induced gut microbial metabolite promotes liver cancer through senescence secretome. *Nature* **499**, 97–101 (2013).
185. Ridlon, J. M., Kang, D.-J. & Hylemon, P. B. Bile salt biotransformations by human intestinal bacteria. *J. Lipid Res.* **47**, 241–259 (2006).
186. Warburg, O. The Metabolism of Carcinoma Cells. *J. Cancer Res.* **9**, 148–163 (1925).
187. Hsu, P. P. & Sabatini, D. M. Cancer cell metabolism: Warburg and beyond. *Cell* **134**, 703–707 (2008).
188. Vander Heiden, M. G., Cantley, L. C. & Thompson, C. B. Understanding the Warburg effect: the metabolic requirements of cell proliferation. *Science* **324**, 1029–1033 (2009).
189. Brusselmans, K. & Swinnen, J. V. Increased lipogenesis in cancer cells: new players, novel targets. *Curr Opin. Clin Nutr Metab Care* **9**, 358–65 (2006).
190. Yahagi, N. *et al.* Co-ordinate activation of lipogenic enzymes in hepatocellular carcinoma. *Eur. J. Cancer* **41**, 1316–1322 (2005).
191. Calvisi, D. F. *et al.* Increased lipogenesis, induced by AKT-mTORC1-RPS6 signaling, promotes development of human hepatocellular carcinoma. *Gastroenterology* **140**, 1071–83 (2011).
192. Yamashita, T. *et al.* Activation of lipogenic pathway correlates with cell proliferation and poor prognosis in hepatocellular carcinoma. *J. Hepatol.* **50**, 100–110 (2009).

193. Swinnen, J. V. *et al.* Fatty acid synthase drives the synthesis of phospholipids partitioning into detergent-resistant membrane microdomains. *Biochem. Biophys. Res. Commun.* **302**, 898–903 (2003).
194. Rakheja, D., Kapur, P., Hoang, M. P., Roy, L. C. & Bennett, M. J. Increased ratio of saturated to unsaturated C18 fatty acids in colonic adenocarcinoma: Implications for cryotherapy and lipid raft function. *Med. Hypotheses* **65**, 1120–1123 (2005).
195. Simons, K. & Ikonen, E. Functional rafts in cell membranes. *Nature* **387**, 569–572 (1997).
196. Simons, K. & Toomre, D. Lipid rafts and signal transduction. *Nat. Rev. Mol. Cell Biol.* **1**, 31–39 (2000).
197. Rysman, E. *et al.* De novo lipogenesis protects cancer cells from free radicals and chemotherapeutics by promoting membrane lipid saturation. *Cancer Res.* **70**, 8117–8126 (2010).
198. Sun, Z. & Lazar, M. a. Dissociating fatty liver and diabetes. *Trends Endocrinol. Metab.* **24**, 4–12 (2013).
199. Corbett, J. W. Review of recent acetyl-CoA carboxylase inhibitor patents: mid-2007-2008. *Expert Opin Ther Pat* (2009).
200. Tong, L. & Harwood, H. J. Acetyl-coenzyme A carboxylases: Versatile targets for drug discovery. *J. Cell. Biochem.* **99**, 1476–1488 (2006).
201. Hoehn, K. L. *et al.* Acute or Chronic Upregulation of Mitochondrial Fatty Acid Oxidation Has No Net Effect on Whole-Body Energy Expenditure or Adiposity. *Cell Metab.* **11**, 70–76 (2010).
202. Olson, D. P., Pulinilkunnil, T., Cline, G. W., Shulman, G. I. & Lowell, B. B. Gene knockout of *Acc2* has little effect on body weight, fat mass, or food intake. *Proc. Natl. Acad. Sci. U. S. A.* **107**, 7598–7603 (2010).
203. Reddy, J. K. & Rao, M. S. Lipid metabolism and liver inflammation. II. Fatty liver disease and fatty acid oxidation. *Am. J. Physiol. Gastrointest. Liver Physiol.* **290**, G852–8 (2006).
204. Randle, P. J., Garland, P. B., Hales, C. N. & Newsholme, E. A. The glucose fatty-acid cycle. Its role in insulin sensitivity and the metabolic disturbances of diabetes mellitus. *Lancet* **1**, 785–9 (1963).

205. Chakravarthy, M. V. *et al.* Identification of a Physiologically Relevant Endogenous Ligand for PPAR α in Liver. *Cell* **138**, 476–488 (2009).
206. Yang, L. *et al.* The fasted/fed mouse metabolic acetylome: N6-acetylation differences suggest acetylation coordinates organ-specific fuel switching. *J. Proteome Res.* **10**, 4134–4149 (2011).
207. Wang, Q. *et al.* Acetylation of metabolic enzymes coordinates carbon source utilization and metabolic flux. *Science* **327**, 1004–1007 (2010).
208. Sterner, D. E. & Berger, S. L. Acetylation of histones and transcription-related factors. *Microbiol. Mol. Biol. Rev.* **64**, 435–459 (2000).
209. Roth, S. Y., Denu, J. M. & Allis, C. D. Histone acetyltransferases. *Annu. Rev. Biochem.* **70**, 81–120 (2001).
210. Cai, L. & Tu, B. P. On acetyl-CoA as a gauge of cellular metabolic state. *Cold Spring Harb. Symp. Quant. Biol.* **76**, 195–202 (2011).
211. Karamanlidis, G. *et al.* Mitochondrial complex I deficiency increases protein acetylation and accelerates heart failure. *Cell Metab.* **18**, 239–250 (2013).
212. Chow, J. D. Y. *et al.* Genetic inhibition of hepatic acetyl-CoA carboxylase activity increases liver fat and alters global protein acetylation. *Mol. Metab.* **3**, 419–431 (2014).
213. Cohen, P., Nimmo, H. & Proud, C. How does insulin stimulate glycogen synthesis? *Biochem Soc Symp* 69–95 (1978).
214. Schwarz, J.-M., Linfoot, P., Dare, D. & Aghajanian, K. Hepatic de novo lipogenesis in normoinsulinemic and hyperinsulinemic subjects consuming high-fat, low-carbohydrate and low-fat, high-carbohydrate isoenergetic diets. *Am. J. Clin. Nutr.* **77**, 43–50 (2003).
215. El-Serag, H. B. & Rudolph, K. L. Hepatocellular Carcinoma: Epidemiology and Molecular Carcinogenesis. *Gastroenterology* **132**, 2557–2576 (2007).
216. Starley, B. Q., Calcagno, C. J. & Harrison, S. a. Nonalcoholic fatty liver disease and hepatocellular carcinoma: A weighty connection. *Hepatology* **51**, 1820–1832 (2010).
217. Davila, J. a, Morgan, R. O., Shaib, Y., McGlynn, K. a & El-Serag, H. B. Diabetes increases the risk of hepatocellular carcinoma in the United States: a population based case control study. *Gut* **54**, 533–539 (2005).

218. El-Serag, H. B., Tran, T. & Everhart, J. E. Diabetes Increases the Risk of Chronic Liver Disease and Hepatocellular Carcinoma. *Gastroenterology* **126**, 460–468 (2004).
219. Wideroff, L. *et al.* Cancer incidence in a population-based cohort of patients hospitalized with diabetes mellitus in Denmark. *J. Natl. Cancer Inst.* **89**, 1360–1365 (1997).
220. Jee, S. H. *et al.* Fasting serum glucose level and cancer risk in Korean men and women. *JAMA* **293**, 2210–2211; author reply 2211 (2005).
221. Rossi, M. *et al.* Dietary glycemic load and hepatocellular carcinoma with or without chronic hepatitis infection. *Ann. Oncol.* **20**, 1736–1740 (2009).
222. Verna, L., Whysner, J. & Williams, G. M. N-Nitrosodiethylamine mechanistic data and risk assessment: Bioactivation, DNA-adduct formation, mutagenicity, and tumor initiation. *Pharmacol. Ther.* **71**, 57–81 (1996).
223. Farazi, P. a & DePinho, R. a. Hepatocellular carcinoma pathogenesis: from genes to environment. *Nat. Rev. Cancer* **6**, 674–87 (2006).
224. Heindryckx, F., Colle, I. & Van Vlierberghe, H. Experimental mouse models for hepatocellular carcinoma research. *Int. J. Exp. Pathol.* **90**, 367–386 (2009).
225. Turner, N. *et al.* Enhancement of muscle mitochondrial oxidative capacity and alterations in insulin action are lipid species dependent: potent tissue-specific effects of medium-chain fatty acids. *Diabetes* **58**, 2547–2554 (2009).
226. Evert, M. *et al.* V-AKT murine thymoma viral oncogene homolog/mammalian target of rapamycin activation induces a module of metabolic changes contributing to growth in insulin-induced hepatocarcinogenesis. *Hepatology* **55**, 1473–1484 (2012).
227. Nagai, Y. *et al.* The Role of Peroxisome Proliferator-Activated Receptor γ Coactivator-1 β in the Pathogenesis of Fructose-Induced Insulin Resistance. *Cell Metab.* **9**, 252–264 (2009).
228. Messier, C., Whately, K., Liang, J., Du, L. & Puissant, D. The effects of a high-fat, high-fructose, and combination diet on learning, weight, and glucose regulation in C57BL/6 mice. *Behav. Brain Res.* **178**, 139–145 (2007).
229. Garbow, J. R. *et al.* Hepatic steatosis, inflammation, and ER stress in mice maintained long term on a very low-carbohydrate ketogenic diet. *Am. J. Physiol. Gastrointest. Liver Physiol.* **300**, G956–67 (2011).

230. Cao, C. *et al.* AMP-activated protein kinase contributes to UV- and H₂O₂-induced apoptosis in human skin keratinocytes. *J. Biol. Chem.* **283**, 28897–28908 (2008).
231. He, G. *et al.* AMP-Activated Protein Kinase Induces p53 by Phosphorylating MDMX and Inhibiting Its Activity. *Mol. Cell. Biol.* **34**, 148–157 (2013).
232. Luo, J. *et al.* Negative control of p53 by Sir2alpha promotes cell survival under stress. *Cell* **107**, 137–148 (2001).
233. Leandro, G. *et al.* Relationship Between Steatosis, Inflammation, and Fibrosis in Chronic Hepatitis C: A Meta-Analysis of Individual Patient Data. *Gastroenterology* **130**, 1636–1642 (2006).
234. Caldwell, S. H., Crespo, D. M., Kang, H. S. & Al-Osaimi, A. M. S. Obesity and hepatocellular carcinoma. *Gastroenterology* **127**, 97–103 (2004).
235. Regimbeau, J. M. *et al.* Obesity and diabetes as a risk factor for hepatocellular carcinoma. *Liver Transpl.* **10**, S69–S73 (2004).
236. Wanless, I. R. & Lentz, J. S. Fatty liver hepatitis (steatohepatitis) and obesity: an autopsy study with analysis of risk factors. *Hepatology* **12**, 1106–10 (1990).
237. Juakim, W., Torres, D. M. & Harrison, S. A. Nutrition in cirrhosis and liver disease. *Clin. Liver Dis.* **18**, 179–90 (2014).
238. Montella, M., Crispo, A. & Giudice, A. HCC, diet, and metabolic factors. *Hepat Mon* **11**, 159–162 (2011).
239. Hill-Baskin, A. E. *et al.* Diet-induced hepatocellular carcinoma in genetically predisposed mice. *Hum. Mol. Genet.* **18**, 2975–2988 (2009).
240. Kahle, M. *et al.* Phenotypic comparison of common mouse strains developing high-fat diet-induced hepatosteatosis. *Mol. Metab.* **2**, 435–446 (2013).
241. Nicholson, A. *et al.* Diet-induced obesity in two C57BL/6 substrains with intact or mutant nicotinamide nucleotide transhydrogenase (Nnt) gene. *Obesity (Silver Spring)*. **18**, 1902–1905 (2010).
242. Nordenstedt, H., White, D. L. & El-Serag, H. B. The changing pattern of epidemiology in hepatocellular carcinoma. *Dig. Liver Dis.* **42**, 206–214 (2010).
243. Misra, A. & Bhardwaj, S. Obesity and the metabolic syndrome in developing countries: focus on South Asians. *Int. Nutr. Achiev. Millenium Goals Beyond*.

- Nestle Nutr Inst Work. Ser. Nestec Ltd. Veyvey/S. Karger AG Basel* **78**, 133–40 (2014).
244. Neuschwander-Tetri, B. a. & Caldwell, S. H. Nonalcoholic steatohepatitis: Summary of an AASLD Single Topic Conference. *Hepatology* **37**, 1202–1219 (2003).
245. Ascha, M. S. *et al.* The incidence and risk factors of hepatocellular carcinoma in patients with nonalcoholic steatohepatitis. *Hepatology* **51**, 1972–1978 (2010).
246. Zen, Y. *et al.* Hepatocellular carcinoma arising in non-alcoholic steatohepatitis. *Pathol. Int.* **51**, 127–131 (2001).
247. Brass, E. P. & Vetter, W. H. Interleukin-6 , but not tumour necrosis factor-a , increases lipogenesis in rat hepatocyte primary cultures. **197**, 193–197 (1994).
248. Brass, E. P. & Vetter, W. H. Stimulation of lipogenesis by interleukin-6 and misoprostol-free acid in isolated rat hepatocytes. *Am J Ther* **2**, 706–10 (1995).
249. Menendez, J. a & Lupu, R. Fatty acid synthase and the lipogenic phenotype in cancer pathogenesis. *Nat. Rev. Cancer* **7**, 763–777 (2007).
250. Aleksandrova, K. *et al.* Inflammatory and metabolic biomarkers and risk of liver and biliary tract cancer. *Hepatology* 858–871 (2014). doi:10.1002/hep.27016
251. Saxena, N. K. *et al.* Adiponectin modulates C-Jun N-terminal kinase and mammalian target of rapamycin and inhibits hepatocellular carcinoma. *Gastroenterology* **139**, 1762–1773.e5 (2010).
252. Ran, J. *et al.* Angiotensin II infusion decreases plasma adiponectin level via its type 1 receptor in rats: An implication for hypertension-related insulin resistance. *Metabolism.* **55**, 478–488 (2006).
253. Rezvani, R. *et al.* Effects of sugar-sweetened beverages on plasma acylation stimulating protein, leptin and adiponectin: Relationships with Metabolic Outcomes. *Obesity* **21**, 2471–2480 (2013).
254. Arao, T. *et al.* FGF3/FGF4 amplification and multiple lung metastases in responders to sorafenib in hepatocellular carcinoma. *Hepatology* **57**, 1407–1415 (2013).
255. Cabibbo, G. *et al.* A meta-analysis of survival rates of untreated patients in randomized clinical trials of hepatocellular carcinoma. *Hepatology* **51**, 1274–1283 (2010).

256. Li, C. *et al.* SREBP-1 has a prognostic role and contributes to invasion and metastasis in human hepatocellular carcinoma. *Int. J. Mol. Sci.* **15**, 7124–7138 (2014).
257. Su, Q. & Bannasch, P. Relevance of hepatic preneoplasia for human hepatocarcinogenesis. *Toxicol. Pathol.* **31**, 126–133 (2003).
258. Hardwick, J. P., Osei-Hyiaman, D., Wiland, H., Abdelmegeed, M. a. & Song, B. J. PPAR/RXR Regulation of fatty acid metabolism and fatty acid ω -hydroxylase (CYP4) isozymes: Implications for prevention of lipotoxicity in fatty liver disease. *PPAR Res.* **2009**, (2009).
259. Bhalla, K. *et al.* PGC1 α promotes tumor growth by inducing gene expression programs supporting lipogenesis. *Cancer Res.* **71**, 6888–98 (2011).
260. Charos, A. E. *et al.* A highly integrated and complex PPARGC1A transcription factor binding network in HepG2 cells. *Genome Res.* **22**, 1668–1679 (2012).
261. Louet, J. F., Hayhurst, G., Gonzalez, F. J., Girard, J. & Decaux, J. F. The coactivator PGC-1 is involved in the regulation of the liver carnitine palmitoyltransferase I gene expression by cAMP in combination with HNF4 α and cAMP-response element-binding protein (CREB). *J. Biol. Chem.* **277**, 37991–38000 (2002).
262. Abramson, H. N. The lipogenesis pathway as a cancer target. *J. Med. Chem.* **54**, 5615–5638 (2011).
263. Lee, J. *et al.* Regulator of fatty acid metabolism, acetyl coenzyme a carboxylase 1, controls T cell immunity. *J. Immunol.* **192**, 3190–9 (2014).
264. Freeman, H. C., Hugill, A., Dear, N. T., Ashcroft, F. M. & Cox, R. D. Deletion of nicotinamide nucleotide transhydrogenase: A new quantitative trait locus accounting for glucose intolerance in C57BL/6J mice. *Diabetes* **55**, 2153–2156 (2006).
265. Chow, J. D. Y., Jones, M. E. E., Prella, K., Simpson, E. R. & Boon, W. C. A selective estrogen receptor α agonist ameliorates hepatic steatosis in the male aromatase knockout mouse. *J. Endocrinol.* **210**, 323–334 (2011).
266. Healy, M. E. *et al.* Dietary effects on liver tumor burden in mice treated with the hepatocellular carcinogen diethylnitrosamine. *J. Hepatol.* **62**, 599–606 (2015).
267. Berglund, E., Li, C., Poffenberger, G. & Ayala, J. Glucose metabolism in vivo in four commonly used inbred mouse strains. *Diabetes* **57**, 1790–1799 (2008).

268. Millar, J. S., Cromley, D. a, McCoy, M. G., Rader, D. J. & Billheimer, J. T. Determining hepatic triglyceride production in mice: comparison of poloxamer 407 with Triton WR-1339. *J. Lipid Res.* **46**, 2023–2028 (2005).
269. Kojiro, M. Pathological diagnosis at early stage: Reaching international consensus. *Oncology* **78**, 31–35 (2010).
270. Kudo, M. Early hepatocellular carcinoma: definition and diagnosis. *Liver cancer* **2**, 69–72 (2013).
271. Schlaeger, C. *et al.* Etiology-dependent molecular mechanisms in human hepatocarcinogenesis. *Hepatology* **47**, 511–20 (2008).
272. Folch, J., Lees, M. & Stanley, S. G. H. A simple method for the isolation and purification of total lipides from animal tissues. *J Biol Chem* **226**, 497–509 (1957).
273. Severgnini, M. *et al.* A rapid two-step method for isolation of functional primary mouse hepatocytes: Cell characterization and asialoglycoprotein receptor based assay development. *Cytotechnology* **64**, 187–195 (2012).
274. Byrne, F. L. *et al.* Metabolic Vulnerabilities in Endometrial Cancer. *Cancer Res.* **74**, 5832–5845 (2014).
275. Kenwood, B. M. *et al.* Identification of a novel mitochondrial uncoupler that does not depolarize the plasma membrane. *Mol. Metab.* **3**, 114–123 (2014).
276. Bengtsson, C. *et al.* Design of small molecule inhibitors of acetyl-CoA carboxylase 1 and 2 showing reduction of hepatic malonyl-CoA levels in vivo in obese Zucker rats. *Bioorganic Med. Chem.* **19**, 3039–3053 (2011).
277. Gao, L. *et al.* Simultaneous quantification of malonyl-CoA and several other short-chain acyl-CoAs in animal tissues by ion-pairing reversed-phase HPLC/MS. *J. Chromatogr. B Anal. Technol. Biomed. Life Sci.* **853**, 303–313 (2007).
278. Boersema, P. J., Raijmakers, R., Lemeer, S., Mohammed, S. & Heck, A. J. R. Multiplex peptide stable isotope dimethyl labeling for quantitative proteomics. *Nat. Protoc.* **4**, 484–494 (2009).
279. Rappsilber, J., Mann, M. & Ishihama, Y. Protocol for micro-purification, enrichment, pre-fractionation and storage of peptides for proteomics using StageTips. *Nat. Protoc.* **2**, 1896–1906 (2007).

280. Beausoleil, S. a, Villén, J., Gerber, S. a, Rush, J. & Gygi, S. P. A probability-based approach for high-throughput protein phosphorylation analysis and site localization. *Nat. Biotechnol.* **24**, 1285–1292 (2006).
281. Liberzon, A. *et al.* Molecular signatures database (MSigDB) 3.0. *Bioinformatics* **27**, 1739–1740 (2011).
282. Pagliarini, D. J. *et al.* A Mitochondrial Protein Compendium Elucidates Complex I Disease Biology. *Cell* **134**, 112–123 (2008).
283. Smoot, M. E., Ono, K., Ruscheinski, J., Wang, P. L. & Ideker, T. Cytoscape 2.8: New features for data integration and network visualization. *Bioinformatics* **27**, 431–432 (2011).
284. Huang, D. W., Sherman, B. T. & Lempicki, R. a. Systematic and integrative analysis of large gene lists using DAVID bioinformatics resources. *Nat. Protoc.* **4**, 44–57 (2009).